The role of cosurfactants in adsorption and emulsification

The Role of Cosurfactants in

Adsorption and Emulsification

Gert Tuin

THE ROLE OF COSURFACTANTS IN ADSORPTION AND EMULSIFICATION

THE ROLE OF COSURFACTANTS IN ADSORPTION AND EMULSIFICATION

PROEFSCHRIFT

ter verkrijging van de graad van doctor aan de Technische Universiteit Eindhoven, op gezag van de Rector Magnificus, prof.dr. J.H. van Lint, voor een commissie aangewezen door het College van Dekanen in het openbaar te verdedigen op dinsdag 13 juni 1995 om 14.00 uur

door

Gert Tuin

geboren te Winschoten

Dit proefschrift is goedgekeurd door de promotoren:

prof.dr. H.N. Stein
prof.dr. W.G.M. Agterof

Contents

Contents

CHAPTER 1

INTRODUCTION

1.1 Introduction

Surfactants find applications in various chemical industrial activities, such as detergency, paints, cosmetics, pharmaceuticals, pesticides, fibres, and plastics. Surfactants have also frequently been used in the oil industry, for example in enhanced recovery. The fundamental understanding of the properties of surfactants is therefore very important. In this chapter a survey of the following aspects of surfactants will be given: the properties of surfactants with respect to molecular structure, adsorption of surfactant on interfaces and the use of surfactants in emulsions.

1.1.1 Properties of surfactants

Surfactants (surface active agents) have a characteristic structure consisting of two structural groups: one that has very little attraction for the solvent and one that has strong attraction for the solvent. In figure 1.1 a schematic view of a surfactant molecule is shown.

hydrophobic tail   hydrophilic
                            headgroup
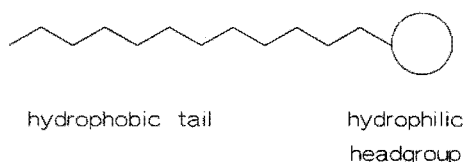
Figure 1.1: Schematic view of a surfactant molecule.

The "tail" of the surfactant molecule is known as the lyophobic (solvent hating) part, whereas the headgroup is known as the lyophilic (solvent loving) part. When water is the solvent, these groups are also called hydrophobic resp. hydrophilic. These two groups in one surfactant molecule are the reason for the amphiphatic character of surfactants. For a more thorough description of surfactants see Rosen [1], Tadros [2] and Myers

[3]. Depending on the nature of the headgroup, ionic or polar, surfactants are termed ionic or non-ionic. In this thesis the surfactant Sodium Dodecylbenzenesulphonate (abbreviated as SDBS) is used. The chemical structure is shown in figure 1.2.

$$C_{12}H_{25} \bigcirc SO_3^- \ Na^+$$
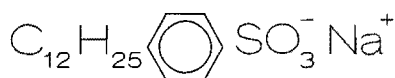
Figure 1.2: Chemical structure of SDBS.

This surfactant was chosen instead of the frequently employed surfactant Sodium Dodecylsulphate (SDS), because the latter hydrolyses in aqueous solution forming dodecanol [4]. In this thesis dodecanol was chosen as a cosurfactant. The occurrence of dodecanol as consequence of hydrolysis of SDS could be a problem in the interpretation of the results.

Due to the amphipathic nature of surfactant molecules, they exhibit a number of un-expected phenomena. Already in 1920, McBain and Salmon [5] investigated the osmotic activity of a 1 M solution of Potassium stearate at 90 °C. They found that the concentration of osmotically active material was 0.42 M and concluded that considerable association had occurred in the solution. McBain suggested to call these associates micelles.

The properties of surfactant solutions were later described by Hartley [6]. The micelle proposed by Hartley was spherical, consisted of approx. 100 surfactant molecules and the process of micellization took place over a narrow range of concentration, indicated by the "critical micelle concentration" (cmc).

This result is still an excellent foundation for present day studies. Nevertheless some deviations from this model have been observed. Hayter [7] found, using small angle neutron scattering, that the surface of the micelles may be somewhat rougher than depicted in the model of Hartley. Various modern techniques have indicated, that in many systems the micelles are not spherical, but cylindrical as found by Debye and Anacker [8]. Evidence for disc-shaped micelles has also been found [9].

The driving force for micellization is the tendency to minimize the Gibbs energy of the

system, which entails the need to minimize unfavourable interactions or to maximize favourable interactions of surfactant molecules with the environment. This minimization of the free energy of the system is also the reason, that surfactants adsorb strongly at liquid-solid (L/S), liquid-liquid (L_1/L_2) and liquid-gas (L/G) interfaces. Surfactants will spend therefore, on average, most of their time interacting at interfaces or with others of their kind (at concentrations higher than the cmc).

The adsorption of surfactant has extensively been studied, both from an academic point of view and because the performance of surfactant systems in practical situations depends strongly on the adsorbed amount at the interface (surface excess).

1.1.2 Emulsions

An emulsion is a suspension of droplets of one liquid in a second immiscible liquid [10], [11]. Emulsions are encountered frequently in daily life. An example is milk (a dispersion of fat globules in water). Many industrial processes involve the production of emulsions, for example food industry, detergency, pharmacy and the spraying of bitumen emulsions on road surfaces.

Two types of emulsions can be distinguished, based on the nature of the dispersed phase: oil-in-water (O/W) and water-in-oil (W/O). The dispersed phase is the discontinuous phase, whereas the other is the continuous phase.

Two immiscible, pure liquids cannot form an emulsion, which is at least temporarily stable. Dispersions of one liquid in another are generally unstable from a thermodynamical point of view. Because of the large increase in surface area when dispersing one liquid in another, there is a large increase in interfacial free energy. This interfacial free energy (determined by the interfacial tension and the interfacial area) is orders of magnitude larger than that of two phases separated by a flat interface. An emulsion is therefore a thermodynamically unstable system. Addition of a surfactant lowers the interfacial tension and thus the free energy, but an emulsion still remains a thermodynamically unstable system.

Emulsions can be formed by the input of kinetic energy (by e.g. stirring). When stirring is stopped, it will eventually separate in two different phases. Emulsions are therefore kinetically stable systems.

Such an emulsion, however, may be kinetically stable requiring a third component, which is usually a surfactant, but solid particles can also be used to stabilize the system [12].

The type of emulsion formed, depends on the solubility of the surfactant in the respective phases. If the surfactant is more soluble in the water-phase, in most cases an O/W emulsion will be formed, whereas an W/O emulsion is obtained if the surfactant is more soluble in the oil-phase. This fact is known as the Bancroft rule [13].

In contrast to emulsions with droplet sizes larger than 1 μm, micro-emulsions have droplet sizes smaller than 100 nm. These micro-emulsions were first described in 1943 by Hoar and Schulman [14]. The term micro-emulsion was, however, used in 1959 for the first time [15]. These systems are transparent (or translucent) and form spontaneously when oil and water are mixed together with large amounts of surfactant and a co-surfactant (e.g. a medium size alcohol).

Micro-emulsions are, in contrast to emulsions, thermodynamically stable. In these system the interfacial tension is so low (but still positive), that the free energy of the interface can be overcompensated by the entropy of the droplets in the medium [16],[17],[18]. For these low interfacial tensions a combination of a surfactant and cosurfactant may be used: for instance SDS and pentanol [19],[20], SDBS and pentanol [21]. Low interfacial tensions can also be obtained by using a single surfactant with two hydrophobic tails per molecule (e.g. AOT) [22] or by using a non-ionic surfactant [23], [24].

1.2 Aim of this thesis

It may be obvious from the foregoing survey that surfactants play a very important role in a number of industrial processes, like e.g. emulsion polymerization. During emulsion polymerization the surfactants can act as loci, in which the polymerization is started and they stabilize the prepared polymer particles.

The use of surfactants during emulsion polymerization has also a number of disadvantages, such as the possibility to foam formation during further processing of the polymers as e.g. paint, ink and adhesive. The surfactants also remain in the dry film of the paints, which in turn leads to a greater sensitivity to water.

It is the aim of the present investigation to determine the influence of cosurfactants on the

physical properties of surfactants in relation to the stability of coarse emulsions (with diameter larger than 1 μm). Emulsion stability is largely determined by the adsorption of surfactant on the oil-water interface, which prevents the emulsion droplets from coalescing.

Addition of a small amount of cosurfactant to a surfactant leads to a smaller interfacial tension. When a certain low value of the interfacial tension is needed to create an emulsion, the required surfactant concentration can be reduced by adding a small amount of cosurfactant, with the total concentration of surfactant and cosurfactant being smaller than the surfactant concentration alone.

1.3 Survey of this thesis

In **chapter 2** the preparation of large monodisperse Polystyrene particles is described. These particles were prepared by a one step surfactant-free emulsion polymerization. In this way model colloids were prepared, without the need to remove surfactants, if a conventional emulsion polymerization procedure had been followed.

Chapter 3 deals with the characterization of the Polystyrene latices in connection with the surface charge density arising from the initiator used during emulsion polymerization. It is found that the surface charge density varies with particle size, but not in a systematic way. To complete the surface characterization, zeta (ζ) potential measurements were performed, which showed that the ζ-potential does not follow the expected decrease of ζ-potential with increasing electrolyte concentration, but that the ζ-potential goes through a maximum upon increasing the electrolyte concentration. It is also found that the charge density behind the electrokinetic shear plane is higher than the surface charge density for one of the latices prepared.

In **chapter 4** the adsorption of ionic surfactant on Polystyrene particles is described. It will be shown that the surface excess (the amount of surfactant adsorbed on the Polystyrene particles per unit surface area) is influenced by variables such as temperature. The adsorption of surfactant in presence of cosurfactant is also studied. It is found, that the area per adsorbed surfactant molecule *decreases* with higher amounts of cosurfactants present. The largest decrease in adsorption area is found at temperatures above the melting point of the cosurfactants and with cosurfactant/surfactant ratios larger than one.

Chapter 5 compares experimental adsorption data with a model for the adsorption of surfactant on the Polystyrene particles. In this model localized adsorption is assumed for the adsorption of the surfactant anion, whereas mobile adsorption is assumed for the adsorption of the surfactant cation. Deviations from this model are included in an excess G-function. Combining this model and an experimentally determined adsorption isotherm, it is found that the standard Gibbs energy of adsorption is not a constant quantity, but that it goes through a maximum as the degree of occupancy of the surface increases. This phenomena is thought to be the result of a change in configuration of the surfactant anion during adsorption.

In **chapter 6** the preparation of decane emulsions in surfactant solutions, in absence and presence of cosurfactant, is described. In absence of cosurfactants the influence of process variables, such as stirrer speed and volume fraction of dispersed phase, is well described by the Weber number theory. To account for the presence of surfactant, a dynamic interfacial tension (instead of the equilibrium interfacial tension) has to be introduced in the Weber number to obtain a good relationship between experimental and theoretical results. This dynamic interfacial tension is a consequence of the fact, that the droplets are expanding every time they come in the vicinity of the stirrer.

In the presence of cosurfactants the emulsification time (the time necessary to reach a steady state droplet size) is shortened with respect to the situation in absence of cosurfactants. This is due to the smaller difference between dynamic and equilibrium interfacial tension in presence of cosurfactant. A second influence of cosurfactants is the average droplet size being reduced as a result of a lower interfacial tension.

In **chapter 7** possible consequences of the use of cosurfactants during emulsion polymerization is described from a theoretical background.

This thesis is based on articles, which have been published (chapter 2 [25], chapter 4 [26]), are accepted (chapter 5 [27]) or will be submitted (chapter 3 [28], chapter 6 [29]).

1.4 References

(1) Rosen, M. J., *Surfactants and Interfacial Phenomena*, J. Wiley and Sons, **1978**.

(2) Tadros, Th. F., *Surfactants*, Academic Press Inc., **1984.**

(3) Myers, D., *Surfactant Science and Technology*, VCH Publishers Inc., **1988**.

(4) Harold, S. P., *J. Colloid Interface Sci.*, **1960**, *15*, 280.

(5) McBain, J. W., Salmon, C. S., *J. Am. Chem. Soc.*, **1920**, *43*, 426.

(6) Hartley, G. S., *Aqueous Solutions of Paraffin Chain Salts*, Hermann and Cie, **1936**.

(7) Hayter, J. B., *Ber. Bunsenges. Phys.* Chem., **1981**, *85*, 887.

(8) Debye, P., Anacker, E. W., *J. Phys. and Colloid Chem.*, **1951**, *55*, 644.

(9) Mazer, N. A., Carey, M. C.,Benedek, G. B., In *Micellization, Solubilization, and Microemulsions*, Mittal, K. L., Ed; Plenum Press, New York; **1977**, p. 359.

(10) Becher, P., *Emulsions, Theory and Practice*, Reinhold Publ. Corp., New York, **1965**.

(11) Sherman, P., *Emulsion Science*, Academic Press, London, **1965**.

(12) Tadros, T. F., Vincent, B., In *Encyclopedia of Emulsion Technology*, Becher, P., Ed.; Marcel Dekker, Inc., New York, **1983**, p. 272.

(13) Bancroft, W. D., *J. Phys. Chem.*, **1913**, *17*, 514.

(14) Hoar, T. P., Schulman, J. H., *Nature*, **1943**, *152*, 102.

(15) Stockenius, W., Schulman, J. H., Prince, L. M., *J. Phys. Chem.*, **1959**, *63*, 1677.

(16) Reiss, H., *J. Colloid Interface Sci.*, **1975**, *53*, 61.

(17) Reiss, H., *Adv. Colloid Interface Sci.*, **1977**, *7*, 1.

(18) Overbeek, J. Th. G., *Faraday Disc. Chem. Soc.*, **1978**, *65*, 7.

(19) Kegel, W. K., Van Aken, G. A., Bouts, M. N., Lekkerkerker, H. N. W., Overbeek, J. Th. G., De Bruyn, P. L., *Langmuir*, **1993**, *9*, 252.

(20) Zhou, J. S., Dupeyrat, M., *J. Colloid Interface Sci.*, **1990**, *134(2)*, 320.

(21) Doe, P. H., El-Emary, H., Wade, W. H., *J. Am. Oil Chem. Soc.*, **1977**, *54*, 570.

(22) Aveyard, R., Binks, B. P., Clark, S., Mead, J., *J. Chem. Soc., Faraday Trans. 1*, **1986**, *82*, 125.

(23) Aveyard, R., Binks, B. P., Lawless, T. A., Mead, J., *J. Chem. Soc., Faraday Trans 1*, **1985**, *81*, 2155.

(24) Overbeek, J. Th. G., De Bruyn, P. L., Verhoeckx, F., In *Surfactants*; Tadros, Th. F., Ed., Academic Press, **1984**, p. 111.

(25) Tuin, G., Peters, A. C. I. A., Van Diemen, A. J. G., Stein, H. N.,
    J. Colloid Interface Sci., **1993**, *158(2)*, 508.

(26) Tuin, G., Stein, H. N., *Langmuir*, **1994**, *10(4)*, 1054.

(27) Tuin, G., Stein, H. N., *Langmuir*, accepted.

(28) Tuin. G., Senders, J. H. J. E., Stein. H. N., submitted.

(29) Tuin, G., Senders, J. H. J. E., Stein, H. N., Agterof, W. G. M., submitted.

CHAPTER 2

PREPARATION OF LARGE MONODISPERSE POLYSTYRENE PARTICLES BY A ONE STEP SURFACTANT-FREE EMULSION POLYMERIZATION

Summary: Large monodisperse polystyrene (PS) particles were prepared by a one step surfactant-free emulsion polymerization using a lower stirrer speed than applied by previous investigators. The largest PS-particles prepared had a diameter of 3.2 μm. SEM-photographs showed no surface roughness on the PS-particles.

2.1 Introduction

Monodisperse Polystyrene (PS) particles are widely used as model colloids. Aqueous PS-latices are usually prepared by an emulsion polymerization. The emulsion polymerization can be performed either with a surfactant or without a surfactant (soap-free or emulsifier-free).

The theory of emulsion polymerization, in which a surfactant is used, was established by Harkins [1] and by Smith and Ewart [2]. The main disadvantage of the use of a surfactant is that the emulsifier is adsorbed at the interface of the PS-particle and water. The removal of the adsorbed emulsifier can be quite difficult and one can never be sure that all emulsifier molecules are removed from the interface.

These drawbacks lead to the development of the emulsifier-free emulsion polymerization. Previous work on this subject has been reported by Matsumoto and Ochi [3], Kotera et al. [4,5] and Goodwin et al. [6,7].

In these polymerization systems [6,7] monomer concentration, initiator concentration, ionic strength and temperature were found to be important variables. Under the conditions used it was impossible to prepare PS-latices with particle sizes larger than 1 μm in a one-step process.

In order to obtain larger particles a seeded-growth procedure seemed to be a reliable way [8], but in many seeded-growth experiments new nucleation occurred and bimodal and even broader distributions occurrred.

Investigations on the one-step surfactant-free emulsion polymerization of styrene in order to obtain large PS-particles (particle size larger than 1 μm) have, to our knowledge, never been published thus far.

In this chapter the preparation and characterization of PS-particles (up to 3.2 μm) made by a one-step emulsion polymerization is described. Variables, such as monomer concentration, initiator concentration, ionic strength and the flow pattern have been found to play a very important role. The particles obtained had a high degree of monodispersity.

2.2   Experimental

2.2.1 Materials

Water used was doubly-distilled from an all glass apparatus. The specific conductance (0.8 μMHO cm^{-1}) and the surface tension (72 $\pm$ 0.3 mN/m) of this water indicated that it was free of surface active impurities.

Styrene: ex Merck (*pro analysi*, purity > 99%), used without further purification.

Sodium chloride, potassium persulphate: ex Merck (*pro analysi*, purity > 99%), used without purification.

2.2.2 Polymerization procedure

All polymerization reactions were carried out in 10 dm^3 reaction vessels fitted with multinecked flanged tops. Normally a reaction volume of 8500 cm^3 was used.

Latices with a particle size below 1 μm were prepared in a round-bottomed reactor with four (L-78) or without (L-80) any baffles, using a stainless steel stirrer. Latices with particle sizes greater than 1 μm were prepared in a flat-bottomed reactor with 4 baffles, using a stainless steel anchor type stirrer. The distance of the stirrer to the bottom of the reaction vessel was the same for all polymerizations.

The reactor was kept at constant temperature by a water thermostat bath circulating water through the double wall of the reactor.

The polymerizations were carried out in the following manner. Initially the major part of the water was added to the reactor. The stirrer and baffles were installed and care was taken to ensure that the stirrer was at the same distance from the bottom of the reactor for each polymerization.

After the reactor cover had been installed the required quantity of sodium chloride (if necessary), dissolved in 100 cm^3 of distilled water, was then added and washed in with a further 20 cm^3 of water. Then under an outflow of nitrogen the styrene was added and the stirrer was adjusted to its required speed. This speed was checked several times with a tachometer.

The mixture was then left to equilibrate for 30 minutes and to attain the reaction temperature to which the thermostat bath had been adjusted a few hours earlier.

After these 30 minutes the reaction was started by addition of the potassium persulphate which had been dissolved in 100 cm^3 distilled water of about 40 °C.

The recipes of the preparation of the latices together with relevant reaction parameters are given in table 2.1. The concentrations of all reactants are based on the aqueous phase, except the styrene percentage which is based on the total volume.

After the reaction times mentioned the reaction mixture was cooled down to room temperature. Then the latex was filtered through a 200 mesh screen to remove any coagulum formed. Conversions were always higher than 90%.

Table 2.1: Details of latex preparation.

	Latex				
	L-78	L-80	L-86	L-88	L-89
Water (g)	7484	7725	7500	7500	7500
Styrene (g)	998	769	906	906	906
$K_2S_2O_8$ (g)	8.48	5.16	8.50	6.43	5.74
NaCl (g)	9.98	0	15	20	20
[Styrene] (% v/v)	12.8	9.9	11.8	11.8	11.8
[$K_2S_2O_8$] (mM)	3.70	2.25	3.65	2.80	2.50
[NaCl] (M)	0.02	0	0.03	0.04	0.04
Reaction temperature (°C)	70	70	68	67	66
Reaction time (min)	290	510	960	960	960
Stirrer speed (rpm)	300	150	160	160	160
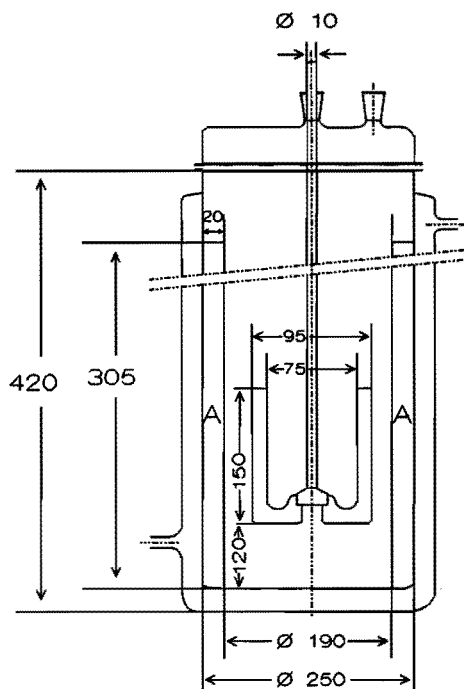
Figure 2.1: Schematic drawing of the reaction vessel and the stirrer used for the preparation of latices with particle diameters > 1 μm. Dimensions are in mm; the baffles are denoted by A.

2.2.3 Particle size measurements

Particle sizes of the polystyrene latices were determined with the Coulter Counter (Coulter Electronics), the Coulter LS 130 (Coulter Electronics) and with Scanning Electron Microscopy (SEM, Cambridge S 200).

2.2.3.1 Coulter Counter

The measurements with the Coulter Counter (equipped with channel expander and 30 μm orifice tube) are useful for particles with diameters larger than 1 μm. In this way the particle size and the particle size distribution (number, surface and volume average) were determined. The results are given in table 2.2.

Table 2.2: Particle sizes determined with Coulter Counter and Coulter LS 130.

Latex	Coulter Counter				Coulter LS 130			
	D_n (nm)[a]	D_a (nm)[b]	D_v (nm)[c]	P_n[d]	D_n (nm)[a]	D_a (nm)[b]	D_v (nm)[c]	P_n[d]
L-78	-	-	-	-	736	754	764	1.04
L-80	-	-	-	-	381	398	407	1.07
L-86	1309	1357	1386	1.06	1224	1247	1258	1.03
L-88	2165	2217	2252	1.04	2018	2086	2116	1.05
L-89	3124	3253	3279	1.02	3166	3252	3302	1.04

[a] number average diameter

[b] surface average diameter

[c] volume average diameter

[d] degree of polydispersity (D_v/D_n)

2.2.3.2 Coulter LS 130

In the particle size measurements with the Coulter LS 130 two techniques are combined: light scattering measurement (Photon Correlation Spectroscopy) and light diffraction measurement (Polarized Intensity Differential Scattering).

With the former method particles which are much larger particle diameter than the wave length of light (≥ 0.8 μm) can be measured while the latter method is especially suitable for measuring particles that are just of about the size of the wavelength (0.4 - 0.8 μm).

By this combination of measurement techniques particles in the range of 0.1 - 10 μm can be measured. Therefore all five latices were measured with the Coulter LS-130. The measured particle sizes are also given in table 2.2.

2.2.3.3 SEM

To obtain insight in the monodispersity and possible roughness of the particle surface, all latices were scanned by means of Scanning Electron Microscopy (SEM). A drop of a dilute sample of each latex was placed onto a brass surface. The sample was then left to evaporate to dryness in a dust-free environment at room temperature. The samples were then coated with gold and scans were taken at 90° angle. Typical SEM-photographs are represented by the SEM-photograph of latex L-89 in figure 2.2.

Particle sizes and particle size distributions were determined by measuring at least 100 particles for each latex. The obtained particle sizes are also listed in table 2.3.

Table 2.3: Particle sizes determined with SEM.

Latex	D_n (nm)[a]	D_a (nm)[b]	D_v (nm)[c]	$P_n^{\ d}$
L-78	672	673	675	1.01
L-80	413	415	416	1.01
L-86	1230	1233	1235	1.01
L-88	1997	2001	2005	1.01
L-89	3086	3091	3092	1.01

[a] number average diameter

[b] surface average diameter

[c] volume average diameter

[d] degree of polydispersity (D_v/D_n)

2.3 Results and discussion

In table 2.1 the recipes for the preparation of the latices are shown. As can be seen from table 2.1 a combination of factors (such as initiator concentration, ionic strength, temperature and stirrer speed) determine the final particle size of the latices. A low reaction temperature results in the formation of less radicals than at a higher temperature and larger particles are obtained.

The fact that the monomer was used without purification (i.e. without distillation, thus without removing the inhibitor) does not seem to have any influence on the preparation of these latices.

We found that the flow pattern during the reaction (determined by the geometry of the reactor, the stirrer speed and the type of stirrer) plays a very important role in this type of emulsion polymerization. In the present investigation, the stirrer speed was adjusted such as to let a styrene layer form on top of the aqueous phase, but detaching regularly droplets from the styrene layer, dispersing them in the water. This is a lower stirrer speed than used by other investigators.

Particle sizes determined with various methods are listed in table 2.2 and table 2.3, where
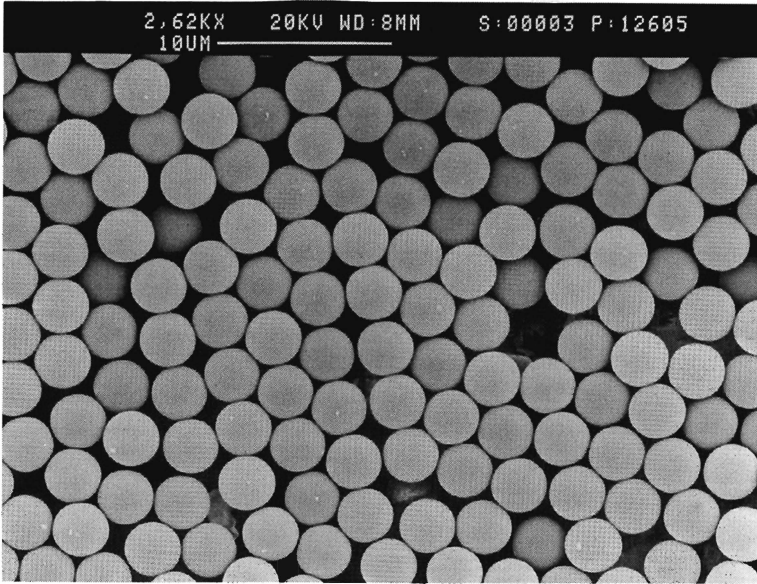
Figure 2.2: *SEM photograph of latex L-89: the bar represents 5 μm.*
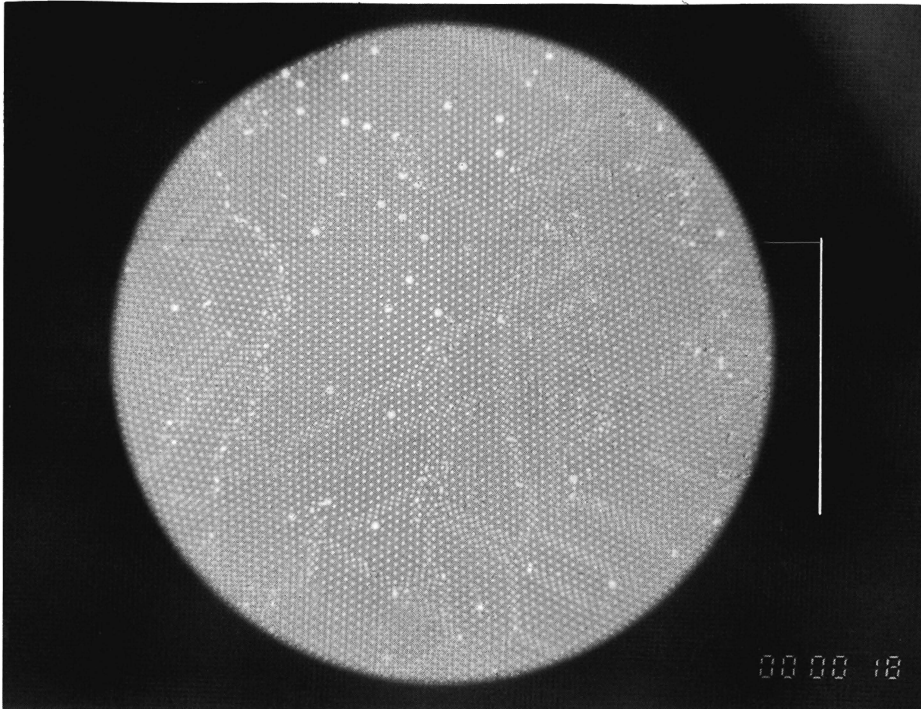
Figure 2.3: *Light microscope photograph of latex L-78: the bar represents 100 μm.*

the particle sizes are listed as number average diameter ($D_n = \sum n_i D_i / \sum n_i$), surface average diameter ($D_a = \sum n_i D_i^2 / \sum n_i D_i$), volume average diameter $D_v = \sum n_i D_i^3 / \sum n_i D_i^2$) and the degree of polydispersity P_n (D_v / D_n) where n is the number of particles with diameter D.

As can be seen from table 2.2 and table 2.3 all the particles are monodisperse, especially the larger ones (latex L-88 and L-89). The degree of polydispersity P_n is always smaller than 1.07. Highly monodisperse particles have a degree of polydispersity smaller than 1.05. This is the case for latices L-86, L-88 and L-89.

Comparing the results of the measurements with the Coulter Counter and the Coulter LS 130 one can see that the differences in particle size measured by these instruments are very small. In table 2.3 the results for the measurements by Scanning Electron Microscopy (SEM) are shown. The determined particle sizes are smaller (except latex L-80) than with the other two methods, but the differences in the particle sizes are not pronounced. The fact, that the particle sizes measured with SEM are smaller, is explained by the fact that when the particles are exposed to an electron beam shrinking can occur. The fact that latex L-80 as measured by SEM is larger than as measured by the Coulter LS 130 remains, however, unexplained.

Concluding one can say that the three methods of measuring particle sizes are very well comparable, although the measuring methods are different.

In figure 2.2 a typical SEM-photograph of latex L-89 is shown. As can be seen from this picture the latex particles are spherical, monodisperse and a hexagonal packing is present. Surface roughness is not visible on the scale of the SEM photograph. The degree of monodispersity is also testified for the latices L-86, L-88 and L-89, by the large close packed regions present. These large close packed regions were also seen when examining the latices under a light microscope, which is also shown for latex L-89 in figure 2.3. Examining the latices under a light microscope reveals also the interference colours. These observations confirm that the particles are highly monodisperse.

2.4 Conclusions

Surfactant-free emulsion polymerization is an important technique to produce PS-latices. By our approach it is possible to prepare PS-latices with particle sizes larger than 1 μm in a one step process. This method avoids some disadvantages of seeded-growth emulsion

polymerization. The prepared latices are extremely useful for adsorption studies.

2.5 References

(1) Harkins, W. D., *J. Amer. Chem. Soc.*, **1947**, *69*, 1428.

(2) Smith, W. V., Ewart, R. H., *J. Chem. Phys.*, **1948**, *16*, 592.

(3) Matsumoto, T., Ochi, A., *Kobunshi Kagaku*, **1965**, *22*, 481.

(4) Kotera, A., Furasawa, K., Takeda, Y.,*Kolloid-Z. u. Z. Polymere*, **1970**, *239*, 677.

(5) Kotera, A., Furasawa, K., Kudo, K. *Kolloid-Z. u. Z. Polymere*, **1970**, *240*, 837.

(6) Goodwin, J. W., Hearn, J., Ho, C. C., Ottewill, R. H.,
     Br. Polymer J., **1973**, *5*, 347.

(7) Goodwin, J. W., Hearn, J., Ho, C. C., Ottewill, R. H.,
     Colloid and Polymer Sci., **1974**, *252*, 464.

(8) Hearn, J., Ottewill, R. H., Shaw, J. N., *Br. Polymer J.*, **1970**, *2*, 116.

ELECTROPHORETIC PROPERTIES OF MONODISPERSE POLYSTYRENE PARTICLES

Summary: In this chapter the electrophoretic properties of the latices, of which the preparation was presented in chapter 2, is described. The latices were characterized by conductometric titration. The charged groups, arising from initiator fragments, were all strong acid groups and no carboxyl groups could be detected. The amount of surface charge groups varies with particles size.

Electrophoresis measurements have shown, that the electrophoretic mobility passes through a maximum as the electrolyte concentration is increased. Converting the electrophoretic mobility to ζ-potentials gives the same picture. The same phenomenon is observed with increasing H^+-concentration. Only at very high electrolyte or H^+-concentrations the ζ-potential reaches values close to zero.

The ζ-potentials were converted to charge densities behind the electrokinetic shear plane (σ_ζ), using the Gouy-Chapman theory and assuming no influence of surface conductivity. In general PS-particles behave as expected without discrepancies between experiment and theory: $|\sigma_0|$ is larger than $|\sigma_\zeta|$. For one particular latex, however, a $|\sigma_\zeta|$ larger than $|\sigma_0|$ was found. This fact was attributed to chemisorption of NO_3^- ions. Chemisorption of NO_3^--ions is not a common fact, but may be attributed to the pronounced hydrophobic character of the PS-particles.

3.1 Introduction

Monodisperse Polystyrene (PS) particles are widely used as model colloids for e.g. adsorption studies. Aqueous PS-latices are usually prepared by an emulsion polymerization. The emulsion polymerization can be performed either with a surfactant or without an intentionally added surfactant ("soap-free" or emulsifier-free polymerization). The surfactant-free emulsion polymerization has the advantage, that the only charged groups present on the PS-latex surface are sulphate groups, arising from the initiator fragments. The preparation of PS-particles by surfactant-free emulsion polymerization is well described [1]-[5]. The particle size of these latices is usually below 1 μm, when prepared by a one-step surfactant-free emulsion polymerization. Recently, we described a method to obtain particle sizes up to 3.2 μm in a one-step surfactant-free emulsion polymerization [6].

However, it has been reported that the model PS-particles have an anomalous electrokinetic behaviour. Theoretically it is expected, that if there is no chemisorption of ions present, an increasing electrolyte concentration at a constant pH should lead to a continuous decrease in the absolute value of the electrophoretic mobility or zeta-potential (ζ), because of compression of the electric double layer. This decrease is indeed observed, but only at rather high electrolyte concentrations (> 0.01 M) [7]. As the electrolyte concentration is increased from low to high concentrations, the electrophoretic mobility (or the zeta-potential calculated from it) first increases in absolute value and it decreases only when a certain electrolyte concentration is surpassed. The zeta-potential versus electrolyte concentration curves therefore exhibit a maximum in absolute value. This phenomenon has been observed by many authors [7]-[22]. The observed maximum is explained by the hairy layer model, the co-ion adsorption model [7], [16]-[19] or by surface conductivity [22].

The hairy layer model assumes that the latex particle is covered by a layer of protruding, rather flexible, polymer chains ("hairs") having terminal end groups (the sulphate groups introduced by the initiator fragments) [7]-[15]. As the ionic strength decreases the repulsion between these charged groups increases and the hairy layer expands. This results in the slipping plane moving outwardly and the net charge transported electro-kinetically decreases.

The co-ion adsorption model assumes, in the case of negatively charged particles, that anions, which are less hydrated than cations, are closer to the apolar surface [7],[16]-[19]. These anions are not believed to be chemisorbed on specific sites and the magnitude of the electrokinetic potential depends on the valency of the co-ions.

In the surface conductivity model, the presence of mobile Stern-layer anions causes the mobility to decrease and the conductivity to increase, in comparison with the case where surface conductivity is absent [22]. According to this model, not only the diffuse double layer contributes to the surface conductance, but also a process of additional conductance between slipping plane and particle interface is operative.

It is obvious that there seems to be a controversy about the explanation of the electrokinetic behaviour of the PS-latices. In this chapter the electrophoretic properties of the PS-particles, described in chapter 2, are investigated. By varying the particle size of

these latex particles, κa values larger than 10 are reached (where κ is the Debye-Hückel parameter and a is the particle radius). For these κa values the theory for calculating ζ-potentials from measured mobilities [23] is reliable, as long a surface conductivity can be neglected. The PS-particles are prepared by a one step surfactant-free emulsion polymerization. In this way PS-particles are obtained with a uniform surface composition.

3.2 Experimental

3.2.1 Materials

Water was twice distilled from an all glass apparatus. The specific conductance (0.8 μS cm^{-1}) and the surface tension (72 mN/m) of this water indicated that it was free of surface active impurities.

Sodium nitrate, potassium nitrate, sodium hydroxide and nitric acid (Titrisol) were obtained from Merck (*pro analysi*, purity > 99%) and used without purification.

The ion exchange resins DOWEX 50W-X4 (H$^+$-form) and DOWEX 1-X4 (OH$^-$-form) were obtained from Fluka and purified as described by Van den Hul and Vanderhoff [24].

3.2.2 Latices

The preparation of the latices used is described elsewhere [6]. The particle size of the latices are listed in table 2.2 and 2.3 in chapter 2.

3.2.3 Cleaning of the latices

All latices were dialysed by the serum replacement technique as described by Vanderhoff et al. [25] and Ahmed et al. [26] in Amicon serum replacement cells. For a description of the dialysis cells see [26].

The latex was first diluted to a solid content less than 5 percent (w/v) with twice-distilled water. Then a volume of 300 cm^3 of the latex was placed in the stirred cell. This cell was equipped with a Nucleopore membrane (Poretics Corporation, USA) with a pore size approx. 10-20% smaller than the particle size of the latex. Then a continuous stream of twice-distilled water was flown through the cell until the conductivity of the outlet water reached the same value as that of the inlet twice-distilled water (0.8 μS cm^{-1}).

Normally this took about 24 hours. All the dissolved electrolyte had then been removed

and then the latex was removed from the cell. This procedure was applied to all samples of latex.

3.2.4 Determination of solids content
The solids percentage of the different PS-latices were determined by drying a known amount of the latex in an oven at 105 °C, until constant weight was reached.

3.2.5 Latex titration
3.2.5.1 Conditioning of the ion-exchange resins
The ion-exchange resins used in this study were the DOWEX 50W$\times$X4 (cation exchange, H$^+$-form) and the DOWEX 1$\times$X4 (anion exchange, OH$^-$-form). These ion-exchange resins were separately cleaned according to the same procedure as described by Van den Hul and Vanderhoff [24].

After the cleaning procedure the wash water of the ion-exchange resins exhibited no surface active impurities (surface tension 72 mN/m at 20 °C) and the conductivity of the wash water had the same value as the inlet water used (0.8 μS cm^{-1}).

Equal quantities of the two ion-exchange resins were then mixed together. The wash water from the mixed resin had a considerably lower conductivity (0.25 μS cm^{-1}) than the water used.

3.2.5.2 Preparation of the latices in the H$^+$-form
The freshly cleaned latices (by the serum replacement technique) were diluted with ion-exchanged water to a solids percentage lower than 5% and were transferred into a pyrex glass bottle with a large amount of mixed ion-exchange resin. The bottles were placed on a roll-bank and were rolled for 3 to 24 hours. At specific times (3, 6, 9 and 24 hours) samples were taken to be analyzed by conductometric titration.

Latex and ion-exchange resin were, after their contact, separated by decantation followed by filtration through a glass-filter.

3.2.5.3 Conductometric titration procedure
Conductometric titrations of the ion-exchanged latices were performed at 20 °C under a

nitrogen atmosphere. The solid content was always low (1-2 % w/v). The conductivity was measured using a conductivity meter (Radiometer Kopenhagen) equipped with a Schott conductivity cell. A 2.1 mM NaOH-solution (nitrogen flushed) was added with a constant rate pump (LC-5000 syringe pump, ISCO). The change in conductivity was continuously monitored using a computer.

The influence of the rate of adding NaOH-solution on the titration was checked for several rates (0.1 to 40 ml/hour), but no difference was found for the endpoint of the conductometric titration. Therefore a moderate rate of 15 ml/hour was chosen. A typical titration curve (specific conductivity κ_c versus quantity of NaOH-solution added) is shown in figure 3.1.
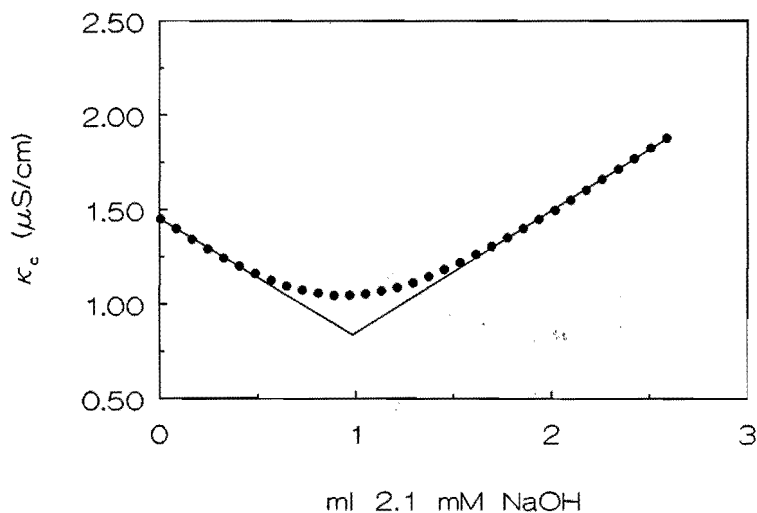
Figure 3.1: Change in specific conductivity (κ_c) versus added volume 2.1 mM NaOH-solution for the conductometric titration of latex L-78.

The samples of the latices (taken after various ion-exchange times) were titrated three to four times and the average value was used. When the determined endpoints, obtained after different ion-exchange times, were the same (within experimental error), this was

assumed to be the endpoint. This endpoint was always reached within 4 ion-exchange cycles. The endpoint (assuming complete dissociation of charged groups at the end of the conductometric titration and complete charge compensation of the charged groups by H^+ at the start of the titration) was then converted to the surface charge (σ_0) and the area per negative charge (A_n) assuming a quadratic arrangement of charged sites on the particle surface. This is shown in figure 3.2 for latex L-78 (as an example) and also in table 3.1.
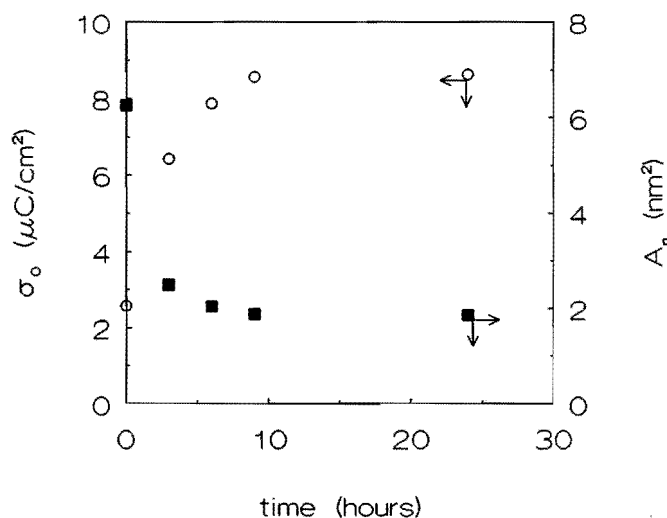
Figure 3.2: *Change in surface charge density (σ_0) and area per negative group (A_n) versus time for the ion-exchange cycles of latex L-78. "Time" is the duration of the ion-exchange process.*

3.2.6 ζ-Potential measurements

ζ-Potential measurements were performed using a Malvern Zetasizer 3 (Malvern Instruments, Malvern, England) equipped with an AZ-4 cell. This apparatus uses the Laser-Doppler effect to measure the electrophoretic mobility. The latices used were the ion-exchanged PS-latices in the H^+-form. In case of measuring the ζ-potential as function of pH the electrolyte used was either potassium nitrate or sodium nitrate and nitric acid was used to set the pH to the desired value.

Table 3.1: Change in σ_0 and A_n with ion-exchange cycles for latex L-78.

time (hours)	σ_0 ($\mu C/cm^2$)	A_n (nm^2)
0	2.57	6.26
3	6.43	2.50
6	7.87	2.04
9	8.56	1.88
24	8.63	1.86

3.3 Results and discussion

3.3.1 Latex titration

In table 2.2 and 2.3 in chapter 2 the particle sizes of the latices are listed. As can be seen from table 2.2 and 2.3 the particle sizes of the latices are fairly monodisperse (indicated by $P_n = D_v/D_n$). Particles are often called monodisperse if the value of P_n is < 1.05. This is especially the case for the larger particles.

In figure 3.1 can be seen, that both the descending and ascending legs of the plot of conductivity versus quantity of NaOH-solution added are linear, with the exception of a region near the intersection point, which means that only one type of surface groups is observed. This was found for all latices investigated.

The charged surface groups are in origin sulphate groups ($-SO_4^-$) [27], but carboxyl ($-COO^-$) groups have also been reported [4],[28],[29] originating from oxidation of inter-mediate alkanol groups. In the polymerization procedure the so-called Kolthoff reaction can occur [30], resulting in the loss of sulphate groups and the appearance of hydroxyl ($-OH$) groups. These hydroxyl groups can be present at the PS-water interface as non-charged groups. The Kolthoff reaction can be suppressed by using $KHCO_3$ as supporting electrolyte [31]; however this was considered not to be necessary in view of the titration data (see later).

The chemical instability of the PS-particles, prepared by using $K_2S_2O_8$ as initiator, has also become apparent from other studies (see e.g. Hearn et al. [30]). The PS-latices may loose their sulphate groups upon storage by hydrolysis of the sulphate groups [31],[32]. The rate of hydrolysis appears to vary widely. Goodall et al. [33] e.g. found rates of

hydrolysis varying from 2% to 37% per month (at 25 °C), whereas Vanderhoff [34] reports the complete loss of sulphate groups of an ion-exchanged latex in 14 days. Most reports only mention the removal of the sulphate groups upon storage as a result of hydrolysis. Vanderhoff [34] and Goodall et al. [33] observed the appearance of weak acid groups.

From this literature survey, it is obvious that the preparation and handling of the PS-particles can have a large influence on the surface charge groups present. The PS-particles used in this study were titrated nine months after preparation. The fact, that only one type of acid group could be detected, might suggest that only weak acid groups are present. It is, however, difficult to deduct which type of acid groups at the PS-surface is detected by conductometric titration. The additional presence of surface hydroxyl groups is, of course, not excluded.

In figure 3.2 and table 3.1 the change in surface charge (σ_0) and the area per surface charge group (A_n) with ion-exchange time for latex L-78 is shown as an example. The increase in σ_0 and thus decrease in A_n vanishes after the third ion-exchange cycle (after 9 hours). Further ion-exchange does not lead to an increase in σ_0. A possible explanation for this could be, that the ion-exchange resin is exhausted. The amount of ion-exchange resin was, however, large and using an excess of fresh ion-exchange resin did not result in a change in σ_0. When treating tap water with the used ion-exchange resin the conductivity decreased to values as described before. The fact, that the conductivity of the wash water from the used ion-exchange resin was still as low as before the titration, supports the fact that the obtained value for σ_0 is the correct one.

In figure 3.3 and table 3.2 the determined values of σ_0 and A_n are given, together with the particle sizes of the latices. From figure 3.3 and table 3.2 it can be seen, that the surface charge density measured increases slightly and the area per negative charge decreases slightly with increasing particle size. The only exception in this respect is latex L-78, which was made by a different polymerization procedure (in a different reactor) [6]. The surface charge of latex L-78 is almost as high as that of latex L-89, but the particle size of latex L-89 is more than 4 times larger than latex L-78. This means that the polymerization procedure can have a large influence on the final latex.
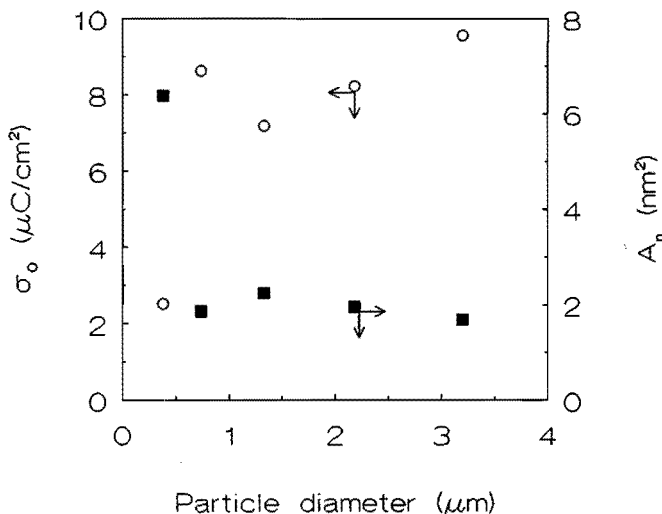
Figure 3.3: The final determined surface charge densities (σ_0) and area per negative group (A_n) for the different particle sizes used.

Table 3.2: Final σ_0 and A_n after ion-exchange for all latices.

latex	D_n (nm)	σ_0 ($\mu C/cm^2$)	A_n (nm^2)
L-80	381	2.52	6.14
L-78	736	8.63	1.86
L-86	1224	7.18	2.24
L-88	2018	8.23	1.95
L-89	3166	9.56	1.68

3.3.2 Electrophoresis

In figure 3.4 the dependence of the electrophoretic mobility (E_m) on the concentration of HNO_3 is shown for the different latices used. In these experiments, the latices were in the H^+-form. As can be seen from figure 3.4 the electrophoretic mobilities of all latices show a maximum at a concentration of about 10^{-3} M. The electrolyte, HNO_3, provides H^+ as potential determining ion.

The latices used have acid groups, either sulphate or carboxyl groups. The sulphate groups have a pK_a in the range 1 to 2 [35]. Clint et al. [36] observed independence of electrophoretic mobility on pH between pH 4.3 and pH 9 in 10^{-2} M KNO_3, suggesting the presence of $-SO_4^-$-groups only. Ottewill and Shaw [37] reported pK_a-values of carboxyl groups between pH 4 and pH 6. When the pH is raised from pH 4.6 to pH 6 this would cause a steady increase in electrophoretic mobility up to pH 6.

The measurements presented in figure 3.4 show, that even when the HNO_3 concentration is raised to 10^{-3} M (pH $\approx$ 3) the electrophoretic mobility still increases. At a pH of 3 any carboxyl groups present are certainly not fully dissociated.
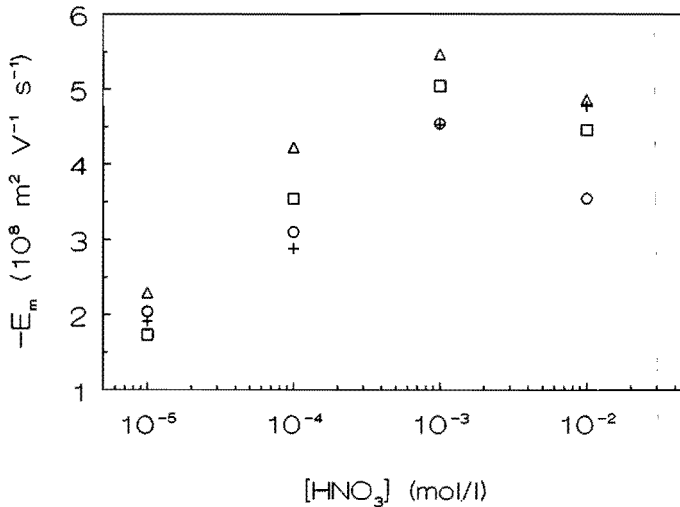
Figure 3.4: Electrophoretic mobility (E_m) versus concentration of HNO_3 for different latices; ○ latex L-78, + latex L-80, □ latex L-86, △ latex L-89.

The decrease in electrophoretic mobility at concentrations higher than 10^{-3} M HNO_3 is too pronounced to be due to a shift of the dissociation equilibria of charged groups ($-SO_4^-$ and $-CO_2^-$) and can best be explained by the larger H^+-ion concentration leading to more counterions being present, resulting in a reduction of the net charge behind the slipping plane. A similar maximum in electrophoretic mobility was found by Voegtli and Zukoski

[16] on measuring their PS-particles in HCl and HClO$_4$. Their PS-latices also did not contain any carboxyl groups detectable by conductometric titration. The maximum was, however, found at a concentration of 10^{-2} M. Comparing their results with ours, we can conclude that our latices contain no detectable carboxyl groups, but only -SO$_4^-$-groups.

The measured electrophoretic mobilities were converted to ζ-potentials by using the equations of Ohshima et al. [23]. These equations are an approximation of the numerical results obtained by O'Brien et al. [38], which are valid with neglect of the possibility of contribution to conductance by ions behind the electrokinetic slipping plane. The equations of Ohshima are valid for $\kappa a > 10$ (where κ is the reciprocal double layer thickness and a is the particle radius). The difference between Ohshima's approximate equations and O'Brien's exact numerical result for $\kappa a > 10$ is smaller than 1%. The κa-values for the different PS-particles and the different salt concentrations used in the present investigation are larger than 10 and the equations of Ohshima can therefore be used safely, in the absence of electrical conductance behind the electrokinetic shear plane.

In figure 3.5 the dependence of the ζ-potential of the latices used on the concentration of NaNO$_3$ at pH 5.5 is shown. About the absolute value of the ζ-potential the following remarks can be made.

At a pH of 5.5 the charged surface groups can be assumed to be fully dissociated. As can be seen from figure 3.5 the $|\zeta|$-potential exhibits also a maximum, as was also shown for the electrophoretic mobility dependence on the HNO$_3$ concentration. Under these circumstances a maximum in electrophoretic mobility leads to a maximum in $|\zeta|$. The maximum is found at a concentration of about $6*10^{-3}$ M NaNO$_3$.

Measuring the electrophoretic mobility (and calculating the ζ-potential) of the latices in a different salt (KNO$_3$) gives approximately the same results, as shown in figure 3.6. Although the cations are different (Na$^+$ versus K$^+$) the measured ζ-potentials again show a maximum at a concentration of about $6*10^{-3}$ M KNO$_3$. However, the value of the maximum of the $|\zeta|$ for the latices used is higher when using KNO$_3$.

The nature of the cation has an effect on the value of the ζ-potential, but the maxima are found at approximately the same electrolyte concentration. An explanation for this behaviour is the size of the cations. The molar conductivity at infinite dilution of Na$^+$ is lower than that of K$^+$, because the radius of a hydrated Na$^+$ is larger than that of K$^+$.
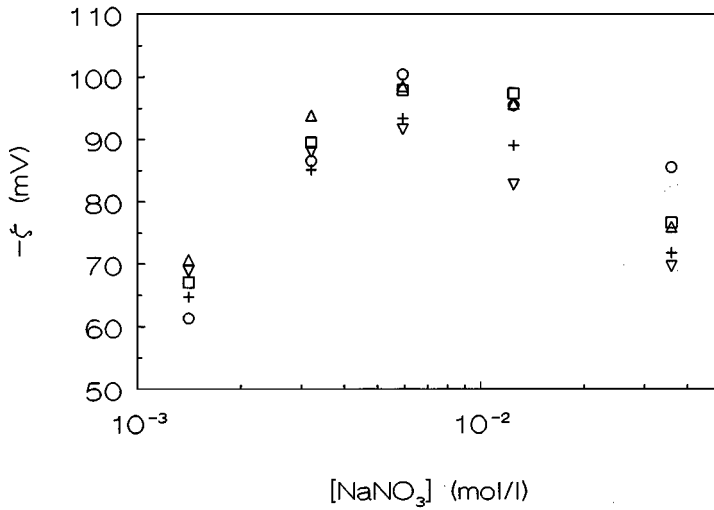
Figure 3.5: Zeta-potential (ζ) versus NaNO₃-concentration for different latices at pH 5.5; ○ latex L-78, + latex L-80, □ latex L-86, ▽ latex L-88, △ latex L-89.
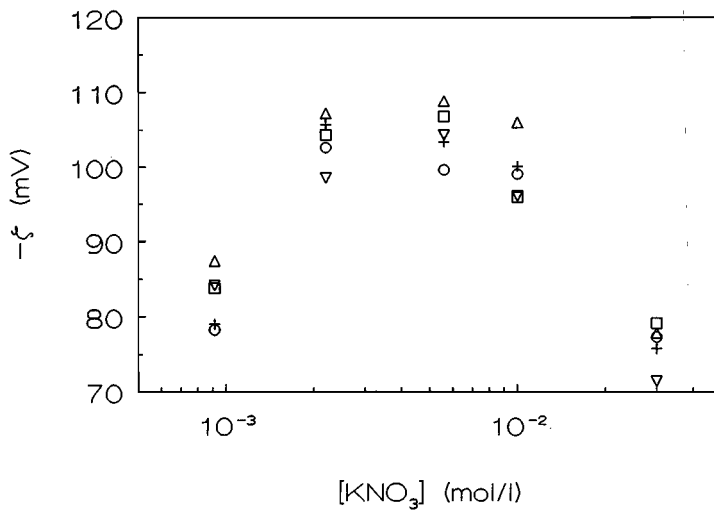
Figure 3.6: Zeta-potential (ζ) versus KNO₃-concentration for different latices at pH 5.5; ○ latex L-78, + latex L-80, □ latex L-86, ▽ latex L-88, △ latex L-89.

Between the PS-particle surface and the electrokinetic shear plane a larger amount of K^+-ions can be present than for Na^+ and consequently the effective charge is lower for K^+ than for Na^+. This behaviour is shown in figure 3.7 for latex L-86 as an example. As can be seen from figure 3.7 the maximum in $|\zeta|$ is found at a somewhat higher concentration in KNO_3 than in $NaNO_3$ solutions. A similar behaviour was found for positively charged latices in different electrolytes by Hidalgo Alvarez et al. [13]. The location of the maximum in the electrophoretic mobility versus electrolyte concentration curve depended on the nature of the counterion in their measurements. At concentrations below $6*10^{-3}$ M the $|\zeta|$ of latex L-86 in $NaNO_3$ is considerably higher than in KNO_3. This behaviour can be explained by the difference in radius of the hydrated cations. However at concentrations higher than $6*10^{-3}$ M (both $NaNO_3$ and KNO_3) the $|\zeta|$-values are similar (within experimental error) at the same concentration.
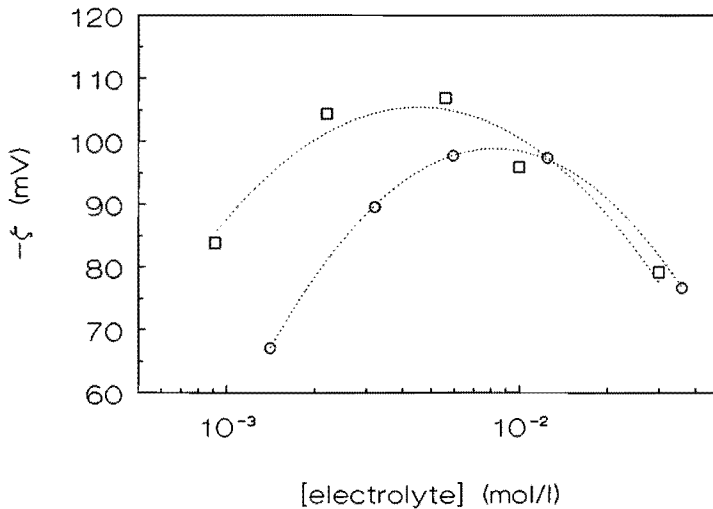
Figure 3.7: Zeta-potential (ζ) versus electrolyte concentration for latex L-86 at pH 5.5; ○ electrolyte KNO_3, □ electrolyte $NaNO_3$; the lines are just a guide to the eye.

Having established the behaviour of the latices in different electrolyte solutions at pH 5.5, we now will present the behaviour of the latices in at different pH-values in $NaNO_3$- or

KNO$_3$- solutions of 3.3*10^{-2} M. For changing the pH a HNO$_3$-solution was used. At pH-values larger than 2.5 the concentration of Na$^+$- or K$^+$-ions is much larger than the concentration of H$^+$-ions. At the lowest pH-value used (pH 2) the concentrations of the different cations are rather equal.

In figure 3.8 the $|\zeta|$ of the latices in 3.3*10^{-2} M KNO$_3$ at different pH-values is shown. The concentration of 3.3*10^{-2} M KNO$_3$ is higher than the concentration (6*10^{-3} M) where the maximum occurs at pH = 5.5 (see figure 3.7). As can be seen from figure 3.8, $|\zeta|$ is almost constant in the pH range from 6 to 4, which can be expected, when there are only strong acid groups present at the PS-surface. It is obvious, that only at pH 2 a significant decrease in $|\zeta|$ is seen. At this pH the $|\zeta|$ of all latices investigated is the same (within experimental error), although their surface charge densities varies from 2.52 to 9.56 μC/cm^2. Latex L-78, however, shows a more steady decrease in $|\zeta|$ going from pH 6 to pH 2. This could possibly be due to the presence of weak acid (carboxyl) groups. These groups were, however, not detected by the conductometric titrations.
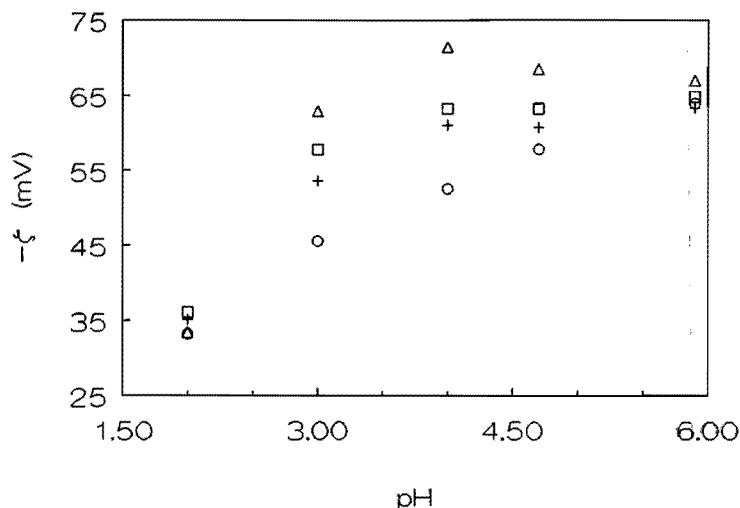
*Figure 3.8: Zeta-potential (ζ) versus pH for different latices at [KNO$_3$] = 3.3*10^{-2} M; ○ latex L-78, + latex L-80, □ latex L-86, △ latex L-89.*

At a concentration of $3.3*10^{-2}$ M NaNO$_3$ and varying pH-values a different picture is found, which is shown in figure 3.9. The constant decrease with decreasing pH of the $|\zeta|$ of latex L-78 has disappeared. The $|\zeta|$-values of all latices have a constant value (within experimental error) in the pH-range 6 to 4. From pH 4 to pH 2 a decrease in $|\zeta|$ is seen. At pH 2 the $|\zeta|$-values of the latices are still the same (within experimental error), as was the case for KNO$_3$. It is again noted that the $|\zeta|$ is larger in NaNO$_3$- than in KNO$_3$-solutions for the latices studied.
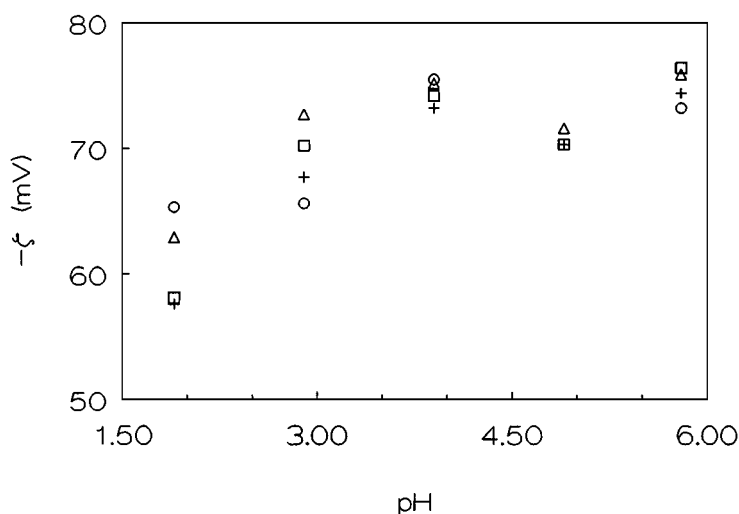
Figure 3.9: Zeta-potential (ζ) versus pH for different latices at [NaNO$_3$] = $3.4*10^{-2}$ M; ○ latex L-78, + latex L-80, □ latex L-86, △ latex L-89.

The $|\zeta|$-values of latex L-80 in $3.3*10^{-2}$ M KNO$_3$ and NaNO$_3$ at different pH-values are shown in figure 3.10 as an example. In this figure it can be seen that the $|\zeta|$-values for latex L-80 are higher in NaNO$_3$ than in KNO$_3$ over the whole pH-range. This difference in $|\zeta|$ for latex L-80 seems not to strongly depend on pH over the whole pH-range studied.
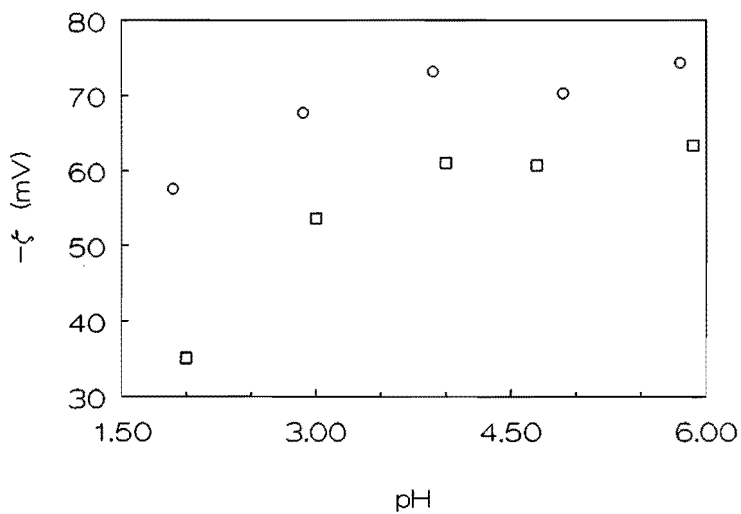
Figure 3.10: *Zeta-potential (ζ) versus pH latex L-80 for different electrolytes;*
○ [NaNO$_3$] = 3.4*10^{-2} M, □ [KNO$_3$] = 3.3*10^{-2} M.

3.3.3 Double layer characteristics

Conversion of the zeta-potential into the charge density behind the electrokinetic shear plane and comparing this value to the surface charge density, gives information on the charge distribution in the electrical double layer. For high κa-values the Gouy-Chapman theory (see e.g. Hunter [39]) for flat double layers, gives the following conversion:

$$\sigma_\zeta = -\sqrt{8000 \ c\epsilon_0\epsilon_r N_A kT} \ \sinh\left(\frac{ze_0\zeta}{2kT}\right) \tag{3.1}$$

where c is the bulk-concentration of ions (moles/liter), N_A is Avogadro's number, ϵ_0 is the permittivity of vacuum, ϵ_r is the solvent dielectric constant, z is the valency, e_0 is the elementary charge, ζ is the zeta-potential, k is Boltzman's constant and T is the temperature.

The difference between the surface charge density and the charge density behind the electrokinetic shear plane is the charge density in the Δ-layer (the distance between the surface of the latex particle and the electrokinetic shear plane). This can be calculated using the following equation:

$$\sigma_\zeta + \sigma_\Delta + \sigma_0 = 0 \tag{3.2}$$

where σ_ζ is the charge density behind the electrokinetic shear plane (calculated assuming absence of contribution to surface conductance by ions behind the electrokinetic slipping plane), σ_Δ is the charge density in the delta layer and σ_0 is the surface charge density.

In figure 3.11 the surface charge density of latex L-78 and the charge density at the electrokinetic shear plane at different concentrations of the electrolytes $NaNO_3$ and KNO_3 at a pH of 5.5 is shown as an example. This picture is found for all latices, except latex L-80. At this pH the charged groups at the PS-surface are fully dissociated. At low electrolyte concentrations the charge densities at the electrokinetic shear plane (ζ-plane) for both electrolytes used is the same. Only at rather high electrolyte concentrations the surface charge density at the ζ-plane is lower in KNO_3 than in $NaNO_3$. At these high concentrations, a large part of the surface charge is compensated by cations behind the electrokinetic shear plane.
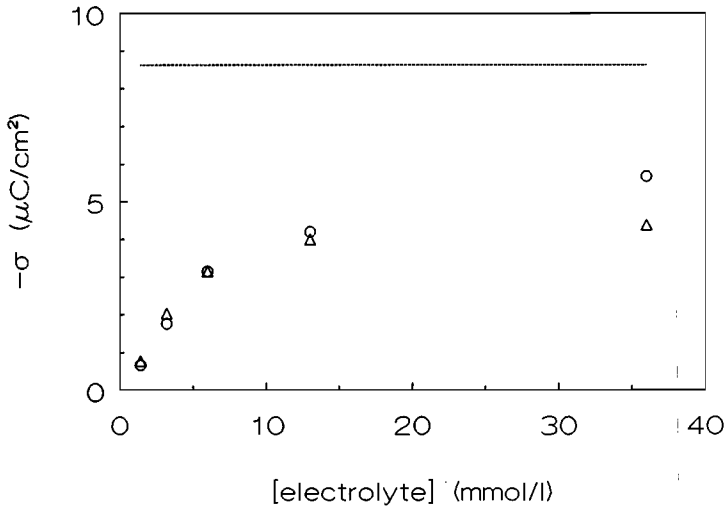
Figure 3.11: σ_0 and σ_ζ for latex L-78 at pH = 5.5; dashed line σ_0, ○ σ_ζ for NaNO$_3$ as electrolyte, △ σ_ζ for KNO$_3$ as electrolyte.
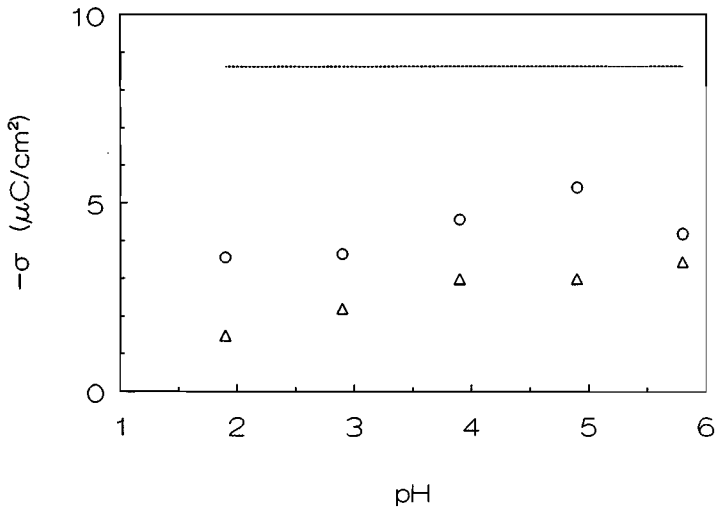
Figure 3.12: σ_0 and σ_ζ for latex L-78 at different pH-values; dashed line σ_0, ○ σ_ζ for [NaNO$_3$] = 3.4×10^{-2} M, △ σ_ζ for [KNO$_3$] = 3.3×10^{-2} M.

In figure 3.12 the σ_ζ and σ_0 for latex L-78 at different pH-values in $NaNO_3$- and KNO_3-solutions of $3.4*10^{-2}$ mol/l and $3.3*10^{-2}$ mol/l resp. are shown. At these high electrolyte concentrations, the calculated value of σ_ζ shows a very small decrease going from pH 6 (fully dissociated) to pH 2 (incompletely dissociated acid groups). In this case, also the values in $NaNO_3$-solution are higher than in KNO_3-solution, as was shown in the previous section. In both cases the same trend can be observed.

In most cases investigated here, $|\sigma_0|$ is larger than $|\sigma_\zeta|$ as appears to be obvious. However, in one case $|\sigma_\zeta|$ is larger than $|\sigma_0|$ (latex L-80). A possible source of error is, that during ion-exchange of latex L-80 not all the Na^+ are converted to H^+. However both repeated ion-exchange cycles for latex L-80 and titration gave the same results. This suggests, that the ion-exchange process and the titration can not be regarded as a source of error. In addition, duplicate electrophoresis experiments also gave the same results.

Similar cases of $|\sigma_\zeta| > |\sigma_0|$ have been reported by Ma et al. [40]. These authors even found negative ζ-potentials on Polystyrene particles in the absence of any titratable surface charge. Abramson [41] also reported negative ζ-potentials for paraffin wax in KNO_3-solution. The only way to account for this phenomenon, as far as we see, is to assume chemisorption of NO_3^- ions.

This is surprising, since NO_3^- ions are usually assumed to be inert. This is based on experiments with other surfaces, e.g. of oxides or AgI. However, in the case of surfaces with a pronounced hydrophobic character such as Polystyrene, the situation may be different, as remarked by Voegtli and Zukoski [16].

The chemisorption of NO_3^- ions in the case at hand may be ascribed to the pronounced hydrophobic character of the PS-particles concerned. The difference with other PS-particles may tentatively be thought to be connected with the different circumstances present during the preparation of the latex concerned.

Figure 3.13 shows σ_Δ, at various constant σ_0 values, as a function of $NaNO_3$ concentrations. It is seen, that in all cases the net charge between the phase boundary and the electrokinetic slipping plane shifts in the negative direction. Although the discussion is concerned with the electrolyte $NaNO_3$, the same observations and conclusions can be made for the electrolyte KNO_3.
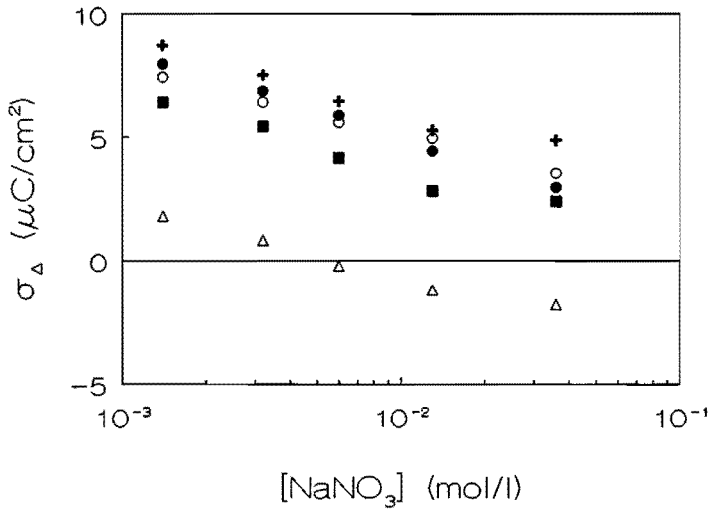
Figure 3.13: Change in σ_Δ versus [NaNO$_3$] at pH 5 for the different latices investigated: ● latex L-78, △ latex L-80, ■ latex L-86, ○ latex L-88, + latex L-89.
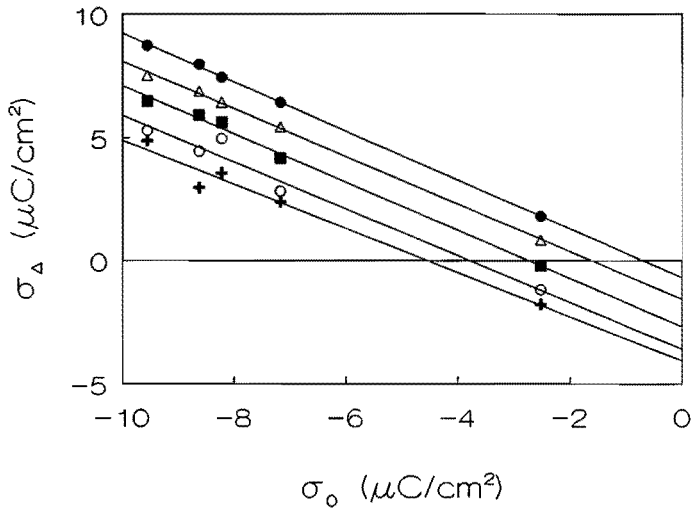
Figure 3.14: Change in σ_Δ versus surface charge density (σ_0) at pH 5.5 at different [NaNO$_3$]: ● $1.4*10^{-3}$ M, △ $3.2*10^{-3}$ M, ■ $6.0*10^{-3}$ M, ○ $1.3*10^{-2}$ M, + $3.6*10^{-2}$ M.

Figure 3.14 shows σ_Δ as function of σ_0 in various [NaNO$_3$]. It is seen, that in all cases straight lines are obtained, with slopes almost equal to each other. These pictures were also found for the other different experimental conditions.

The interpretation of the σ_Δ values starts from the following facts:

1) σ_Δ is, at constant [NaNO$_3$], within experimental error a decreasing linear function of σ_0 (see figure 3.14);

2) $d\sigma_\Delta/d\sigma_0$ decreases with increasing [NaNO$_3$], starting from a value for $d\sigma_\Delta/d\sigma_0$ slightly lower than 1 for [NaNO$_3$] close to 0 (see figure 3.15). This decrease is not very pronounced, however, being confined within the limits 1 and 0.89 in the range of experimental data available.

3) σ_Δ is, at constant σ_0 a non-linear decreasing function of [NaNO$_3$]; it is approximately a linear function of log [NaNO$_3$] (see figure 3.13).

4) $d\sigma_\Delta/d(\log$ [NaNO$_3$]) is not a distinct function of σ_0 (see figure 3.16); its average value is -3.21.

These data are compatible with the following mechanism:

In the absence of NaNO$_3$, the whole charge between the particle surface and the electrokinetic slipping plane consists of Na$^+$ ions, which are adsorbed in such quantity as to nearly compensate the charge of the surface groups ($d\sigma_\Delta/d\sigma_0$ is slightly lower than one as the [NaNO$_3$] tends to zero).

The shift of σ_Δ with increasing [NaNO$_3$] is due to chemisorption of NO$_3^-$ ions on positions far from the charged -OSO$_3^-$ groups. This explains the only slight effect of σ_0 on $d\sigma_\Delta/d\sigma_0$, and the absence of a distinct effect of σ_0 on $d\sigma_\Delta/d(\log$ [NaNO$_3$]), as distinct from the phenomena observed both for the adsorption of inorganic ions on CaSiO$_3$ surfaces [42]-[44] and the adsorption of short chain tetra-alkylammonium ions on silica [45].

Places on the PS-surface which are far from the -OSO$_3^-$ groups may be assumed to have a pronounced hydrophobic character, inducing in the nearby solution a hydrophobic hydration. Thus, in the presence of NaNO$_3$ in the solution, the charge between the phase boundary consists of both Na$^+$ and NO$_3^-$ ions; the Na$^+$ ions are attracted by the charged surface -OSO$_3^-$ groups and will be present predominantly in the hydrophilic regions of the surface near the charged groups, the NO$_3^-$ ions are repelled by the negative charge of the surface groups, but are attracted by the hydrophobic parts of the PS-surface, because the

presence of only slightly hydrated NO_3^- ions in a part of the solution which is subject to hydrophobic hydration leads to a decrease of Gibbs free energy.
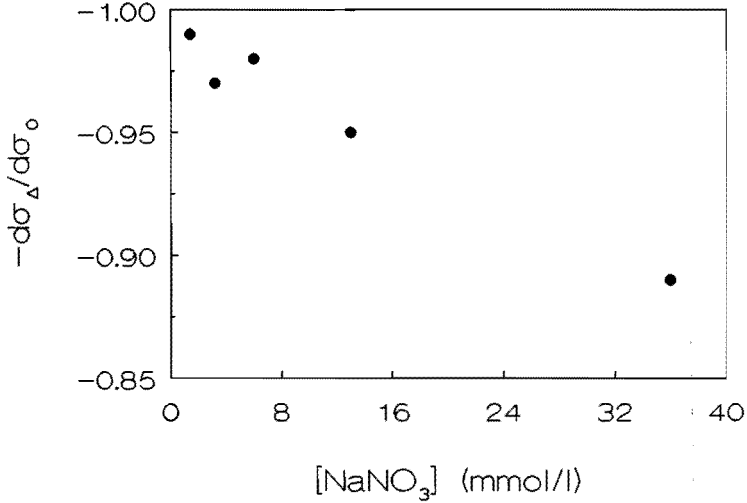
Figure 3.15: *$d\sigma_\Delta/d\sigma_0$ versus [NaNO₃] at pH 5.5, calculated from figure 3.14.*
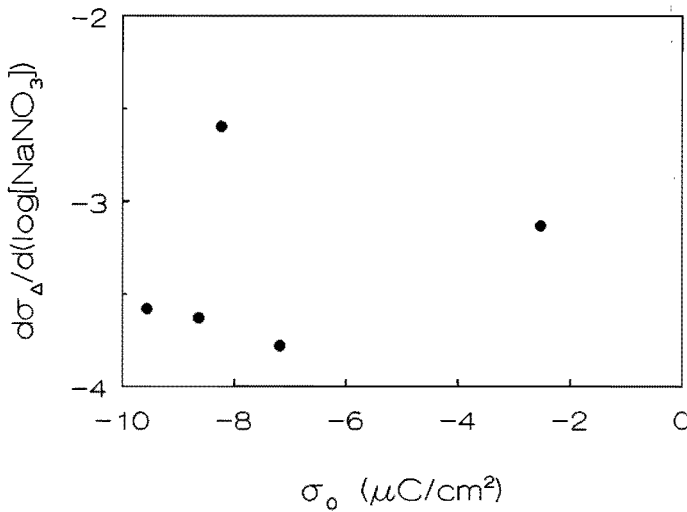
Figure 3.16: *$d\sigma_\Delta/d(log[NaNO_3]$ versus σ_0 at pH 5, calculated from figure 3.13.*

It should be noted that in the results presented here, the influence of surface conductivity is neglected. This process is, if present, only operative at low electrolyte concentrations, resulting in a too low value of $|\zeta|$ calculated from the theory used. This does not, however, influence our results, because $|\sigma_{\zeta}|$ is larger than $|\sigma_0|$ only at high electrolyte concentrations, where the process of surface conductivity is not operative.

The value of $\partial\sigma_\Delta/\partial\sigma_0$ increases with increasing [NaNO$_3$], not only in the region (low electrolyte concentrations) where surface conductivity can be operative, but also at high electrolyte concentrations where $|\zeta|$ is not significantly influenced by the process of surface conductivity.

With increasing $|\sigma_0|$ not only more Na$^+$ ions, but also more NO$_3^-$ ions are adsorbed. This can be understood if $\partial\sigma_\Delta/\partial\sigma_0$ is written as:

$$\frac{\partial\sigma_\Delta}{\partial|\sigma_0|} = e_0\frac{\partial n_{Na}}{\partial|\sigma_0|} - e_0\frac{\partial n_{NO_3}}{\partial|\sigma_0|} \tag{3.3}$$

where n is the number of adsorbed ions.

As

$$\frac{\partial^2\sigma_\Delta}{\partial|\sigma_0|\,\partial[NaNO_3]} < 0 \tag{3.4}$$

this results in:

$$\frac{\partial^2 n_{Na}}{\partial|\sigma_0|\,\partial[NaNO_3]} - \frac{\partial^2 n_{NO_3}}{\partial|\sigma_0|\,\partial[NaNO_3]} < 0 \tag{3.5}$$

The first term of equation (3.5) is positive, this implies that the second term of equation (3.5) must be larger than the first term. This agrees with our remark, that chemisorption takes place.

3.4 Conclusions

In this chapter the electrophoretic properties of the latices, of which the preparation was presented in chapter 2, is described. The latices were characterized by conductometric titration. The charged groups, arising from initiator fragments, were all strong acid groups and no carboxyl groups could be detected. The amount of surface charge groups varies with particles size.

Electrophoresis measurements have shown, that the electrophoretic mobility passes through a maximum as the electrolyte concentration is increased. Converting the electro-phoretic mobility to ζ-potentials gives the same picture. The same phenomenon is observed with increasing H^+-concentration. Only at very high electrolyte or H^+-concentrations the ζ-potential reaches values close to zero.

The ζ-potentials were converted to charge densities behind the electrokinetic shear plane (σ_{ζ}), using the Gouy-Chapman theory and assuming no influence of surface conductivity. In general PS-particles behave as expected without discrepancies between experiment and theory: $|\sigma_0|$ is larger than $|\sigma_{\zeta}|$. For one particular latex, however, a $|\sigma_{\zeta}|$ larger than $|\sigma_0|$ was found. This fact was attributed to chemisorption of NO_3^- ions. Chemisorption of NO_3^--ions is not a common fact, but may be attributed to the pronounced hydrophobic character of the PS-particles.

3.5 References

(1)   Matsumoto, T., Ochi, A., *Kobunshi Kagaku*, **1965**, *22*, 481.

(2)   Kotera, A., Furasawa, K., Takeda, Y.,*Kolloid-Z. u. Z. Polymere*, **1970**, *239*, 677.

(3)   Kotera, A., Furasawa, K.,Kudo, K. *Kolloid-Z. u. Z. Polymere*, **1970**, *240*, 837.

(4)   Goodwin, J. W., Hearn, J., Ho, C. C., Ottewill, R. H., *Br. Polymer J.*,
      1973, *5*, 347.

(5)   Goodwin, J. W., Hearn, J., Ho, C. C., Ottewill, R. H., *Colloid and Polymer Sci*,
      1974, *252*, 464.

(6)   Tuin, G., Peters, A. C. I. A., Van Diemen, A. J. G., Stein, H. N.,
      J. Colloid Interface Sci., **1993**, *158*, 508; see chapter 2 of this thesis.

(7)   Verdegan, B. M., Anderson, M. A., *J. Colloid Interface Sci.*, **1993**, *158*, 372.

(8) Midmore, B. R., Diggins, D., Hunter, R. J., *J. Colloid Interface Sci.*, **1989**, *129*, 153.

(9) Chow, R. S., Takamura, K., *J. Colloid Interface Sci.*, **1988**, *125*, 226.

(10) Midmore, B. R., Hunter, R. J.,, *J. Colloid Interface Sci.*, **1988**, *122*, 521.

(11) Brouwer, W. M., Zsom, R. L. J., *Colloids Surfaces*, **1987**, *24*, 195.

(12) Van den Hoven, Th. J. J., Bijsterbosch, B. H., *Colloids Surfaces*, **1987**, *22*, 187.

(13) Hidalgo Alvarez, R., De las Nieves, F. J., Van der Linde, A. J., Bijsterbosch, B. H., *Colloids Surfaces*, **1986**, *21*, 259.

(14) Goff, J. R., Luner, P., *J. Colloid Interface Sci.*, **1984**, *99*, 468.

(15) Van der Put, A. G., Bijsterbosch, B. H., *J. Colloid Interface Sci.*, **1983**, *92*, 499.

(16) Voegtli, L. P., Zukoski, C. F., *J. Colloid Interface Sci.*, **1991**, *141*, 92.

(17) Elimelech, M, O'Melia, C., *Colloids Surfaces*, **1990**, *44*, 165.

(18) Zukoski, C. F., Saville, D. A., *J. Colloid Interface Sci.*, **1986**, *114*, 32.

(19) Zukoski, C. F., Saville, D. A., *J. Colloid Interface Sci.*, **1986**, *114*, 45.

(20) Zukoski, C. F., Saville, D. A., *J. Colloid Interface Sci.*, **1985**, *107*, 322.

(21) Bensley, C. N., Hunter, R. J., *J. Colloid Interface Sci.*, **1983**, *92*, 448.

(22) Van der Linde, A. J., Bijsterbosch, B. H., *Croatica Chemica Acta*, **1990**, *63(3)*, 455.

(23) Ohshima, H., Healy, T. W., White, L. R., *J. Chem. Soc., Faraday Trans. 2*, **1983**, *73*, 1613.

(24) Van den Hul, H. J., Vanderhoff, J. W., *J. Electroanal. Chem.*, **1972**, *37*, 161.

(25) Vanderhoff, J. W., Van den Hul, H. J., Tausk, R. J. M. and Overbeek, J. Th. G., in *Clean Surfaces: Their preparation and characterization for interfacial studies*; Goldfinger, G., Ed., Marcel Dekker, Inc, New York, **1970**, p. 15.

(26) Ahmed, S. M., El-Aasser, M. S., Pauli, G. H., Poehlein, G. W., Vanderhoff, J. W., *J. Colloid Interface Sci.*, **1980**, *73(2)*, 388.

(27) Van den Hul, H. J., Vanderhoff, J. W., *Br. Polym. J.*, **1970**, *2*, 121.

(28) Stone-Masui, J., Watillon, A., *J. Colloid Interface Sci.*, **1975**, *52*, 479.

(29) Laaksonen, J., Lebell, J. C., Stenius, P., *J. Electroanal. Chem.*, **1975**, *64*, 207.

(30) Kolthoff, I. M., Miller, I. K., *J. Amer. Chem. Soc.*, **1955**, *73*, 3055.

(31) Hearn, J., Wilkinson, M. C., Goodall, A. R., *Adv. Colloid Interface Sci*, **1981**, *14*, 173.

(32) Furasawa, K., *Bull. Chem. Soc. Jpn*, **1982**, *55*, 48.

(33) Goodall, A. R., Hearn, J., Wilkinson, M. C., *J. Polym. Sci., Polym. Chem. Ed.*, **1979**, *17*, 1019.

(34) Vanderhoff, J. W., *Pure Appl. Chem.*, **1980**, *52*, 1263.

(35) James. R. O., in *Polymer Colloids*; Buscall, R., Corner, T., Stageman, J. F., Eds., Elsevier, Amsterdam, **1985**, p. 69-104.

(36) Clint, G. L., Clint, J. H., Corkill, J. M., Walker, T., *J. Colloid Interface Sci*, **1973**, *44*, 121.

(37) Ottewill, R. H., Shaw, J. N., *Kolloid-Z. Z. Polym*, **1967**, *218*, 34.

(38) O'Brien, R. W., White, L. R., *J. Chem. Soc., Faraday Trans. 2*, **1978**, *74*, 1607.

(39) Hunter, R. J., *Foundations of Colloid Science, Volume 1*, Clarendon Press, Oxford, **1991**, p. 335.

(40) Ma, C. M., Micalle, F. J., El-Aasser, M. S., Vanderhoff, J. W., in *Emulsion Polymers and Emulsion Polymerization;* Basset, D. R., Hamielec, A. E., Eds., *ACS Symp. Ser.*, **1981**, *165*, p. 251.

(41) Abramson, M. D., *Electrokinetic Phenomena and their Application to Biology and Medicine*, ACS Monograph Series No. 66, Chem. Catalog Co., New York, **1934**.

(42) Siskens, C. A. M., Stein, H. N., Stevels, J. M., *J. Colloid Interface Sci.*, **1975**, *52*, 244.

(43) Van Diemen, A. J. G., Stein, H. N., *J. Colloid Interface Sci.*, **1975**, *67*, 213.

(44) Van Diemen, A. J. G., Stein, H. N., *Science of Ceramics*, **1977**, *9*, 264.

(45) Van der Donck, J. C. J., Vaessen, G. E. J., Stein, H. N., *Langmuir*, **1993**, *9*, 3553.

CHAPTER 4

ADSORPTION OF IONIC SURFACTANT ON POLYSTYRENE PARTICLES IN ABSENCE AND PRESENCE OF COSURFACTANT

Summary: The adsorption of Sodium Dodecylbenzenesulphonate (SDBS) on polystyrene particles was investigated. Monodisperse polystyrene particles were prepared by a one step surfactant-free emulsion polymerization and their particle size varied from 0.4 to 3 µm. The surface charge density varies with particle size. Differences in the surface charge density have an effect on the adsorption behaviour of surfactants at very high surface charge densities only.

The areas per adsorbed SDBS-molecule were determined by Maron's soap titration method and were 50-60 Å² at 22 °C and 60-80 Å² at 60 °C for the latices depending on the surface charge density. The higher areas per adsorbed molecule at higher temperatures are explained by the larger thermal motion of the adsorbed molecules.

The addition of long chain fatty alcohols (cosurfactants) such as dodecanol or cetylalcohol influences the adsorption behaviour of the surfactants. When adding the alcohols at low cosurfactant/surfactant ratios there is only little influence, whereas at higher ratios the average area per adsorbed molecule of SDBS decreases sharply.

This is explained by the fact that when adding alcohols there is a positive attraction between the tails of surfactant and alcohol, without simultaneously introducing additional repulsion through negatively charged groups. This positive effect is more pronounced at larger ratios of cosurfactant/surfactant than at lower ratios. At higher temperatures smaller average areas per adsorbed SDBS molecule are found.

4.1 Introduction

During emulsion polymerization reactions, the surfactant used plays an important role. It emulsifies the monomer, influences the polymerization rate and morphology of the product and it also stabilizes the formed polymer particles. The adsorption behaviour of ionic surfactants on polymer particles has therefore been investigated extensively [1-10]. The adsorption of ionic surfactants on polymer particles is due to their amphipathic nature: the polar headgroups are bound to the water phase, while the apolar tails are bound by the apolar polymer surface. In a similar way surfactant molecules also are adsorbed at the water-air interface. If an aqueous dispersion of polystyrene (PS) is in contact with a gas phase an equilibrium of surfactant molecules adsorbed at the water-air and at the water-polymer interface will be established. The concentration of surfactants in

the water phase can be determined by surface tension measurements, because the surface tension is determined predominantly by the amount of surfactant molecules adsorbed at the water-air interphase. This principle was already used by Maron et al. [1] in their "soap-titration" technique. The addition of surfactant is continued up to a concentration at which the surface tension reaches an almost constant value, because the surfactant molecules aggregate and form micelles. By measuring the surface tension at different solids percentages, they were able to determine the amount of adsorbed surfactant molecules at the polymer surface. Since then many investigations have been done for the adsorption behaviour of various surfactants on different polymer surfaces [2-10]. The differences found were attributed to various factors, such as polarity of the polymer surface, the number of ionic groups (initiator fragments) on the polymer surface and the salt present in the aqueous phase.

In micro-emulsions [11-13] and mini-emulsions [14-17] so called cosurfactants are used to stabilise the emulsion droplets. In micro-emulsions mostly short chain alcohols (such as pentanol) are used as cosurfactant, whereas in mini-emulsions long chain alcohols (such as dodecanol or cetylalcohol) are used. The cosurfactants used change the adsorption behaviour of the surfactants at the oil-water (L1/L2) interface. Most research on the adsorption behaviour of mixed emulsifier systems has been done at the L1/L2 interfaces. However, it is expected that addition of a cosurfactant (a higher alcohol or amine) can change the adsorption behaviour of anionic surfactants on polymer surfaces as well. There has been little research on this subject. Chou [18] found that SDS (Sodium Dodecyl Sulphate) has a larger molecular area per surfactant molecule on the PS-latex in presence of cetyl-alcohol on the PS-surface than in its absence. This means that there is a simple replacement of SDS by cetyl-alcohol taking place.

The molecular area per surfactant molecule, A_m, here means: the total area of the interface divided by the number of adsorbed surfactant molecules in absence of cosurfactants. This has to be distinguished from the effective molecular area per surfactant molecule, which is the molecular area of the surfactant in presence of cosurfactants. In the presence of cosurfactant, the effective molecular area per surfactant molecule, A_a, is calculated as $(A_{total} - N_{cosurf} * A_{cosurf}) / N_{surf}$, where A_{total} is the total area, N_{cosurf} is the number of cosurfactant molecules, A_{cosurf} is the area per adsorbed cosurfactant molecule

for both dodecanol and cetylalcohol (20 Å^2) [18,24] and N_{surf} is the number of surfactant molecules.

The present investigation concerns (i) the effect of the solids percentage on the adsorption of the surfactant, (ii) the effect of the PS particle size on the adsorption of the surfactant, (iii) the influence of cosurfactants on the adsorption of surfactants and (iiii) the influence of the temperature on the adsorption.

4.2 Theory

The soap titration method, developed by Maron et al. [1], can be used to determine the molecular area (A_m) of an adsorbed surfactant. The method involves the titration of a latex with surfactant until the critical micelle concentration (cmc) of the surfactant in solution is attained. The cmc can be determined either by surface tension or conductivity measurements. At the cmc it is assumed that the aqueous phase as well as the interfacial layers (air/liquid and polymer/liquid) have become saturated with surfactant. Because of the large difference between the magnitudes of the air/liquid and polymer/liquid interfacial areas, the amount of surfactant adsorbed at the air/liquid interface can be neglected.

However, the amount of surfactant in the aqueous phase may be significant compared with the adsorbed quantity, especially for large PS-particles (≥ 1 μm). Therefore it is necessary to subtract this amount from the total surfactant added in order to obtain the amount of surfactant adsorbed on the particle surface.

The amount of surfactant dissolved in the aqueous phase can be determined by titrating several samples of the same latex at different solids percentages. Neglecting the surfactant adsorbed at the air/liquid interface, the total amount of surfactant present in a latex at the titration end point C_t is given by:

$$C_t = C_a + C_f \qquad (4.1)$$

where C_t is the total concentration of surfactant (mol per liter of suspension), C_a is the concentration of adsorbed surfactant (mol per liter of suspension) and C_f is the concentration unadsorbed surfactant (mol per liter of suspension). On division and multiplication of C_a in equation (4.1) by m_p (grams of polymer per liter of suspension), we obtain:

$$(4.2)$$

$$C_t = \left(\frac{C_a}{m_p}\right) m_p + C_f = S_a m_p + C_f$$

where S_a is the surfactant added that has been adsorbed on the latex particles (mol per gram polymer). Maron et al. [1] assumed that C_f is constant and equal to I, the cmc of surfactant in pure water (mol per liter). As shown by Abbey et al. [20] it is more reasonable to assume that the aqueous concentration of the free surfactant at the cmc is a constant quantity and is equal to I. Therefore the corrected Maron equation becomes:

$$C_f = I\left(1 - \frac{m_p}{\rho_p}\right)$$ $$(4.3)$$

where ρ_p is the density of the latex particles in (1.05 gram per liter). Combining equation (4.2) and equation (4.3) the corrected Maron equation is obtained:

$$C_t = \left(S_a - \left(\frac{I}{\rho_p}\right)\right) m_p + I$$ $$(4.4)$$

When various end points are plotted as a function of the amount of polymer, a straight line is obtained. S_a can be calculated from this plot by adding the intercept I divided by ρ_p to the slope. This intercept I corresponds with the cmc of the aqueous phase. From the value of S_a the molecular area of the surfactant can be calculated.

If A_i is the molecular area in Å^2 of surfactant or cosurfactant initially present on the latex particles and A_a is the molecular area of added surfactant, then the surface area A in Å^2 per gram of polymer is given by:

$$A = (S_i A_i + S_a A_a) N_A$$ $$(4.5)$$

where N_A is Avogadro's number and S_i is the amount of surfactant or cosurfactant initially present. The volume V_p of 1 gram of polymer in Å^3 is:

$$V_p = \frac{10^{24}}{\rho_p}$$ $$(4.6)$$

where ρ_p is the density of the polymer particles (gram/ml). Combining equations (4.5) and (4.6) we find for V_p/A:

$$\frac{V_p}{A} = \frac{10^{24}}{(S_i A_i + S_a A_a) N_A \rho_p}$$

(4.7)

For spherical monodisperse particles with diameter D_s (surface average diameter) V_p/A equals $D_s/6$. Substitution of this relation in equation (4.7) then gives for A_a the molecular area of the added surfactant:

$$A_a = \frac{9.961}{S_a \rho_p D_s} - \frac{S_i A_i}{S_a}$$

(4.8)

For particles prepared by surfactant-free emulsion polymerization S_i is zero (because there are no surfactant or cosurfactant molecules initially present at the latex surface) and equation (4.8) can be simplified into:

$$A_m = A_a = \frac{9.961}{S_a \rho_p D_s}$$

(4.9)

Equation (4.9) is used to calculate the A_m (molecular area of the adsorbed surfactant) for the adsorption of surfactant in absence of cosurfactant. In the case of adsorption of surfactant in presence of cosurfactant the values of S_i (the amount of cosurfactant present) and A_i (the area per adsorbed alcohol molecule) can be substituted in equation (4.8) and by measurement of S_a it is possible to calculate A_a. A_m is used for the molecular area of a surfactant in absence of cosurfactants, whereas A_a is used for the effective molecular area of a surfactant in presence of cosurfactants.

4.3 Experimental

4.3.1 Materials

Sodium dodecylbenzenesulfonate (SDBS): ex. Albright and Wilson (Nansa 1260, 25% w/v in water) was used without further purification, because surface tension (γ) measurements showed no minimum in the γ versus concentration curves, indicative for the absence of surface active impurities.

Dodecanol and cetylalcohol: ex Merck (purity > 98%) were used without further purification.

Water was twice distilled using an all glass apparatus.

4.3.2 PS-latices

In this study 5 different PS-latices are used. Their preparation and characterization is described elsewhere [21,22]. The diameters of the latices were measured shortly before use. In table 4.1 the properties of these latices are given: number average diameter (D_n), surface average diameter (D_s), volume average diameter (D_v), degree of polydispersity ($P_n = D_v/D_n$) and the surface charge density (σ_0).

Table 4.1: *Characterization of the PS-latices.*

latex	D_n (nm)	D_s (nm)	D_v (nm)	P_n	σ_0 (μC/cm^2)
L-78[a]	669	690	701	1.05	8.63
L-80[a]	404	422	432	1.07	2.52
L-86[b]	1288	1335	1362	1.06	7.18
L-88[b]	2157	2204	2241	1.04	8.23
L-89[b]	3230	3278	3308	1.02	9.56

[a] The particle size was determined by the Coulter LS 130 [21].

[b] The particle size was determined by the Coulter Counter [21].

4.3.3 Cleaning of the latices

All latices were dialysed by the well-known serum replacement technique as described by Vanderhoff [23] in Amicon serum replacement cells. For a description of the serum replacement cells see [24]. The latex was first diluted to a solid content of a few percent with double-distilled water. Then a volume of 300 cm^3 of the latex was placed in the stirred cell. This cell was equipped with a Nucleopore membrane (Poretics Corporation, USA) with a pore size somewhat smaller than the particle size of the latex. Then a continuous stream of twice distilled water was flown through the cell until the conductivity of the outlet water reached the same value as that of the inlet double-distilled water (ca. 0.8 μS cm^{-1}).

Normally this took about 24 hours. All the dissolved electrolyte had then been removed and then the latex was removed from the cell. This procedure was repeated with a new sample of uncleaned latex.

4.3.4 Determination of solids content

The solids percentage of the different PS-latices were determined by drying a known amount of the latex in an oven at 105 °C, until constant weight was reached.

4.3.5 Procedure of the surface tension measurements

Surface tension measurements were performed using a Krüss K10T automatic tensiometer (Krüss GmbH, Hamburg) equipped with a Du Nouy ring. Before the measurements the glass vessel (diameter 4 cm, height 2 cm, ground upper edges) was cleaned using chromic acid and washed with twice distilled water. The dry vessel was then heated in the gas flame of a Bunsen burner. During a measurements series the Du Nouy ring was also heated in a gas flame between measurements.

After adding 20.0 grams of PS-latex to the glass vessel and waiting for 10 minutes for thermal equilibrium, the surface tension was measured twice. Then 0.5 ml of 0.03 M SDBS-solution in water was added and after 10 minutes the surface tension was measured. This procedure was repeated until the cmc was reached (the point where further addition of SDBS-solution effects only a very slight surface tension decrease). All surface tension measurements were performed at 22 °C.

4.3.6 Procedure of the conductivity measurements

Conductivity measurements were performed using a conductivity meter (Radiometer Kopenhagen). In a thermostatted measurement cell of 50 cm^3 20.0 g of latex, with known polymer content, was placed. A small magnetic stirrer was added and the conductivity electrode was immersed in the latex. Under stirring a small amount (0.25 or 0.50 ml) of SDBS-solution (0.01 or 0.03 M) was added and after every increment the conductivity was measured. The addition of SDBS-solution was continued until 10 to 15 ml of SDBS-solution were added. Conductivity measurements were performed at 22 °C and at 60 °C.

4.3.7 Procedure of measurements with cosurfactants

In case of added cosurfactant the measurements were performed by measuring the conductivity. Precise amounts of cosurfactant were added to the latex in glass bottles, in such a way that different percentages of coverage of the PS-particles were obtained. The

glass bottles were then placed in a waterbath at 60 °C (above the melting point of the cosurfactants) for at least one day. The measurements were performed in the same way as without cosurfactant at temperatures of 22 °C and 60 °C.

4.4 Results and discussion

4.4.1 Results in absence of cosurfactants

In table 4.1 the parameters of the used PS-latices are given. As can be seen from table 4.1 the latices are monodisperse, indicated by the value of P_n. This is especially the case for the larger particles. It can also be seen in table 4.1, that the surface charge density σ_0 is rather different for the used latices. The surface charge density arises from the initiator fragments depending on the polymerization procedure and is larger for larger particles. The only exception of this trend is latex L-78, which has a larger surface charge density than expected from its diameter. This latex was prepared in a slightly different way [21]. The surface charge density can have an influence on the molecular areas of surfactants [4],[5].

In figure 4.1 a typical example is shown of a titration curve obtained by surface tension measurements of latex L-78. The logarithm of the surface tension is plotted versus the added amount of SDBS-solution. As can be seen from figure 4.1 the surface tension (γ) decreases as more SDBS-solution is added. This decrease continues up to the point where further addition of SDBS-solution results in a much smaller decrease in surface tension (the critical micelle concentration, cmc). In the presence of a larger solids percentage of PS-particles a larger amount of SDBS-solution has to be added to reach the cmc. The cmc is indicated in figure 4.1 by the two arrows.

The determination of the cmc was performed from a graph of $\log(\gamma)$ versus the quantity of SDBS-solution added, by approximating the datapoints not very close to the cmc by straight lines, using linear regression (see figure 4.1). There is some uncertainty with regard to the exact position of the cmc, which is related in final instance to the fact, that the cmc is an idealization of what is in reality a gradual transition from a micelle-poor to a micelle-rich situation. Errors with regard to the position of the cmc are not considered to be serious, since only the difference between the values of SDBS-solution added, in absence and presence of PS-particles, is important in the context of the present paper.

The procedure used in the present work was preferred over that used in the work of Maurice [4], because the latter relies heavily on the data-points close to the cmc, in which case the errors of the fitted curve are more pronounced.

The error in the determination of the surface tension is 0.2 mN/m, which is less than 1%. However, the error in the determined endpoint is larger than the error in the surface tension measurements, because of the gradual character of the transition at the cmc. Duplicate values differ by less than 6%.

Surface tension measurements were only performed at room temperature (22 °C), because experimentally it was not possible to perform them at higher temperatures. Therefore conductivity measurements were performed both at room temperature (22 °C) and at 60 °C. The conductivity measurements were performed at these two temperatures, for comparing both the difference in A_m obtained with two different techniques at the same temperature and the difference in A_m obtained with the same technique at two different temperatures.

In figure 4.2 a typical conductivity measurement is shown for latex L-80 for the two different temperatures. As can be seen from figure 4.2 the conductivity increases as more SDBS-solution is added. The increase is less pronounced after the cmc has been passed. The conductivity versus added quantity of SDBS-solution can be represented very well by two straight lines, if the data points close to the cmc are omitted. The best fit of these lines was determined using linear regression. The line before the free surfactant concentration reaches the cmc has a larger slope than the line after the cmc has been passed. The cmc is located at the intersection point of these two lines. With regard to the exact position of the cmc, the same restrictions apply as in the case of cmc determination by surface tension measurements; but again this will not lead to serious errors, since it is the difference between values obtained in the absence and presence of PS-particles which is important. Duplicate values differed by less than 5%. Again a higher solids percentage results in more SDBS-solution to be added to reach the cmc.

In this way the determined cmc varied between 2 and 3.5 mmol/l; these values show reasonable agreement with literature values ranging from $3.2*10^{-4}$ mol/l [25] to $2.0*10^{-2}$ mol/l [26].
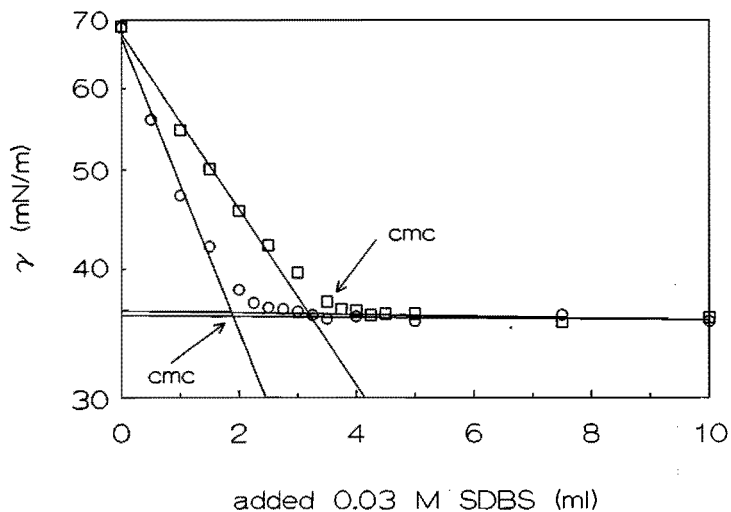
Figure 4.1: *Surface tension (γ) versus added 0.03 M SDBS for latex L-78:*
○ 3.6 % solids, □ 17.43 % solids; arrows indicate the cmc.
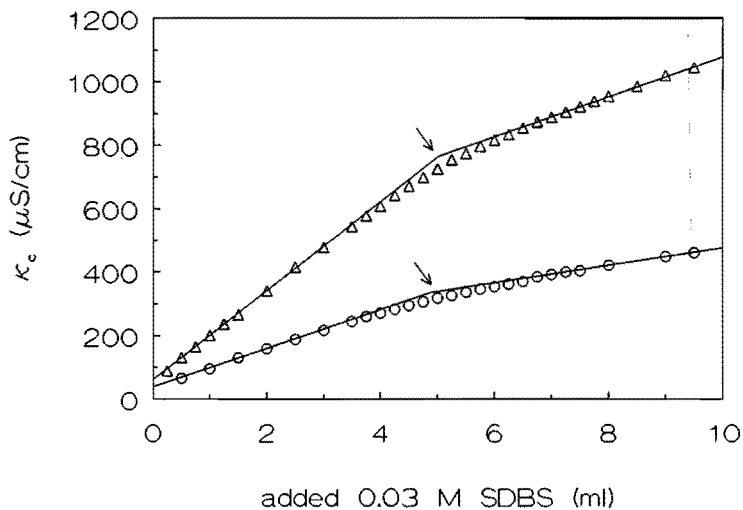
Figure 4.2: *Specific conductivity (κ_c) versus added 0.03 M SDBS for latex L-80:*
○ conductivity measurement at 22 °C, Δ conductivity measurement at 60 °C;
arrows indicate the cmc.

The cmc's obtained with the two different techniques (surface tension and conductivity measurements) and at different temperatures can be used to calculate S_a, from which A_m (the molecular area per adsorbed SDBS-molecule) can be calculated. This is shown in figure 4.3, where the concentration of SDBS-solution at the cmc is plotted versus the concentration of PS-particles at the cmc. As can be seen from figure 4.3 all obtained points are on straight lines, in agreement with the theory. This confirms the absence of serious errors in the determination of the cmc. The slope of these lines and the intersection points (the cmc) are used to calculate A_m using equation (4.9). In table 4.2 the obtained values for A_m are given for the different techniques and the different temperatures used. The A_m values are too low to be compatible with an adsorption of the surfactant in the form of trains and loops, as postulated in the Scheutjens-Fleer theory [27]. At least at large surface coverages, adsorption can not involve more than one or two -CH_2- or -CH_3-groups.
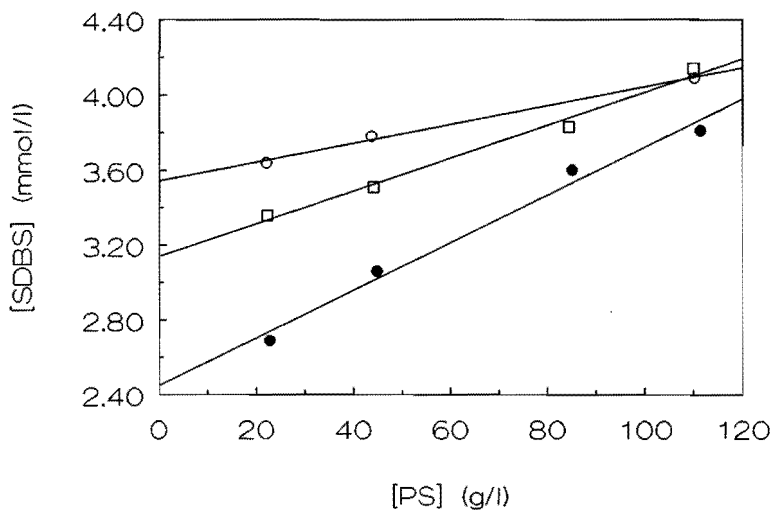
Figure 4.3: Plot of the concentration of SDBS versus concentration of PS for the determination of S_a: ● *surface tension at 22 °C,* □ *conductivity at 22 °C,* ○ *conductivity at 60 °C.*

A_m values obtained by surface tension measurements depend on the particle size or the surface charge density. In literature different values of A_m for SDBS on PS (in absence of added electrolyte) are reported: 62 Å^2 [2], 81 Å^2 [4] and for SDS 14.5 Å^2 [3], 14.5 Å^2 and 32.7 Å^2 [5] and 47.1 Å^2 [7]. An A_m of 53 Å^2 for SDBS on PS in 0.005 N salt is reported by Paxton [2]. The differences are described to various factors, such as the presence of charged surface groups [4],[5], surface irregularities [5] and polymer surface polarity [5]. The differences for the value of A_m found in presence of salt, are explained by the shielding of the charged head groups of the surfactant [2].

All values found in the present investigation are very close to the literature values. The values of A_m for the latices L-80, L-86 and L-88 are very close to each other. Although the surface charge density increases from 2.52 to 8.23 $\mu C/cm^2$, the value for A_m increases only by 14%. The appearance of charged groups on the surface has only a small effect on the adsorption area of the surfactant. The values of A_m obtained for latex L-78 and L-89 can therefore not be explained by the appearance of charged groups at the surface. A possible explanation for the difference for A_m for latex L-89 is that the total adsorbing surface area per gram PS is much smaller than for the other latices, because of the larger diameter. The possibility of errors by determining the cmc is therefore increased and the value of S_a (determined by the position of the cmc) is subject to serious error. However, for latex L-78 this can not be the explanation, because the surface area is much larger than for latex L-89. The surface charge densities of latex L-78 and L-88 are comparable, but the values for A_m differ by as much as 66 %. The only explanation for this difference, which we can see, is the surface area used for the calculations. This surface area was determined from the diameter of the latex measured by the Coulter Counter and is thus related to the macroscopic area. Adsorption, however, is related to a surface area on a molecular scale.

Surface irregularities may explain the difference between the calculated surface area (macroscopic) and the real surface area (microscopic). On SEM-photographs this kind of surface roughness could be seen only for latex L-78. All other latices used showed no surface roughness.

Table 4.2: Molecular area (A_m) for different latices measured at different temperatures and with different techniques.

latex	A_m (Å^2), γ, 22 °C[a]	A_m (Å^2), Λ, 22 °C[b]	A_m (Å^2), Λ, 60 °C[c]
L-78	80	92	117
L-80	49	52	64
L-86	48	60	84
L-88	56	_[d]	_[d]
L-89	78	_[d]	_[d]

[a] Surface tension measurement at 22 °C

[b] Conductometric measurement at 22 °C

[c] Conductometric measurement at 60 °C

[d] Not measured

In table 4.2 also the values of A_m obtained with conductometric measurements are listed, both at 22 °C and 60 °C. The latices used for the conductometric measurements are L-78, L-80 and L-86: with the latices L-88 and L-89, the increase in conductivity on addition of SDBS-solution up to the cmc, was too small for accurate determination of the endpoint of the titration. This is ascribed to the smaller surface area per gram PS of these latices.

The results of the surface tension measurements and the conductometric measurements at 22 °C are compared in table 4.2 and show, that there is some difference between the values of A_m determined. The values obtained with conductometric measurements are larger than those obtained with surface tension measurements. This is in agreement with data reported by Urban [9] (compare, however, ref. [1]). The difference between the values of A_m obtained by conductometric and surface tension measurements are, however, rather small in the experiments reported here.

The values of A_m obtained with conductometric titrations at 60 °C are all larger than those obtained at 22 °C. This is in agreement with data reported by Piirma and Chen [7]. They studied the adsorption of SDS on PS-particles at temperatures varying from 22 °C to 47 °C. Raising the temperature from 22 °C to 47 °C resulted in an increase of A_m from 47.1 Å^2 to 52.4 Å^2. This difference was attributed to the larger thermal motion of

the molecules. In our case the temperature is even more raised and consequently an even larger value of A_m was found.

4.4.2 Results in presence of cosurfactants

For the measurements with cosurfactants two latices were chosen, latex L-80 and L-86. These latices have a relatively large surface area per gram and the values for the adsorption without cosurfactant are very close to literature values. In figure 4.4 the titration of latex L-86 with a surface coverage of dodecanol of $1.5 * 10^{-6}$ mol/m^2 is shown as an example. This titration and the titrations without cosurfactants are very similar, with the exception that in the case with cosurfactants, the transition from the situation poor in micelles to that rich in micelles, can be approximated by three straight lines with two intersection points. These are indicated in figure 4.4 with the two arrows.

Such a more complicated character of the conductivity versus added amount of surfactant in the presence of alcohol is ascribed to the excess of alcohol being solubilized in the micelles.
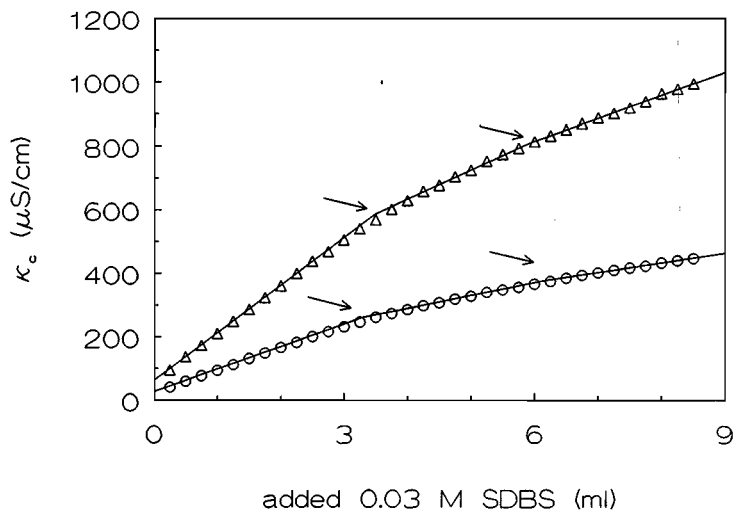
Figure 4.4: *Specific conductivity (κ_c) versus added 0.03 M SDBS for latex L-86:*
○ conductivity measurement at 22 °C, Δ conductivity measurement at 60 °C;
arrows indicate intersection points.

In view of the (in reality) gradual character of the transition from solutions poor in micelles to solutions rich in micelles, it is plausible that solubilization of the alcohols in the micelles is more pronounced at surfactant concentrations which exceed the cmc by some amount, than at surfactant concentrations which only slightly exceed the cmc. That such a gradual transition can be approximated, when following the electrical conductivity as a function of added amount of surfactant, by three straight lines was already observed by Chou [18]. The first intersection point found in the latex titration with cosurfactant can be regarded as the cmc. Such two intersection points are found for both cosurfactants used (dodecanol and cetylalcohol), the two temperatures studied (22 °C and 60 °C) and the two surface coverages studied ($1.5 * 10^{-6}$ mol/m^2 and $5 * 10^{-6}$ mol/m^2). The first intersection points are used to determine the value of S_a, similar as described before.

In order to determine A_a (the adsorption area of SDBS in presence of cosurfactant) some additional assumptions are needed:

1: All the cosurfactant added is assumed to be adsorbed on the PS-particles. The solubility of the cosurfactants (dodecanol and cetylalcohol) in water is very low, as long as the cosurfactants are not solubilized in the micelles. The addition of the cosurfactants refers to the situation before adding surfactants, therefore it is reasonable to assume that all the alcohol molecules are adsorbed on the PS-particles. Desorption of the alcohol, even after addition of surfactant, is only expected to a significant degree at surfactant concentrations larger than the cmc. Measurements of the surface tension, after the alcohols had been adsorbed, gave the same surface tension, as in the case where no alcohols were used. The decrease in surface tension at very low concentrations of dodecanol is very pronounced. In our case no surface tension decrease was found. This confirms, that the alcohols are indeed all adsorbed on the PS-particles.

2: The cosurfactants are assumed to be adsorbed in a monolayer. Absorption of cetyl-alcohol or dodecanol by the PS-particles is excluded, since it is very unlikely that diffusion of such large molecules into solid PS-particles might be fast enough to lead to any perceptible absorption at the time-scale of our experiments.

3: The added cosurfactants are assumed to be adsorbed in a random way on PS-particles and not patch-wise.

If the first two assumptions are granted, the smallest surface area per adsorbed alcohol

molecule before addition of surfactant becomes 33 $Å^2$. This value was calculated by the amount of alcohols added divided by the calculated surface area. This is larger than the value of 20 $Å^2$ reported by Chou [18] for cetylalcohol in a close packed monolayer. A similar value was found by Sharma et al. [19] for $C_{18}H_{37}OH$ at air/water interfaces.

The third assumption is confirmed by the fact, that at the highest surface coverage the molecular area of an alcohol molecule is larger than that in a close packed monolayer. Then at the titration endpoint the cosurfactant and surfactant molecules are adsorbed in a mixed close packed monolayer with the alkyl chains standing straight up with their polar heads pointing to the water phase.

In the mixed close packed monolayer the alcohol molecules occupy an area of 20 $Å^2$. This value was found by Chou [18] for cetylalcohol. If our assumptions are right then dodecanol should also occupy an area of 20 $Å^2$. Using this assumption, the obtained values of A_a (the adsorption area of SDBS in presence of cosurfactants) are listed in table 4.3. It is seen, that A_a values indeed approach 20 $Å^2$ when cetylalcohol is the co-surfactant; when dodecanol is the cosurfactant, this is only observed with latex L-86. Again, the surface area per adsorbed surfactant or cosurfactant molecule is too low to be compatible with a Scheutjes-Fleer-like adsorption by way of trains and loops.

The data in table 4.3 can be understood in the following manner:

The temperature of 22 °C is below the melting point of the alcohols, whereas the temperature of 60 °C is above the melting point of the alcohols. From table 4.3 it can be seen that at 22 °C the values of A_a for the two latices studied, at low surface coverage of both alcohols, are very similar to the values obtained without cosurfactant. This would imply that at low surface coverage the effect of the added alcohols is of minor importance only. At these low surface coverages of cosurfactant the amounts of alcohol and SDBS molecules are more or less equal. The electrostatic repulsion between the charged groups of SDBS is still very important. At high surface coverages of cosurfactants the values of A_a are much smaller than at low surface coverage. In this case the introduction of cosurfactant molecules into a surfactant surface layer leads to additional attraction between the alkyl chains of surfactant and cosurfactant, without simultaneously introducing additional negatively charged ionic head groups.

Table 4.3: Values of A_a, effective molecular area of SDBS ($Å^2$), in the presence of different initial surface coverages, different cosurfactants and different temperatures, assuming a molecular area of the cosurfactants of 20 $Å^2$.

latex	temperature (°C)	without cosurfactant	dodecanol $1.5*10^{-6}$ mol/m^2	cetylalcohol $1.5*10^{-6}$ mol/m^2	dodecanol $5*10^{-6}$ mol/m^2	cetylalcohol $5*10^{-6}$ mol/m^2
L-80	20	52	51	59	45	31
L-86	20	60	59	51	31	24
L-80	60	64	85	103	40	31
L-86	60	84	64	63	25	29

At low temperatures the surface coverage of surfactant can be increased significantly by the presence of cosurfactant, as long as the cosurfactant/surfactant ratio is larger than 1.

At 60 °C a different picture is found. At low surface coverage of cosurfactant the value of A_a for latex L-80 is larger and the value of A_a latex L-86 is smaller than the values obtained without cosurfactants. At this moment it is not quite clear, which of these values is the right one.

The values of A_a obtained at high surface coverage, are even lower than those at 22 °C. In spite of the larger thermal motion of both the surfactant and cosurfactant molecules at higher temperatures, the value of A_a is smaller. The mixed monolayer may be better packed than at lower temperatures. At temperatures of 60 °C it is also important that the ratio of cosurfactant/surfactant should be larger than 1 for reaching a higher surface coverage of surfactant.

4.5 Conclusions

The adsorption of SDBS on PS-particles is only slightly influenced by the charged surface groups, arising from initiator fragments. At higher temperatures, the molecular area of SDBS increases, because of the larger thermal motion of the ionic head groups of SDBS. The values found in literature for A_m, determined from measurement of adsorbed amounts

of surfactant and particle sizes, are very different (ref. [2]-[5], [7]). In this study it is shown, that the differences in A_m found are only scarcely influenced by the presence of charged surface groups. A possible explanation for this difference is the surface roughness of the PS-particles used.

For this study two cosurfactants (higher alcohols) were chosen, dodecanol and cetyl-alcohol. These two cosurfactants were chosen, because in mini-emulsions such cosurfactants are used for their stabilizing properties. Our results show that these alcohols can change the adsorption behaviour of surfactants on solid surfaces as well.

At low surface coverages of cosurfactants little influence on the adsorption of SDBS was found, both at low temperature (22 °C, below the melting point of the cosurfactant) and at higher temperatures (60 °C, above the melting point of the cosurfactants). In this case the electrostatic repulsion of the ionic head groups of SDBS is still very important.

At high surface coverages the adsorption of SDBS is significantly increased (at both temperatures). This may probably be explained by the fact, that the positive interaction of the alkyl-chains is increased, without simultaneously introducing charged ionic head-groups.

The addition of a cosurfactant can stimulate the adsorption of surfactant only at rather high cosurfactant/surfactant ratios.

4.6 References

(1)   Maron, S. H., Elder, M. E., Ulevitch, I. N., *J. Colloid Interface Sci.*, **1954**, *9*, 89.

(2)   Paxton, T. R., *J. Colloid Interface Sci.*, **1969**, *31*, 19.

(3)   Vijayendran, B. R., Bone, T., Gajria, C., *J. Appl. Polym. Sci*, **1981**, *26*, 1351.

(4)   Maurice, A. M., *J. Appl. Polym. Sci*, **1985**, *30*, 473.

(5)   Ali, S. I., Steach, J. C., Zollars, R. L., *Colloids surfaces*, **1987**, *26* ,1.

(6)   Vijayendran, B. R., *J. Appl. Polym. Sci*, **1979**, *23*, 733.

(7)   Piirma, I., Chen, S. R., *J. Colloid Interface Sci.*, **1980**, *74*, 90.

(8)   Painter, D., Hall, D. G., Wyn-Jones, E., *J. Chem. Soc., Faraday Trans 1*, **1988**, *84*, 773.

(9)   Urban, P. C., *J. Disp. Sci. Tech.*, **1981**, *2*, 233.

(10) Connor, P., Ottewill, R. H., *J. Colloid Interface Sci.*, **1971**, *37*, 642.

(11) Gan-zuo, L., Friberg, S. E., *J. Disp. Sci. Tech.*, **1983**, *4*, 19.

(12) Guo, J.S., El-Aasser, M. S., Vanderhoff, J. W., *J. Polym. Sci., Polym. Chem Ed.*, **1989**, *27*, 691.

(13) Verhoeckx, G. J., De Bruyn, P. L., Overbeek, J. Th. G., *J. Colloid Interface Sci.*, **1987**, *119*, 409.

(14) Tadros, Th. F., *Colloids Surfaces*, **1980**, *1*, 3.

(15) El-Aasser, M. S., Lack, C. D., Vanderhoff, J. W., Fowkes, F. M., *Colloids Surfaces*, **1988**, *29*, 103.

(16) Brouwer, W. M., El-Aasser, M. S., Vanderhoff, J. W., *Colloids Surfaces*, **1988**, *21*, 69.

(17) El-Aasser, M. S., Lack, C. D., Choi, Y. T., Min, T. I., Vanderhoff, J. W., Fowkes, F. M., *Colloids Surfaces*, **1984**, *12*, 79.

(18) Chou, Y. J., **1978**, Lehigh University, Ph. D. Thesis, Chapter 3.

(19) Sharma, M. K., Shiao, S. Y., Bansal, V. K., Shah, D. O., In *Macro- and Micro emulsions, Theory and Applications*, (ACS Symposium Series 272); Shah, D. O., Ed; Washington; **1985**; p 91.

(20) Abbey, K. J., Erickson, J. R., Seidewand, R. J., *J. Colloid Interface Sci.*, **1978**, *66(1)*, 203.

(21) Tuin, G., Peters, A. C. I. A., Van Diemen, A. J. G., Stein, H. N., *J. Colloid Interface Sci.*, **1993**, *158(2)*, 508; see also chapter 2 of this thesis.

(22) Tuin, G., Stein, H. N., *J. Colloid Interface Sci.*, to be submitted; see also chapter 3 of this thesis.

(23) Vanderhoff, J. W., Van de Hul, H. J., Tausk, R. J. M., Overbeek, J. Th. G., In *Clean surfaces: Their preparation and characterization for interfacial studies*; Goldfinger, G., Ed; Marcel Dekker, Inc: New York, **1970**; p. 15.

(24) Ahmed, S. M., El-Aasser, M. S., Pauli, G. H., Poehlein, G. W., Vanderhoff, J. W., *J. Colloid Interface Sci*, **1980**, *73*, 388.

(25) Jindal, V. K., Bahadur,P., *Ind. J. Technol.*, **1982**, *20*, 66.

(26) Abe, M., Ohsato, M., Suzuki, N., Ogino, K., *Bull. Chem. Soc. Jpn.*, **1984**, *57*, 831.

(27) Scheutjens, J. M. H. M., Fleer, G. J., *J. Phys. Chem.*, **1980**, *84*, 178.

CHAPTER 5

THE EXCESS GIBBS FREE ENERGY OF ADSORPTION OF SODIUM DODECYLBENZENESULPHONATE ON POLYSTYRENE PARTICLES

Summary: Adsorption of Sodium Dodecylbenzenesulphonate (SDBS) on Polystyrene (PS) particles is described by the Langmuir equation only superficially: on closer look there are small but systematic differences with the experiments. This is expressed here as an excess G function (G^E) of the surfactant electrolyte on adsorption, which changes with increasing degree of occupation of adsorption sites (θ). At low θ values, G^E changes in positive direction with increasing θ; at large θ values, this trend levels off and may even be in the opposite direction (depending on the value assumed for total saturation of the surface with surfactants). This is explained by changes in adsorption energy of the surfactant chain on the polystyrene surface: at very low θ values the chain is adsorbed in a flat configuration; at larger θ values this is no longer possible, but this is partially compensated by interaction between the hydrocarbon chains of surfactant ions adsorbed on neighbouring sites. This explanation is confirmed by the effect of cosurfactant molecules on the adsorption.

5.1 Introduction

Adsorption of ionic surfactants has been investigated frequently, see e.g. [1]-[17]. Much attention has been paid to the case of adsorption of surfactants on mineral surfaces, in which ionic interaction between charged groups on the surface and on the surface active ions are important (see, e.g., ref. [10-17]). Quite different phenomena are expected with regard to the adsorption of ionic surfactants on the surface of a hydrophobic substance such as, e.g., polystyrene, especially when the charges on the surface and on the surface active ions have the same sign such as to lead to repulsive rather than attractive forces between surface and surfactant. In such cases, nevertheless adsorption on a hydrophobic substance may occur, since the hydrophobic tails of the surfactant are attracted by hydrophobic groups on the polystyrene surface. This is the case discussed here.

Adsorption data of surfactants are, in some cases, interpreted by a Langmuir adsorption isotherm [8]-[10]. However, on closer look there are, at least in the cases known to the present authors, small but systematic differences between the data and the linear relation

between $1/\Gamma$ and $1/c$ predicted by the Langmuir equation (where Γ is the quantity adsorbed at concentration c in the surrounding liquid).

This has been remarked, a.o., by Kronberg et al. [18,19]. These authors tried to connect the adsorption of non-ionic surfactants with the interactions between surfactant molecules and solvent molecules, in solution and at the solid-liquid interface, expressed as two χ parameters ($\chi_{solution}$ and $\chi_{surface}$, respectively). However, in order to obtain manageable equations, the assumption was introduced, that the configuration of the surfactant remains unchanged on adsorption and is independent of concentration in solution and of the degree of occupancy of the surface.

Böhmer et al. [20]-[22] calculated the distribution of the adsorbed surfactant on the basis of the Scheutjes-Fleer self consistent field theory [23,24]. Their treatment of the adsorption of ionic surfactants was restricted to cases, in which the first layer of adsorbed surfactants was drawn to the surface primarily by electrostatic attraction (e.g., a cationic surfactant on a negatively charged surface), leading to a two-step adsorption.

However, the application of this theory requires the introduction of a number of interaction parameters, which are obtained as fitting parameters, which makes the application of this theory questionable.

In order to understand the effects observed on adsorption of surfactants, the deviations from the Langmuir equation are expressed here as an excess G-function (G^E) on adsorption. G^E comprises, in principle, all deviations from an idealized adsorption equation. When the idealized adsorption equation does not itself include interactions between the adsorbed molecules or ions (as is the case with the Langmuir equation), G^E includes all entropic and enthalpic effects of interaction between the ions both in the adsorbed state and in the surrounding liquid.

From experimental adsorption data, $(\Delta G^0 + G^E)/RT$ can be calculated, in which ΔG^0 is the change in standard-Gibbs free energy on adsorption of the cations and anions of the surfactant. ΔG^0 is, by definition, independent of the degree of occupation of the adsorption sites and of the concentration in the solution. The change in $(\Delta G^0 + G^E)/RT$ with θ reflects changes in G^E, expressing deviations from situations assumed as ideal both in solution and in the adsorbed state. In solution, the ideal state comprises absence of interaction between the dissolved ions. For adsorbed ionic surfactants, the most appro-

priate definition of an ideal state is localized adsorption for the surface active ions and mobile adsorption for the counter ion, again without interaction.

This attack leads us, according to our point of view, as far in analysis of adsorption data as one can get without other assumptions than the basic ones of statistical thermodynamics. The interpretation of the $(\Delta G^0 + G^E)/RT$ versus θ curves thus obtained, must however make use of more detailed model assumptions.

In order to fully understand the meaning of the excess Gibbs free energy of adsorption G^E, we give in the theoretical section the derivation of the equations concerned. This appears to us to be especially useful since a combination of localized and mobile adsorption, as discussed here, is not frequently employed.

5.2 Theory

The two most simple idealized types of adsorption are: localized adsorption and mobile adsorption [25]-[27].

From the viewpoint of statistical thermodynamics, they are differentiated by the energy barrier which an adsorbed molecule or ion must pass when moving along the surface from one adsorption site to the next. When this is large compared to the thermal energy of a molecule, localized adsorption is the appropriate model, while the mobile adsorption should be regarded as the ideal for comparing experimental data with when this energy barrier is small compared with kT (where k is Boltzman's constant and T is the absolute temperature); it may even be non-existent when there are no distinct adsorption sites as is the case, e.g., on a liquid/liquid interface or for an ion in the diffuse double layer.

This difference leads to an essential difference in the partition function of a monolayer adsorbed in a localized, or in a mobile way, respectively.

5.2.1 Localized adsorption

The partition function of the adsorbed monolayer consisting of m molecules distributed over M sites, can be written as [25]:

$$Q = g(M,m) * a(T)^m \tag{5.1}$$

where a(T) is the partition function for internal degrees of freedom of an adsorbed

molecule referred to the lowest internal state of a molecule in the surrounding solution and $g(M,m)$ is the number of distinguishable ways of distributing the adsorbed molecules over the sites. The partition function $a(T)$ can be written as:

$$a(T) = \exp\left(\frac{\chi}{kT}\right) * j^{S}(T) \tag{5.2}$$

where χ is the minimum energy required to remove a molecule, adsorbed in its lowest energy state, from the surface to the bulk solution and $j^{S}(T)$ is the partition function for internal degrees of freedom of the molecule including vibrations relative to its mean position.

If the molecules are distributed over the sites at random, $g(M,m)$ is given by:

$$g(M,m) = \frac{M!}{m!(M-m)!} \tag{5.3}$$

Therefore the contribution of the monolayer to the thermodynamic A function (Helmholtz free energy) is given by:

$$A = -kT * \ln Q =$$
$$-kT * (M * \ln M - m * \ln m - (M-m) * \ln(M-m) + m * \frac{\chi}{kT} + m * \ln(j^{S}(T)) \tag{5.4}$$

and the chemical potential of an adsorbed molecule becomes:

$$\mu = \left(\frac{\delta A}{\delta m}\right)_{T,V} = \mu^{\square} + kT * \ln\left(\frac{\theta}{1-\theta}\right) \tag{5.5}$$

where $\chi + kT \ln j^{S}(T)$ have been replaced by $\mu^{\square}$ and θ is m/M, the degree of occupation of the adsorption sites.

When equilibrium is reached, the chemical potential of an adsorbed molecule must be equal to that of the molecule in solution. If there is no interaction between the molecules in solution, this chemical potential is given by $\mu^{0} + kT * \ln(c)$ (where c is the concentration of the ion). This leads, in the case of localized adsorption, to the Langmuir adsorption isotherm:

$$\theta = \frac{c * \exp\left(-\frac{\Delta G^0}{RT}\right)}{1 + c * \exp\left(-\frac{\Delta G^0}{RT}\right)} \tag{5.6}$$

where $\Delta G^0 = \mu^0 - \mu^\square$ per mole of surfactant.

Thus, it is seen, that the Langmuir adsorption isotherm can be derived without any assumptions with regard to the equality of size of solvent and solute molecules (as proposed by Kronberg [18]).

5.2.2 Mobile adsorption

In this case, the formulae are quite similar to those given above, with the important difference that the number of distinguishable ways of distributing m identical adsorbed molecules over the surface is now given by 1/m!. Thus, in this case the partition function of the adsorbed monolayer becomes:

$$Q = \frac{1}{m!} * \exp\left(\frac{m\chi}{kT}\right) * l(T)^m * j^S(T)^m \tag{5.7}$$

in which $j^S(T)$ is now the partition function for the internal degrees of freedom of the adsorbed molecule including vibration normal to the surface. The motion of the molecule along the surface is included by $l(T)$, the partition function for translation in two dimensions in an area A, which is given by:

$$l(T) = \frac{2\pi m' kTA}{h^2} \tag{5.8}$$

in which m' is the mass of the adsorbed molecule and h is Planck's constant.

This leads to the following expression of the chemical potential of a molecule adsorbed on a surface in mobile adsorption:

$$\mu = \mu^0 + kT * \ln(\theta) \tag{5.9}$$

It should be borne in mind that in this case, the standard state for the surface referred to by μ^0 is $\theta = 1$, while in equation (5.5) it is $\theta = 0.5$. This does not, however, have any

consequences on the final equation since the difference is a constant term (independent of concentration or degree of occupation of the surface).

On equalizing this to the chemical potential of a dissolved molecule, we obtain a "Henry" type of adsorption isotherm:

$$\theta = c * \exp\left(-\frac{\Delta G^0}{kT}\right) \qquad\qquad (5.10)$$

5.2.3 Adsorption of an ionic surfactant

Thus far, the theory relates to non-electrolytes. In the present investigation, we are dealing with an ionic surfactant, with a surface active anion, adsorbed from an aqueous solution, on a hydrophobic surface which has, from its preparation, already some negative charges. The theory will be restricted to the case of univalent cations and anions. In this case, adsorbed anions will be fixed with their hydrophobic tails to adsorption sites, while the simultaneously adsorbed cations are present as counter ions in the vicinity of the solid where there is nothing like a distinct site. The best model to compare experimental adsorption data with theory is, in such cases, mobile adsorption for adsorbed cations and localized adsorption for adsorbed anions.

When treating electrolytes such as an ionic surfactant (SDBS), the following changes have to be introduced in the equations (5.1)-(5.10):

a) in solution, the chemical potential of a surfactant molecule (cation + anion) is given by:

$$\mu_{cat+an} = \mu_{cat+an}^{\square} + 2RT\ln(x) \qquad\qquad (5.11)$$

b) when we are dealing with an ionogenic surfactant with surface-active anion, the chemical potential of the anion in the adsorbed state, can best be described by localized adsorption; in addition, the electrical work has to be taken into account which is neces-sary to bring an electrically charged group (of charge $-e_0$) to the potential ψ_δ, which is the average potential to which the adsorbed ionic head groups are subjected. Thus, the chemical potential of the adsorbed anion is taken to be described by:

$$\mu_{anion} = \mu_{anion}^{\square} + RT\ln\left(\frac{\theta}{1-\theta}\right) - e_0 N_A \psi_\delta \tag{5.12}$$

where N_A is Avogadro's constant.

c) the adsorption of the cation is taken to be mobile. In addition, the adsorbed cation (electrical charge e_0) should be brought to the potential $\psi_{average}$, which is the average potential to which a counter-ion is subject in the electrical double layer. This leads to:

$$\mu_{cation} = \mu_{cation}^{\square} + RT\ln(\theta) + e_0 N_A \psi_{average} \tag{5.13}$$

The chemical potential of the adsorbed electrolyte (cation + anion) becomes:

$$\mu_{cat+an,ads} = \mu_{cat+an,ads}^{\square} + RT\ln\left(\frac{\theta^2}{1-\theta}\right) - e_0 N_A (\psi_\delta - \psi_{average}) \tag{5.14}$$

However, since the electrostatic terms are dependent upon the surface charge and therefore on the degree of occupation, θ, of the adsorption sites, it is more consequent to include them in G^E, the excess Gibbs free energy of adsorption. This takes into account all deviations from an adsorption determined by chemical potentials described by equation (5.11) for the dissolved electrolyte and by

$$\mu_{cat+an,ads} = \mu_{cat+an,ads}^{\square} + RT\ln\left(\frac{\theta^2}{1-\theta}\right) \tag{5.15}$$

for the adsorbed electrolyte.

The adsorption is thus determined thermodynamically by the equation:

$$\mu_{cat+an,dissolved}^{\square} + 2RT\ln(x) = \mu_{cat+an,ads}^{\square} + RT\ln\left(\frac{\theta^2}{1-\theta}\right) + G^E \tag{5.16}$$

in which G^E takes into account interactions between the ions, both in the solution and in the adsorbed state, including the electrostatic interaction between the head groups of the surfactant mutually, between the counterions mutually and between the counter ions and the head groups. By doing so, one can calculate the quantity

$$\frac{(\Delta G^0 + G^E)}{RT} = 2\ln(x) - 2\ln(\theta) + \ln(1-\theta) \tag{5.17}$$

from an experimentally known relationship between the concentration in the solution (x) and the degree of occupation of adsorption sites (θ). The concentration in the solution x is expressed here as the fraction of positions in the surrounding liquid, which is occupied by solute. ΔG^0 is, by definition, independent of the concentration in solution of the degree of occupation, θ, of the adsorption sites.

The question may be asked, whether a Volmer type of adsorption isotherm [28] would not be more appropriate in the case at hand. This type of equation is employed in cases of mobile adsorption, when the amount of adsorbate which can be accommodated at an interface, is limited by the size of the entity to be adsorbed, corresponding with an expression for the partition function for translation in two dimensions in an area A-mA$_0$:

$$l(T) = \frac{2 \pi m' k T (A - m A_0)}{h^2} \qquad (5.18)$$

instead of equation (5.8). A_0 is the minimum surface area which must be available for a molecule to be adsorbed.

However, in the case at hand, in which we apply a mobile adsorption equation to the cations of an anionic surfactant, the quantity of cations which can be adsorbed, is indeed limited, but not by the size of the cations. The restriction is imposed by the electrostatic charge on the cations: no more cations can be adsorbed than the sum of the negative anionic groups on the surface and the adsorbed anions because this would violate electroneutrality. Such a restriction is imposed by electrostatic potential considerations and thus is included in G^E. Inclusion of the restriction by means of an area A_0 would correspond with an incorrect expression for the entropy of the adsorbed cations.

Recently, Oh and Shah [29] reported that the size of a counterion may limit the distance between adsorbed surface active ion, as shown by differences in area per adsorbed surfactant molecule at maximum surface coverage, between Li-, Na-, K- and Cs-dodecyl-sulphates. This should, however, not be taken as an argument for assuming localized adsorption for the counterions. In solution, below the critical micelle concentration, the deviations from ideal behaviour agree with reasonable accuracy with the predictions of the Debye-Hückel theory [30] and even in micelles, where part of the counterions move (e.g. in electrophoresis) with the surface active ions [31], a considerable part of the counterions is not bound, which suggests that the shift of a bound counterion from one adsorption site

to the next is a process of low activation energy compared with kT. The best way to combine this evidence with the findings of Oh and Shah [29] is to assume that at high degree of coverage groups of surface active ions adsorbed on adjacent sites create a pronounced local potential; additional surface active ions can then only be adsorbed on a neighbouring site when the local potential is partially shielded by the nearby presence of counterions. Since this effect is typical a matter of mutual influence between adsorbed ions, it is incorporated in the theory presented here in G^E. The findings of Oh and Shah [29] should be incorporated only by their influence on the surface area per adsorbed molecule at maximum surface coverage.

5.3 Experimental

5.3.1 Materials

Sodium dodecylbenzenesulfonate (SDBS): ex. Albright and Wilson (Nansa 1260, 25% w/v in water) was used without further purification. Surface tension (γ) measurements showed no minimum in the γ versus concentration curves, indicative for the absence of surface active impurities.

Water was twice distilled using an all glass apparatus.

5.3.2 PS-latex

The preparation and characterization of the latex is described elsewhere [32]. The diameter of the latex particles used (latex L-78) was measured shortly before use. In table 4.1 the properties of this latex are given: number average diameter (D_n), surface average diameter (D_s), volume average diameter (D_v), degree of polydispersity ($P_n = D_v/D_n$) and the surface charge density (σ_0).

5.3.3 Determination of solids content

The solids percentage of the different PS-latices were determined by drying a known amount of the latex in an oven at 105 °C, until constant weight was reached.

5.3.4 Procedure of the surface tension measurements

Surface tension measurements were performed using a Krüss K10T automatic tensiometer (Krüss GmbH, Hamburg) equipped with a Du Nouy ring. Before the measurements the glass vessel (diameter 4 cm, height 2 cm, ground upper edges) was cleaned using chromic acid and washed with twice distilled water. The dry vessel was then heated in the gas flame of a Bunsen burner. During a measurements series the Du Nouy ring was also heated in a gas flame between measurements.

After adding 20.0 grams of PS-latex to the glass vessel and waiting for 10 minutes for thermal equilibrium, the surface tension was measured twice. Then 0.5 ml of 0.03 M SDBS-solution in water was added and after 10 minutes the surface tension was measured. This procedure was repeated until the cmc was reached (the point were further addition of SDBS-solution effects only a very slight surface tension decrease). All surface

tension measurements were performed at 22 °C.

5.3.5 Supernatant titration

For the supernatant titration the latex was centrifuged for 4 hours at 20000 rpm in a Centrikon T-2060 centrifuge (Kontron Instruments, Italy). The supernatant titration was carried out as described for dispersions containing of PS-particles.

5.4 Results and discussion

Adsorbed amounts of surfactant are calculated from surface tension measurements on addition of SDBS ("titration") to latices containing various amounts of PS. On adding SDBS to a latex the surface tension (γ) decreases as more SDBS-solution is added (see figure 4.2, chapter 4). This decrease continues up to the point where further addition of SDBS-solution results in a much smaller decrease in surface tension (the critical micelle concentration, cmc). In the presence of a larger solids percentage of PS-particles a larger amount of SDBS-solution has to be added to reach the cmc.

Similar titrations were performed on supernatant solutions obtained on centrifugation of latices. In figure 5.1 two typical supernatant titration are shown. In this case the surface tension is plotted versus the concentration of SDBS in the waterphase. The concentration of SDBS in the waterphase was calculated from the added amount of SDBS-solution to the sample cell. Because of the small surface area of the measuring vessel, the amount adsorbed at the water-air interface can safely be ignored.

Interpolation between the measured data is effected by adjusting the data to the Szyszkowski equation [34]. This equation relates the surface tension to the concentration of surfactant in the waterphase:

$$\gamma - \gamma_0 = -2RT\,\Gamma^{\mathrm{max}}\,\ln\left(\frac{c+a}{a}\right) \tag{5.19}$$

where γ is the surface tension at a certain concentration of SDBS in the waterphase, γ_0 is the surface tension at concentration 0 of SDBS in the waterphase, R is the gas constant, T is the temperature, c is the concentration of SDBS in the waterphase, a is the Langmuir-Szyszkovski constant and Γ^{max} is the maximum surface excess of SDBS.

Szyszkowski made the assumption, based on empirical data, that the equation is only valid

below the CMC for uncharged particles.

It appeared however, that the Szyszkowski equation has a broader validity. The equation is used by Rosen and Aronson [35] for alcohol and anionic surfactant, by Müller [36] for cationic surfactants and Kegel et al. [37] for the system brine, anionic surfactant, alcohol and cyclohexane. They all obtained good results in using the equation to describe their data. In the present investigation the fitting of the equation was performed using a least-squares method, in the same way as was done by Müller [36].
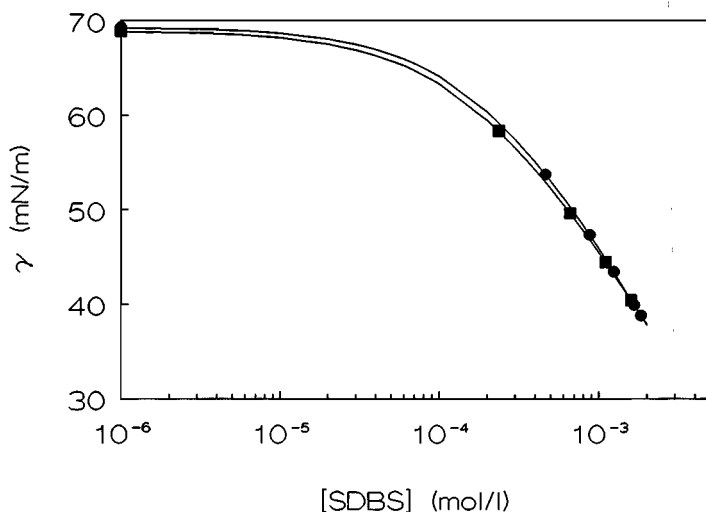
Figure 5.1: Surface tension (γ) versus concentration SDBS in the waterphase for two different supernatant titrations; ● 3.6% solids, ■ 11.8% solids. The drawn lines are the Szyszkowski fits for the two different titrations.

As can be seen from figure 5.1 the Szyszkowski equation fits the data very well. There is, however, a small difference between the two supernatant titrations. Therefore supernatant titrations have been performed for the different solids percentages used.

Using the Szyszkowski equation, it is possible to calculate, on the basis of these data, the adsorption isotherm for adsorption of SDBS on PS. This is shown in figure 5.2 for the different solids percentages used.
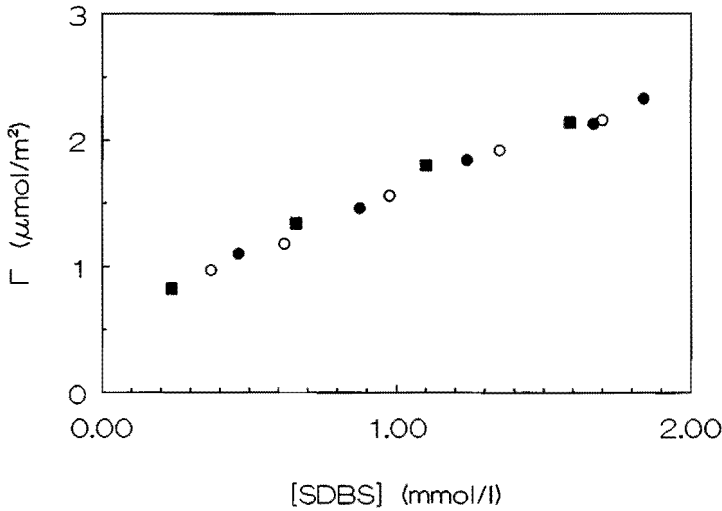
Figure 5.2: Adsorption isotherm for SDBS on latex L-78; ● *3.6 % solids,*
○ *7.6% solids,* ■ *11.8% solids.*

This isotherm is found, on closer look, not to conform to the Langmuir equation. This
equation can be written as:

$$\frac{1}{\Gamma} = \frac{1}{\Gamma^{max}} + \frac{1}{k_L \Gamma^{max}} \left(\frac{1}{c} \right)$$ (5.20)

where k_L is an adsorption/desorption constant (equal to $\exp(-\Delta G^0/RT)$ in equation (5.6)).
Equation (5.20) thus corresponds to a linear relation between $1/\Gamma$ and $1/c$.

As can be seen from figure 5.3, this is certainly not the case. At low concentrations we
observe a lower surface excess than expected from a best fit straight line through the
experimental data points, whereas at higher concentrations we observe a higher surface
excess.

In order to understand this picture, the same data points were used to calculate
$(\Delta G^0 + G^E)/RT$ of the adsorption of SDBS from solution on the basis of equation (5.17).
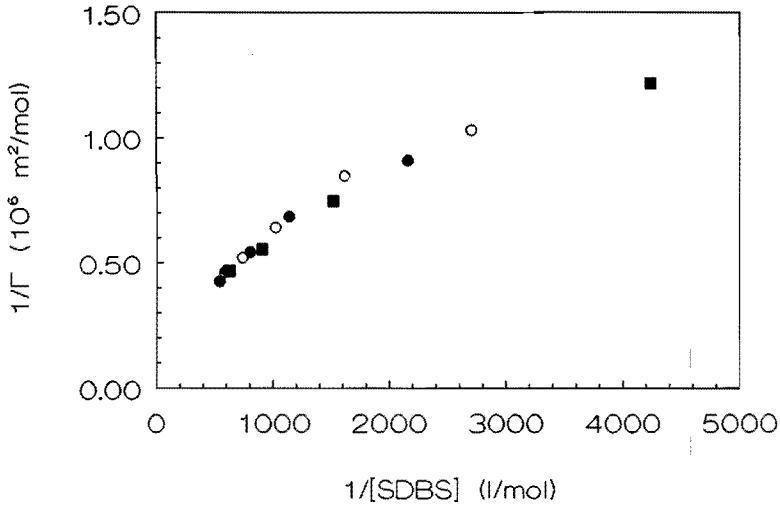
Figure 5.3: *Langmuir plot for the adsorption of SDBS on latex L-78;* ● *3.6 % solids,* ○ *7.6% solids,* ■ *11.8% solids.*

In order to calculate θ, a value for the maximum surface excess has to be assumed. We used, in the first place, the value of $1.5 * 10^{-6}$ mole/m^2. This value was calculated on the basis of an adsorption area of a SDBS molecule of 55 Å^2 [33]. In figure 5.4 the change in Gibbs free energy $((\Delta G^0 + G^E)/RT)$ as function of θ is shown for $\Gamma^{max} = 1.5 * 10^{-6}$ mole/m^2.

It is found that $(\Delta G^0 + G^E)/RT$ is dependent on θ: at low θ values, it is decidedly larger in absolute value than at high θ values. The exact form of the curve in figure 5.4 depends on the value assumed for the value of Γ^{max} used in the calculation. Thus, figure 5.5 shows a similar graph based on $\Gamma^{max} = 1.25 * 10^{-6}$ mole/m^2. The effect of $(\Delta G^0 + G^E)/RT$ being strongly negative at low θ values remains. A similar course of $(\Delta G^0 + G^E)/RT$ as a function of θ can be calculated from adsorption data of surfactants reported by e.g. Kusters [38], Ali et al. [10] and Böhmer et al. [20].
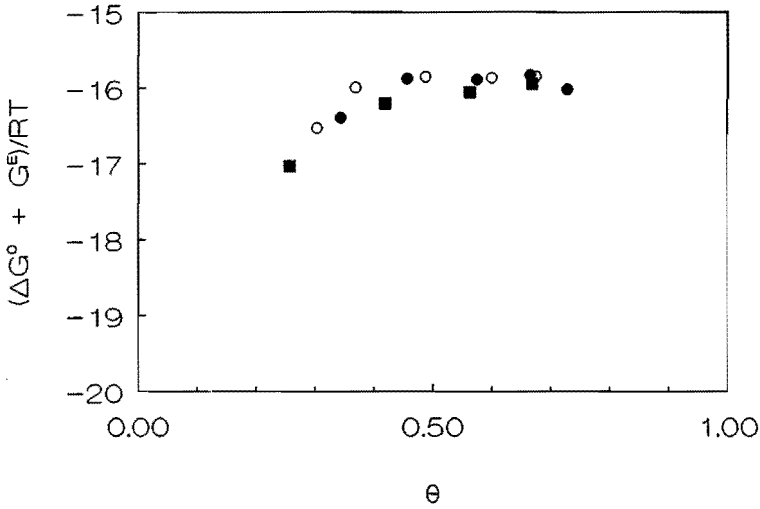
Figure 5.4: *Calculated $(\Delta G^0 + G^E)/RT$ as function of θ for $\Gamma^{max} = 1.5 * 10^{-6}$ mole/m²:*
● *3.6 % solids,* ○ *7.6% solids,* ■ *11.8% solids.*
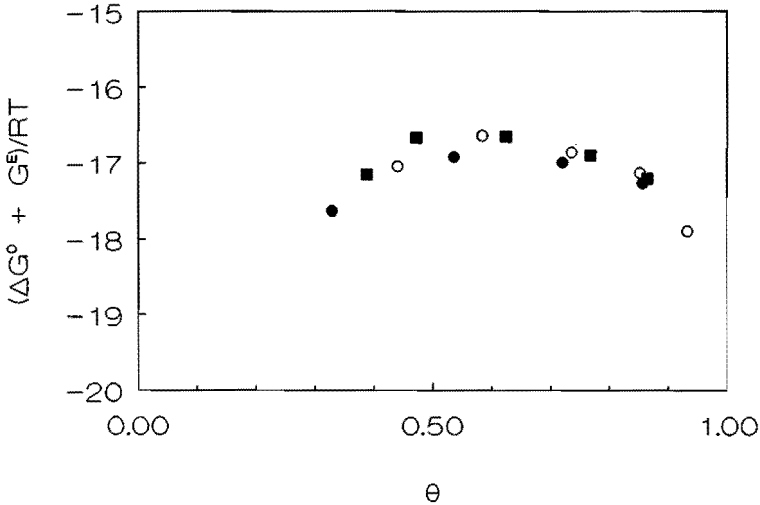
Figure 5.5: *Calculated $(\Delta G^0 + G^E)/RT$ as function of θ for $\Gamma^{max} = 1.25 * 10^{-6}$ mole/m²:*
● *3.6 % solids,* ○ *7.6% solids,* ■ *11.8% solids.*

Paxton [9] found deviations in the Langmuir plot of adsorption of ionic surfactant (SDBS) on PS-particles in absence of salt, similar to those reported here. At low concentrations of surfactant in the aqueous phase, Paxton observed a larger adsorption area than expected from the Langmuir plot. An explanation, however, was not given.

Painter [8] reported the adsorption of sodium hexadecyl sulphate on PS-particles in presence of 10^{-4} mol/l NaBr. He divided the adsorption isotherm into two regions: at low concentrations of surfactant (up to ca. $8*10^{-5}$ mol/l) the adsorption could well be described by a Langmuir adsorption isotherm, whereas at higher concentration a linear relationship between concentration of surfactant and surface excess was obtained. In the first part of the adsorption a large adsorption area for the surfactant was found. This value was comparable to the adsorption area of a surfactant molecule lying flat on the polymer surface.

Ali et al. [10] reported the adsorption of a non-ionic surfactant (octaphenoxy ethoxylate, with 18 ethylene oxide units per molecule) on PS-particles. Their Langmuir plot showed the same kind of deviations as reported here. This behaviour was attributed to the driving force of adsorption, as was given by Kronberg [18] and Kronberg et al. [19]. From thermodynamical analysis, they stated that a large part of the driving force of adsorption was due to replacement of a large number of surfactant-water interactions by surfactant-surfactant interactions. A minor part of the driving force was attributed to the replacement of surface-water contacts by surface-surfactant contacts.

However, Kronberg et al. [18,19] supposed that the configuration of the adsorbed surfactant is independent of surface coverage and concentration. This can only be defended as a first order approximation. Kronberg discusses, a.o., the possibility, that the surfactant is adsorbed in a flat configuration along the PS-surface. This model is equal to the one proposed here at low θ values.

Our data clearly indicate, that $(\Delta G^0 + G^E)/RT$ changes in the positive direction with increasing θ. This differs fundamentally from the phenomena reported by Fuerstenau et al. [12-15], in which a rapid increase of the adsorption above a certain surfactant concentration was found corresponding with hemimicelle formation. This would show up in a change of $(\Delta G^0 + G^E)/RT$ in the negative direction; this is found in the case discussed here only at large θ values.

Since ΔG^0 is, by definition, independent of θ, the variation of the quantity $\Delta G^0 + G^E$ with θ must be due to variations in G^E.

In G^E are included all effects due to interactions between the ions, both in solution and between adsorbed ions. The interactions between the ions in solution can, in the concentration range concerned, be described with reasonable precision by the Debye-Hückel equation which predicts that they are negligible (activity coefficients ranging between 1 and 0.95). The course of $(\Delta G^0 + G^E)/RT$ as a function of θ then should be ascribed to interaction between adsorbed ions.

There are two possible explanations, as far as we see:

a) The presence of negative ions on nearby sites effects an electrostatic repulsion on the ionic head groups of surfactant anions to be adsorbed; at high θ values, this is compensated by an attractive interaction between the hydrocarbon tails of adjacent surfactant ions;

b) At very low θ values, the hydrophobic tail of a surfactant ion is adsorbed onto the surface in a flat configuration, leading to a large (negative) adsorption energy which is equivalent to $\Delta G^0 + G^E$ being negative, but large in absolute sense. Adsorption in a flat configuration is no longer possible when many neighbouring sites are already occupied by other surfactant ions. This leads to a decrease in absolute sense of $\Delta G^0 + G^E$ with increasing θ.

Of these, the electrostatic interactions between the adsorbed ions are accounted for by the term $-N_A e_0(\psi_\delta - \psi_{average})$ (equation (5.14)). This term can be estimated on the basis of the Gouy-Chapman equation, assuming that the head groups of the chemisorbed anions form a kind of Stern plane while the counterions are in the diffuse part of the double layer. Thus, the potential ψ_δ is assumed to be that corresponding to a surface charge $-e_0 * \theta * n_{sites}$, where n_{sites} is the number of adsorption sites per unit surface area. This leads to [39]:

$$\sigma_0 = \epsilon_0 \epsilon_r \left(\frac{d\psi}{dx}\right)_{x=0} = \sqrt{2 n_\infty kT \epsilon_0 \epsilon_r} \left(\exp\left(-\frac{z e_0 \psi_\delta}{2kT}\right) - \exp\left(\frac{z e_0 \psi_\delta}{2kT}\right)\right) \qquad (5.21)$$

where ϵ_0 is the permittivity of the vacuum, ϵ_r is the relative permittivity, k is Boltzman's constant, σ_0 is the surface charge density and n_∞ is the concentration of ions in mole/m^3. From equation (5.21), ψ_δ can be explicitly formulated as:

$$\psi_\delta = -\frac{2kT}{e_0} \ln\left(a + \sqrt{(a^2+1)}\right) \qquad (5.22)$$

in which:

$$a = \frac{\sigma_0}{2\sqrt{2n_\infty kT\epsilon_0\epsilon_r}} \qquad (5.23)$$

The average potential, to which the counter-ions are subject, is calculated from the Gouy-Chapman theory, by:

$$\psi_{aver} = \frac{\int_{x=0}^{x=\infty} \psi\, dn}{\int_{x=0}^{x=\infty} dn} \qquad (5.24)$$

where x is the distance from the plane of the head groups of the adsorbed anions and

$$n = n_\infty \exp\left(\frac{-ze_0\psi}{kT}\right) \qquad (5.25)$$

Using formula (5.24) and (5.25), this leads to:

$$\psi_{aver} = \frac{kT}{ze_0} - \psi_\delta \frac{\exp\left(-\dfrac{ze_0\psi_\delta}{kT}\right)}{1 - \exp\left(-\dfrac{ze_0\psi_\delta}{kT}\right)} \qquad (5.26)$$

In this expression, z is the valency of the counter-ion (sign included). Thus the argument of the exponential function is always > 0: if the negative ions are chemisorbed, then ψ_δ is < 0, while z is > 0; with the minus sign before the quotient in the exponent, the argument as a whole becomes > 0. In the experimental conditions used in the present investigation, the absolute value of ψ_δ always is large enough to lead to:

$$\psi_{aver} \approx \frac{kT}{ze_0} + \psi_\delta \qquad (5.27)$$

in which again z is the valency (sign included) of the counter-ion.

It should be noted, that the assumptions underlying the Gouy-Chapman theory, are too strict for the case at hand. Especially the assumptions of the situation of the negative charges of the ionic headgroups of the adsorbed surfactant anions and of the sulphate groups on the PS-surface, arising from the initiator, in one plane is not strictly applicable. However, even in the absence of surfactant, negative zeta-potentials larger (in absolute sense) than 60 mV have been observed for the PS-latex used here [40]. Thus, the absolute value ψ_δ will be $\geq$ 60 mV. If we introduce this in equation (5.26), we find that the value of $((ze_0(\psi_\delta-\psi_{aver}))/kT$ can only vary between 1.10 and 1. Thus variations in this quantity can only account for a small part of the variation of $(\Delta G^0+G^E)/RT$ with θ.

This means, that at the θ values found in this investigation, the electrostatic term can only partially be held responsible for the dependence of ΔG^0+G^E on θ calculated from the experimental data. Thus, an important part of the change of ΔG^0+G^E at θ values < 0.5 must be due to decrease in interaction energy of the surfactant anion to be adsorbed, with the polystyrene surface. This can be understood as arising from prevention of adsorption of surfactant molecules in a flat configuration along the PS-surface with higher θ-values.

The question may be raised why the attractive interaction between neighbouring chains becomes predominant only at large θ values. This can be understood from the counter-acting effect of freedom of movement of the adsorbed hydrocarbon chains when not bound directly to an adjacent hydrocarbon chain; only at large θ values are the chains so much limited in their movement that the attractive interaction prevails. This effect is analogous to the attractive interaction between dissolved surfactant molecules leading to micelle formation at large concentrations only. In the case of adsorbed surfactant ions, this effect will be strengthened, because at large θ values the surfactant chains will contact the polystyrene surface with their final CH_3- group only (if the explanation offered here for the dependence of ΔG^0+G^E on θ is right); this leads to a large contact zone with an adjacent hydrocarbon chain.

The change of $(\Delta G^0+G^E)/RT$ in the negative direction at large values of θ is analogous to the hemimicelle formation observed by Fuerstenau et al. in the case of adsorption of ionic surfactants on mineral surfaces (ref. [12]-[15]).

Nevertheless, there is a net electrostatic repulsion between adsorbed surfactant ions, since $-e_0*(\psi_\delta-\psi_{average})$ is > 0. Thus, on simultaneous adsorption of a cosurfactant which has an

attractive energy with the surfactant's hydrocarbon chain but no electrostatic repulsion with its head group, the adsorption of the surfactant itself is stimulated [33].

Thus, the increase of surfactant adsorption in the presence of a cosurfactant supports the explanation of the $(\Delta G^0 + G^E)/RT$ versus θ curve given here. In addition, this model agrees with calculations by Böhmer and Koopal [20-22] on the distribution of surfactant segments in the vicinity of a solid surface, although the surfaces considered by these authors differ significantly from those investigated in the present study.

5.5 Conclusions

G^E, the excess change of the Gibbs free energy of adsorption of an ionic surfactant, is calculated here as compromising all effects of interaction between adsorbed ions and between ions in solution. As starting point, localized adsorption is assumed for the surface active ion, while mobile adsorption is assumed for the counter ion.

G^E is found to significantly depend on the degree of occupation, θ, of the adsorption sites. This dependence can be understood as indicating negative adsorption energy, large in absolute sense, at very low θ values, corresponding with adsorption of the surface active ion on the surface in a flat configuration. At higher θ values, this is no longer possible and the absolute value of the adsorption energy decreases, corresponding to a change from a flat to a more dense configuration.

5.6 References

(1) Maron, S. H., Elder, M. E., Ulevitch, I. N., *J. Colloid Interface Sci.*, **1954**, *9*, 89.

(2) Vijayendran, B. R., Bone, T., Gajria, C., *J. Appl. Polym. Sci*, **1981**, *26*, 1351.

(3) Maurice, A. M., *J. Appl. Polym. Sci*, **1985**, *30*, 473.

(4) Vijayendran, B. R., *J. Appl. Polym. Sci*, **1979**, *23*, 733.

(5) Piirma, I., Chen, S. R., *J. Colloid Interface Sci.*, **1980**, *74*, 90.

(6) Urban, P. C., *J. Disp. Sci. Tech.*, **1981**, *2*, 233.

(7) Connor, P., Ottewill, R. H., *J. Colloid Interface Sci.*, **1971**, *37*, 642.

(8) Painter, D., Hall, D. G., Wyn-Jones, E., *J. Chem. Soc., Faraday Trans 1*, **1988**, *84*, 773.

(9) Paxton, T. R., *J. Colloid Interface Sci.*, **1969**, *31*, 19.

(10) Ali, S. I., Steach, J. C., Zollars, R. L., *Colloids Surfaces*, **1987**, *26* ,1.

(11) Bijsterbosch, B. H., *J. Colloid Interface Sci.*, **1974**, *47(1)*, 186.

(12) Fuerstenau, D. W., *J. Phys. Chem.*, **1956**, *60*, 981.

(13) Gaudin, A. M., Fuerstenau, D. W., *Trans. Metal Soc. AIME*, **1964**, *202*, 958.

(14) Fuerstenau, D. W., Healy, T. W., Somasundaran, P., *Trans. Metal Soc. AIME*, **1964**, *229*, 321.

(15) Fuerstenau, D. W., *Pure and Applied Chemistry*, **1970**, *24*, 135.

(16) Goodwin, J. W., *Trans. Brit. Ceram. Soc.* **1971**, *70*, 65.

(17) Welzen, J. Th. A. M, Stein, H. N., Stevels, J. M., Siskens, C. A. M., *J. Colloid Interface Sci.*, **1981**, *81*, 455.

(18) Kronberg, B., *J. Colloid Interface Sci.*, **1983**, *96(1)*, 55.

(19) Kronberg, B., Stenius, P., Igeborn, G., *J. Colloid Interface Sci.*, **1984**, *102(2)*, 418.

(20) Böhmer, M. R., Koopal, L. K., *Langmuir*, **1992**, *8*, 1594.

(21) Böhmer, M. R., Koopal, L. K., *Langmuir*, **1992**, *8*, 2649.

(22) Böhmer, M. R., Koopal, L. K., *Langmuir*, **1992**, *8*, 2660.

(23) Scheutjes, J. M. H. M., Fleer, G. J., *J. Phys. Chem*, **1979**, *83*, 1619.

(24) Scheutjes, J. M. H. M., Fleer, G. J., *J. Phys. Chem*, **1980**, *84*, 178.

(25) Fowler, R., Guggenheim, E. A., *Statistical Thermodynamics*, 2nd Impression, Cambridge University Press, **1956**, p. 421-428.

(26) Jaycock, M. J., Parfitt, G. D., *Chemistry at interfaces*, J. Wiley and Sons, **1981**, p. 183.

(27) Ross, S., Olivier, J. P., *On Physical Adsorption*, Intersciences, **1964**, p. 8.

(28) Aveyard, R., Haydon, D.A., *An Introduction to the Principles of Surface Chemistry*, Cambridge Chemistry Texts, **1973**, p.22.

(29) Oh, S. G., Shah, D. O., *J. Phys. Chem.*, **1993**, *97*, 284.

(30) Clayfield, E. J., Matthews, J. B., *Proceedings of the 2nd International Congress of Surface Activity. Gas/liquid and liquid/liquid interface.* Butterworths Scientific Publications, London, **1957**, p. 172.

(31) Stigter, D., Mysels, K. J., *J. Phys. Chem.*, **1955**, *59*, 45.

(32) Tuin, G., Peters, A. C. I. A., Van Diemen, A. J. G., Stein, H. N., *J. Colloid Interface Sci*, **1993**, *158(2)*, 508; see also chapter 2 of this thesis.

(33) Tuin, G., Stein, H. N., *Langmuir*, **1994**, *10(4)*, 1054; see also chapter 4 of this thesis.

(34) Von Szyszkowski, B., *Z. Phys. Chem*, **1908**, *64*, 385.

(35) Rosen, M. J., Aronson, S., *Colloids Surf.*, **1981**, *3*, 201.

(36) Müller, A., *Colloids Surf.*, **1991**, *57*, 219.

(37) Kegel, W. K., Van Aken, G. A., Bouts, M. N., Lekkerkerker, H. N. W., Overbeek, J. Th. G., de Bruyn, P. L., *Langmuir*, **1993**, *9*, 252.

(38) Kusters, J. H. M., *Ph. D. Thesis*, **1994**, p. 102.

(39) Hiemenz, P. C., *Principles of Colloid and Surface Chemistry*, 2nd ed., Marcel Dekker Inc, **1986**, p. 700.

(40) Tuin, G., Senders, J. H. J. E., Stein, H. N., to be published.

CHAPTER 6

BREAK-UP OF EMULSION DROPLETS IN STIRRED VESSELS

Summary: In this chapter the preparation of emulsions in a stirred vessel is described. It is found, that the equilibrium droplet-size is determined by break-up processes, which have very long time scales. The equilibrium droplet-size was in most of the experiments reached after more than 100 minutes. This time scale seems not to be strongly influenced by process-variables, such as the concentration of surfactant (and consequently the interfacial tension), stirrer speed, volume fraction dispersed phase or temperature.

The Weber number theory has found to be correct, with the exception that in this theory a dynamic interfacial tension should be used instead of the equilibrium value. An attempt has been made to correlate this difference between dynamic and equilibrium interfacial tension ($\Delta\gamma$), by using the elasticity modulus of expanding interfaces. It was found, that the curves of $\Delta\gamma$ and the elasticity modulus versus concentration have the same shape, but the concentration where the maximum is found experimentally, is located at a higher concentration than expected from the theory used. This fact is attributed to the fact, that this theory assumes deformations of the interface at situations close to equilibrium. In our case this is not the case, but theories for deformations far from equilibrium have not been developed so far.

The addition of cosurfactants results in smaller droplet-sizes and a reduction in the time to reach a steady state situation. The smaller droplet-size is attributed to the fact, that the interfacial tension decreases by the addition of cosurfactants. The influence of cosurfactants is the most pronounced, when they are added to the oil-phase. In this case the difference between equilibrium and dynamic interfacial tension is close to zero.

6.1 Introduction

An emulsion, consisting of two liquid phases that are mutually not or only slightly miscible, can be prepared in many different ways. The process of emulsification is usually achieved by applying mechanical energy. Many different apparatuses can be used for the preparation of emulsions [1], like the Ultra-turrax, colloid mill, homogenizers and stirred vessels. Emulsions prepared in stirred vessels usually have larger droplet sizes, then when other techniques are used, because in general the energy input is lower.

In this investigation we used a stirred vessel, to test the theory of droplet break-up in a stirred vessel and to validate the various aspects involved. In the second part of this chapter the influence of a cosurfactant will be investigated.

6.2 Theory

The theory of local isotropic turbulence [2],[3] has been reviewed extensively [4], [5]. Therefore only a very brief summary will be given below.

The "energy cascade of turbulence" model assumes, that fluid eddies range in size from a small scale to a large one, which is determined by the bounds of the vessel. Energy is transferred via an impeller to these large eddies and they, in turn, transfer their energy to the smaller eddies, until energy is transferred to the smallest eddy. These eddies loose their energy by viscous dissipation. The smaller eddies become statistically independent from the larger ones.

Kolmogorov [2],[3] advanced the hypothesis, that in any turbulent flow at sufficiently high Reynolds numbers, the small-scale components of the turbulent flow velocity fluctuations are statistically independent of the main flow and of the turbulence-generating mechanism. The small-scale velocity fluctuations are determined by the local rate of energy dissipation per unit mass of fluid ϵ and the kinematic viscosity ν. This range is called the universal equilibrium range and is subdivided in two subranges: the inertial subrange, where the energy spectrum is independent of ν and solely dependent of ϵ, and the viscous subrange, where the energy spectrum is dependent on both ν and ϵ.

In other words, the spectrum of turbulent velocity fluctuations includes a range of high wave-numbers called the "universal equilibrium range", which is uniquely determined by ϵ and ν. The length scale characteristics of this range were derived from dimensional reasoning by Kolmogorov:

$$L_k = \left(\frac{\nu^3}{\epsilon} \right)^{1/4} \tag{6.1}$$

where L_k is the Kolmogorov length scale. This scale can be used to distinguish between the various break-up mechanisms, which can occur in the stirred vessel. If the maximum droplet size, d_{max}, is small in comparison with L_k than droplet break-up is viscosity dominated, whereas if d_{max} is large in comparison with L_k droplet break-up is inertia dominated.

As will be shown later, most of the emulsion droplets in low viscosity fluids have d_{max}-values larger than the length scale of the Kolmogorov eddy, and consequently the

break-up is inertia dominated. The work of Kolmogorov [2],[3] and Hinze [6] suggests that a drop would deform and break in a turbulent environment, when the shape-restoring interfacial forces and viscous resistive forces set up in the drop are unable to counter the random pressure fluctuations that drive the deformation. Shinnar [7] extended Kolmogorov's concept of locally isotropic turbulence to the flow field inside a stirred vessel and derived theoretically the following expression for d_{max}, the upper limit on the size of a drop that is capable of withstanding the turbulence without further disintegration:

$$\frac{d_{max}}{D_{imp}} = C_1 We_{imp}^{-0.6} \qquad (6.2)$$

where D_{imp} is the impeller diameter, C_1 is a constant and We_{imp} is the impeller Weber number, defined by:

$$We_{imp} = \frac{\rho N^2 D_{imp}^3}{\gamma} \qquad (6.3)$$

where N is the stirrer speed (rps), ρ is the density of the continuous phase and γ is the interfacial tension. Equation (6.2) is valid when the viscous forces in the dispersed phase are not significant. Sprow [8] has found the constant C_1 to vary between 0.126 and 0.15, whereas Lagisetty et al. [9] found the constant to be 0.125.

The work of Shinnar and Church [10] and Chen and Middleman [11], has led to the development and verification of the Weber number theory for prediction of the average equilibrium droplet-size. As applied to dilute suspensions in baffled cylindrical vessels, as was done a.o. by Godfrey et al. [12] and Sharma et al. [13] the correlation is:

$$\frac{d_{3,2}}{D_{imp}} = C_2 We_{imp}^{-0.6} \qquad (6.4)$$

where C_2 is a constant (depending on the vessel geometry and impeller type), $d_{3,2}$ is the surface average diameter (Sauter mean diameter), which is given by:

$$d_{3,2} = \frac{\sum\limits_{i=1}^{i=M} n_i D_i^3}{\sum\limits_{i=1}^{i=M} n_i D_i^2} \tag{6.5}$$

where n_i is the number of droplets with diameter D_i. The Sauter mean diameter $d_{3,2}$ is a convenient diameter, since the interfacial area (a) per unit volume is given by:

$$a = \frac{6\phi}{d_{3,2}} \tag{6.6}$$

where ϕ is the volume fraction.

It is clear that from equations (6.2) and (6.4) follows that:

$$d_{max} = C_3 \, d_{3,2} \tag{6.7}$$

The value of C_3 is approximately 1.5 [14] for low viscosity dispersed phase.

As the dispersed phase volume fraction (ϕ) is increased, the drop size has generally been found to increase, because of the damping of the intensity of the turbulent field. This has been taken into account by a semi-empirical modification in equation (6.2). Various expressions used by different investigators to calculate d_{max} have been reviewed by Coulaloglou and Tavlarides [15]. The general form of the correlation is:

$$\frac{d_{max}}{D_{imp}} = C_3 (1 + C_4 \phi) \, We_{imp}^{-0.6} \tag{6.8}$$

Lagisetty et al. [9] obtained the following expression for a dispersed phase with low viscosity:

$$\frac{d_{max}}{D_{imp}} = 0.125 (1 + 4\phi)^{1.2} \, We_{imp}^{-0.6} \tag{6.9}$$

Equations (6.8) and (6.9) predict, that as ϕ is increases, the d_{max}-value should increase monotonically. This behaviour is indeed found, up to a volume fraction of 0.4 [9]. At higher ϕ-values, the experimental d_{max}-value decreases. Grosso et al. [16] mentioned that for ϕ-values larger than 0.5, the drop size decreases with increasing ϕ.

The influence of surfactants on the break-up of emulsion droplets in stirred vessels was

investigated by Koshy et al. [17]. Addition of surfactant reduces the interfacial tension and consequently the droplet-size will be reduced. Two systems with identical interfacial tension were studied; the water-octanol system had an interfacial tension of 8.3 mN/m in the absence of surfactant, whereas the system water-styrene had an interfacial tension of 34 mN/m before addition of surfactant. The surfactant Teepol was added to the water-styrene system to bring the interfacial tension to 8.3 mN/m. The viscosities of both the dispersed and continuous phases were too low to affect the droplet-size. It was observed that the droplet-size in the water-styrene system was considerably lower than that in the water-octanol system. These results should indicate, that the surfactant not only influences the interfacial tension, but also affects the break-up in a way the models presented above do not account for. Koshy et al. [17] argued that this difference was to be attributed to the difference in static (equilibrium) and dynamic interfacial tension. As a droplet is deformed and break-up takes place, the freshly created interface will have a dynamic (non-equilibrium) interfacial tension, where the non-deformed interface will have the equilibrium interfacial tension. In equation (6.8) the equilibrium interfacial tension was replaced by a dynamic interfacial tension. When the modified equation was used, good correlation was obtained for experimental droplet-sizes and theoretical predictions.

This effect is only operative at dispersed phases with low viscosity. It is expected, that if a high viscosity dispersed phase is present, the surfactant used has a small effect, as the break-up is determined by viscous stress and not by interfacial tension gradients.

In general in dispersion processes, coalescence of droplets is a process that can not be ruled out beforehand. This phenomena will especially take place, if the emulsion is poorly stabilized. From the results presented here, it will become clear that sufficient measures have been taken to prevent coalescence.

In this chapter the break-up of droplets in a stirred vessel will be investigated. Besides the process variables, such as stirrer speed and volume fraction, special attention will be paid to the effects of surfactants and cosurfactants on the break-up behaviour of emulsion droplets.

6.3 Experimental

6.3.1 Materials

Sodium dodecylbenzenesulfonate (SDBS): ex. Albright and Wilson (Nansa 1260, 25% w/v in water) was used without further purification, because surface tension (γ) measurements showed no minimum in the γ versus concentration curves, indicative for the absence of surface active impurities.

Dobanol 91-8: ex. Shell, was used without further purification. The structural formula is H-$(CH_2)_n$-O-$(CH_2$-$CH_2O)_m$-H, with m=8 and n ranges from 9 to 11.

Water was distilled twice using an all glass apparatus.

Decane: ex. Merck (zur Synthese, purity > 99%) was used without further purification.

Dodecanol: ex. Merck (purity > 95%) was used without further purification.

The emulsions were prepared in the stirred vessel shown in figure 6.1. The vessel was filled with surfactant solutions and the stirrer speed was set to the desired value. After all the air bubbles had disappeared along the stirrer shaft, the oil phase was injected using an Orion 940/960 Autochemistry system titrator (Orion Research Inc., USA). At regular intervals a sample was withdrawn, which was measured using the Coulter Counter.

To ensure that single particles are detected in the coulter Counter, the samples have to be diluted by a conducting liquid (Isoton II, Coulter Electronics). Samples were drawn from the mixing vessel, through a sampling probe located at the height of the impeller stream. Samples were also taken at various points in vessel, but no systematic difference was found. Therefore, all samples were taken at the impeller stream.

These samples were diluted with 100 ml Isoton II. This solution was gently stirred, to keep the emulsion droplets suspended while measuring. At least 20000 particles were counted for each sample drawn.

The emulsions prepared were sufficiently stable to be determined by the Coulter Counter. After emulsions had been prepared, they were kept standing for several weeks without stirring. During this time, creaming was observed. Of these emulsions samples were taken, diluted with Isoton and suspended while gently stirring. The stability is testified by the fact, that emulsions had the same particle size distributions after several weeks. Additional, emulsions were prepared as described before. After an equilibrium droplet-size had developed, 5 ml of a 5 M NaCl solution was added, while stirring. No change in

droplet-size was observed, even while stirring was stopped.

6.3.2 Vessel

The perspex vessel used had a flat bottom, four vertical baffles, a tilted cover with angle α and a height equal to the tank diameter. The vessel was completely filled with surfactant solution. The top cover was placed at an angle α, to remove air bubbles introduced on filling the vessel. The stirrer, a standard Rushton disc turbine impeller, had a diameter of one third of the vessel diameter and was placed in the middle of the vessel, giving qualitative similar flow patterns in top and bottom section. The stirrer motor (Jahnke & Kunkel, IKA Labor Technik, Germany) had a facility to keep the stirrer speed constant with variations less than $\pm 1\%$.

In the vessel a sampling probe and a dispenser outlet were fitted.

The vessel was surrounded by water regulated by a temperature bath, so that the temperature could be varied between 20 °C and 70 °C.

The dimensions of the vessel and stirrer are summarized in table 6.1. In figure 6.1 the vessel is shown from side and top view.

The total power input was measured using a torque meter (Visco-Mix, ATP-Engineering, The Netherlands), which was placed between the stirrer motor and the stirrer. The torque meter was checked by measuring the viscosity of water, which was within 1% of the expected value.

6.3.3 Methods

Particle sizes and particle size distributions were measured with the Coulter Counter (Coulter Electronics Ltd., England), equipped with an 200 μm orifice and range expander. The Coulter Counter was regularly calibrated using a calibration latex of 18.3 μm.

The Coulter Counter determines both the number and the size of the emulsion droplets suspended in an electrically conductive liquid, by forcing the droplets through a small aperture between two electrodes. The resistance between the electrodes changes as a particle goes through the aperture and this change is converted to a voltage pulse. These pulses are counted and are approximately proportional to the particle volume.
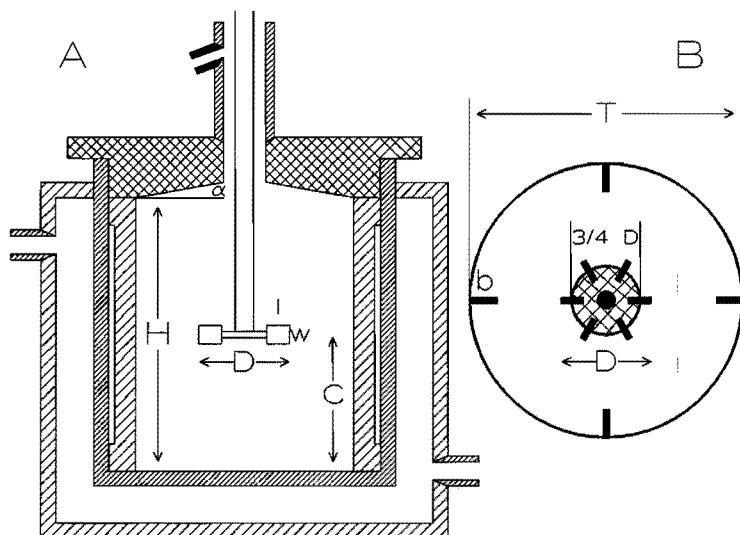
Figure 6.1: Schematic view of the stirred vessel used; A side view, B top view. The symbols are listed in table 6.1.

Table 6.1: Dimensions of the vessel and turbine impeller used[a].

vessel diameter T	90
vessel height H	90
width baffle	9
thickness baffle	2
impeller diameter D	30
blade width w	6
blade length l	7.5
blade thickness d	2
disc diameter	22.5
disc thickness	2
shaft diameter	6
height of stirrer from bottom C	30 or 45

[a] All dimensions are in mm.

Therefore the diameter, corresponding to a particular particle count, can be established. For the principles of operation and analysis of data, see e.g. [18]. The accuracy of the Coulter Counter was found to be within 0.5 μm (less than 3% of the average value). In appendix A a comparison is made for droplet-size measurements with Coulter Counter, Coulter LS 130 (light scattering) and light microscopy.

Interfacial tension measurements are described in appendix B.

6.4 Results

The results in this chapter are all related to break-up processes, because the process of coalescence does not occur in our system. This is testified by the fact, that the same droplet-size distributions are found in regions with high shear (near the impeller tip) and in regions with low shear (near the walls of the vessel). It was also observed, that the droplet-size distribution did not change, when prepared emulsions were left standing for 4 weeks.

6.4.1 Impeller power numbers

The power number (N_p) of the impeller is given by [19]:

$$N_p = \frac{P}{\rho N^3 D_{imp}^5}$$
(6.10)

where P is the impeller power input (J/s), ρ is the fluid density, N is the impeller rotational speed and D_{imp} is the impeller diameter.

The impeller Reynolds number Re_D, is given by:

$$Re_D = \frac{N D_{imp}^2}{\nu}$$
(6.11)

where ν is the kinematic viscosity of the bulk liquid.

In figure 6.2 the impeller power number, N_p, versus the impeller Reynolds number, Re_D, is shown for two different heights of the stirrer (C/H is 0.33 and 0.5; for a definition of C and H see figure 6.1).

As can be seen from figure 6.2, the impeller power numbers for the two different heights are equal (about 4.4) and almost constant, as expected for closed baffled vessels at large

impeller Reynolds numbers [20].

The value of 4.4, found in this investigation for the impeller power number, is within the values found by other investigators for geometrically similar vessels: Höcker [21] found a value of 5.0 for C/H = 0.33, whereas Einekel [22] found a value of 3.55 for C/H = 0.3. Differences for N_p can be attributed to small scale effects and improper scaling of the minor dimensions [23].
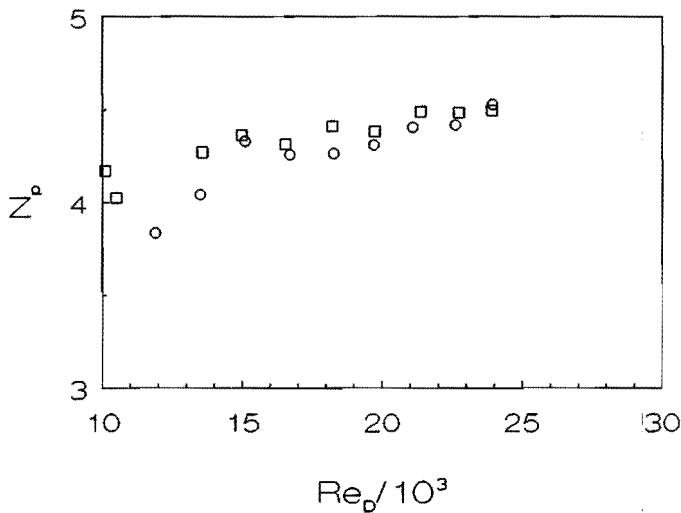
Figure 6.2: Impeller power number (N_p) versus impeller Reynolds number (Re_D):
O C/T = 0.5, □ C/T = 0.33.

For large impeller Reynolds numbers ($Re_D \geq \approx 10^4$) the power consumption on baffled stirred vessels originates fully from turbulent energy dissipation [24]. Therefore, for large Re_D, the mean turbulent energy dissipation rate (ϵ_{av}) in stirred vessels may be estimated by:

$$\epsilon_{av} = \frac{P}{\rho V} = \frac{N_p N^3 D_{imp}^5}{V} \qquad (6.12)$$

where V is the volume of the liquid in the vessel. Droplet break-up is determined by the maximum ϵ prevailing in the impeller regime. The maximum ϵ might be a factor of 10

higher than the ϵ-value averaged over the impeller regime [25]. In addition the ϵ-value averaged over the impeller regime is considerably larger than ϵ_{av}: for D_{imp}/D_{vessel} of 0.5 a factor 8 was experimentally found by Okamoto et al. [26]. The calculation of L_k is possible using equation (6.12). For a stirrer speed of 25 rps, the value of $N_p = 4.4$ and using ϵ_{av}, we obtain a L_k of 24.3 μm. This value is probably lower because of the higher ϵ prevailing in the impeller regime, where break-up is thought to take place (ϵ_{max} is approx. 80 times ϵ_{av}). All emulsions presented in this chapter have a d_{max} of 30-40 μm or larger, which is larger than L_k. The droplet break-up process is therefore predominantly inertia dominated.

6.4.2 Verification of the Weber-number theory

Emulsions were prepared in solutions with different concentrations SDBS (both below and above the cmc) at 20 °C, with different volume fractions, ranging from $4.3*10^{-3}$ to 0.03 and a stirrer speed of 1500 rpm.

In figure 6.3 the change in $d_{3,2}$ and d_{max} with time is shown for emulsion E62 (see table 6.2), with a ϕ of 0.03, a [SDBS] of $3.5*10^{-3}$ mol/l and a stirrer speed 1500 rpm, as an example.

A typical distribution is presented in appendix A. The value of d_{max} is determined from the cumulative distribution as the diameter which presents 99% of the distribution.

As can be seen from figure 6.3, both d_{max} and $d_{3,2}$ change in time, reaching a steady droplet-size after approximately 120 minutes. This long time-scale is found for emulsions with different ϕ-values (up to 0.1). When preparing the emulsions, the initial division of the dispersed phase into droplets occurs rather fast, whereas further break-up is rather slow.

This is more clearly shown in figure 6.4, where the logarithm of the droplet-size is shown as function of the logarithm of time. As can be seen from figure 6.4, there are two regimes to be distinguished. The first regime is where the droplet-size is decreasing and the second regime where the droplet-size remains constant (within experimental error).

As the average circulation time is of the order of one second [35], the droplets have to pass the impeller region several thousands of times, before a stable droplet-size is reached. Similar results are also found in the literature [27],[28]. It is also shown

in figure 6.3 and figure 6.4, that the decrease in size of d_{max} is more pronounced than that of $d_{3,2}$, although both processes have the same time scale.
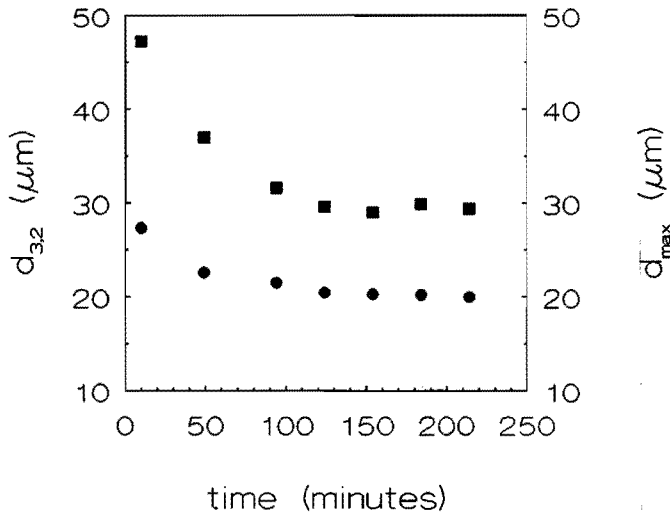

Figure 6.3: Change in $d_{3,2}$ (●) and d_{max} (■) with time for emulsion E62: ϕ = 0.03, [SDBS] = $3.5*10^3$ mol/l, stirrer speed 1500 rpm.
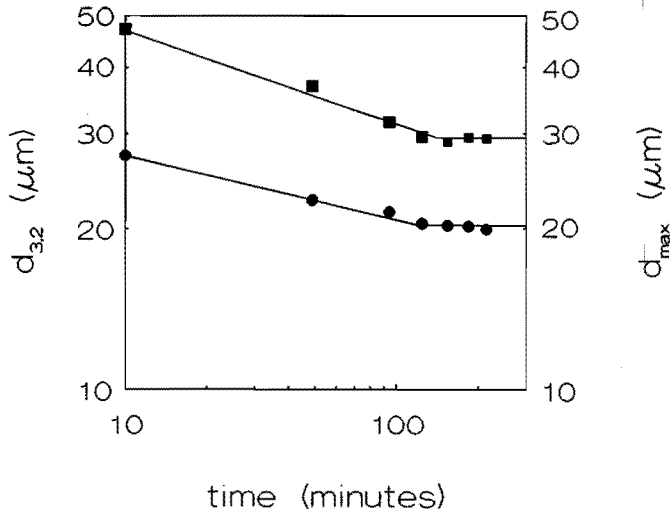

Figure 6.4: Logarithm of $d_{3,2}$ (●) and d_{max} (■) versus logarithm of time for emulsion E62: ϕ = 0.03, [SDBS] $3.5*10^3$ mol/l, stirrer speed 1500 rpm.

In table 6.2 the obtained final values for $d_{3,2}$ and d_{max} for the different emulsions investigated are listed, together with values for the constants C_1 (equation (6.2)) and C_2 (equation (6.4)). From table 6.2 it can be seen, that although there is some scatter in the constants C_1 and C_2, these differences are not very pronounced. For the constant C_1 an average value of 0.126 ± 0.014 was calculated, whereas for the constant C_2 an average value of 0.0778 ± 0.011 was found. The average value of the constant C_1 is within the values found in the literature [8],[9]. From the constants C_1 and C_2 the mean $d_{max}/d_{3,2}$ can be calculated and was found to be 1.62, close to literature values [14], which are approximately 1.5.

Table 6.2: Calculated values for the constants c_1 and c_2 for different emulsions, prepared at 20 °C and a stirrer speed of 1500 rpm.

Emulsion	ϕ	[SDBS] (mol/l)	γ (mN/m)	d_{max} (μm)	C_1	$d_{3,2}$ (μm)	C_2
E91	$4.3*10^{-3}$	$1.0*10^{-3}$	12.1	41.5	0.107	22.2	0.0571
E88	$4.3*10^{-3}$	$1.0*10^{-2}$	5.8	30.3	0.122	18.4	0.0739
E72	$8.5*10^{-3}$	$3.4*10^{-3}$	6.1	35.3	0.137	21.1	0.0820
E69	$3*10^{-2}$	$3.4*10^{-3}$	6.1	38.4	0.149	23.3	0.0903
E68	$3*10^{-2}$	$3.4*10^{-3}$	6.1	32.3	0.125	22.1	0.0857
E62	$3*10^{-2}$	$3.4*10^{-3}$	6.1	29.4	0.114	20.0	0.0776

6.4.3 Influence of stirrer speed

The influence of the stirrer speed is described by equations (6.2) and (6.4). In figure 6.5 the evolution of the droplet-size of an emulsion is shown at different stirrer speeds. The stirrer speed was started at 1000 rpm and subsequently increased as a stable droplet-size has developed. As can be seen from figure 6.6, the plots of log $d_{3,2}$ versus log N are linear and the slope, calculated by linear regression, was found to be -1.24. This value is very close to the value predicted by equation (6.4), which can be rewritten as:

$$d_{3,2} = C_2 D_{imp} \left(\frac{\gamma}{\rho D_{imp}^3 N^2} \right)^{0.6} \qquad (6.13)$$
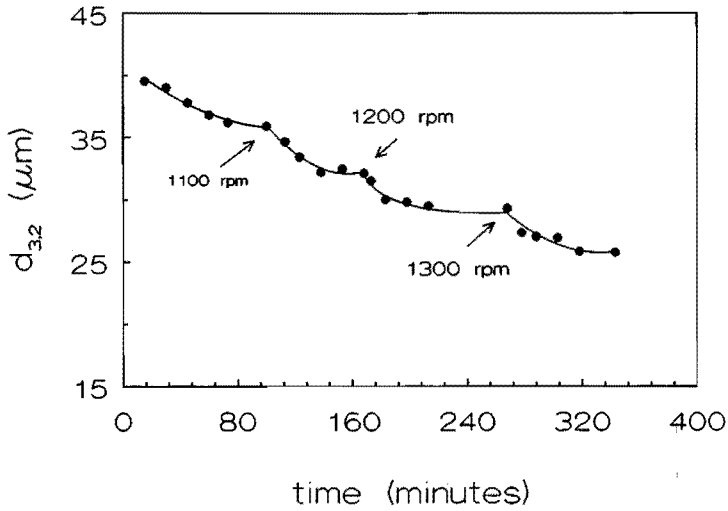
Figure 6.5: *Change in $d_{3,2}$ with increasing stirrer speed. Emulsion prepared with $\phi = 0.03$, [SDBS] $= 3.5*10^{-3}$ mol/l. At $t = 0$ the emulsification was started with a stirrer speed of 1000 rpm. The lines are just a guide to the eye.*
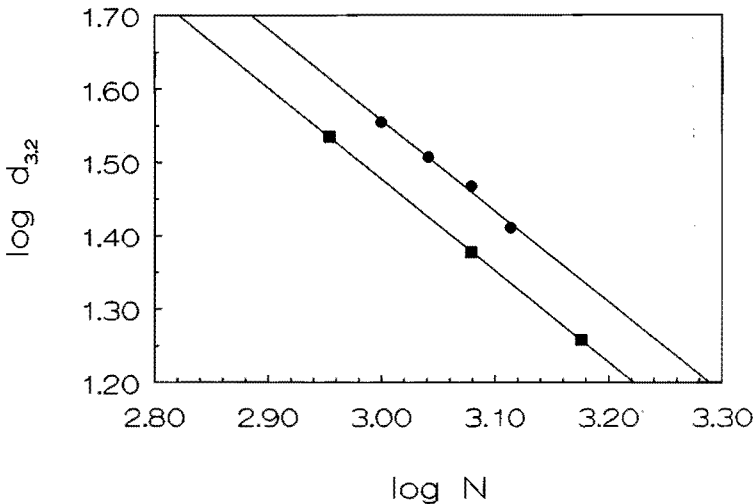
Figure 6.6: *Logarithm of $d_{3,2}$ versus logarithm of stirrer speed (N); ■ Emulsion EG10, $\phi = 0.01$, [SDBS] $= 0,01$ M, $T=30$ °C; ● Emulsion E66, [SDBS] $= 3.5*10^{-3}$ M, $T = 20$ °C, $\phi = 0.03$.*

6.4.4 Influence of temperature

The influence of the temperature on the emulsification process is related to more than one process. The first influence is the change in interfacial tension. At higher temperatures usually a lower interfacial tension is found. According to equation (6.2) this would result in a lower droplet-size. However, the density becomes also lower at higher temperatures and according to the same equation this would result in a larger droplet-size. The lower viscosity at higher temperature, does not influence the break-up process, because this is inertia dominated.

The final droplet-size is thus dependent upon the strongest influence of these two processes. With the apparatus available, it was not possible to measure accurately the interfacial tension at higher temperatures; consequently the discussion on the influence on the temperature must remain rather empirical.

Although the emulsions presented in figure 6.7 have different volume fractions, it is clear from figure 6.7, that a higher temperature results in a lower $d_{3,2}$. As stated earlier, this is probably due to the interfacial tension being lower at higher temperatures.
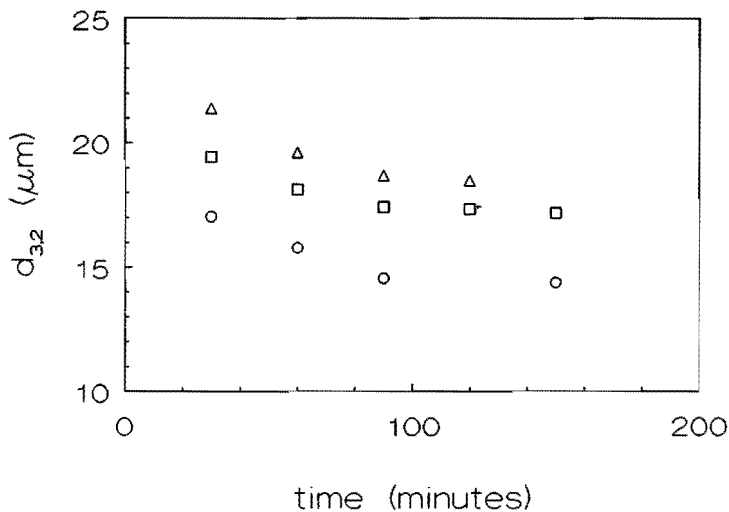
*Figure 6.7: Influence of temperature on the change of $d_{3,2}$ with time; for all emulsions [SDBS] = 0.01 M, stirrer speed 1500 rpm; Δ T = 20 °C, ϕ = 4.3*10^{-3}; $\square$ T = 30 °C, ϕ = 0.01; $\bigcirc$ T=65 °C, ϕ = 4.3*10^{-3}.*

6.4.5 Influence of volume fraction

In equation (6.8) the influence of the volume fraction on the value of d_{max} was given. It is also possible to rewrite this equation into:

$$\frac{d_{3,2}}{D_{imp}} = C_5(1 + C_6\phi) \, We_{imp}^{-0.6} \tag{6.14}$$

In order to calculate the constants C_5 and C_6, this equation was rewritten as:

$$\frac{d_{3,2} \, We_{imp}^{0.6}}{D_{imp}} = Q_{We} = C_5(1 + C_6\phi) \tag{6.15}$$

Here Q_{We} represents all input parameters not related to the volume fraction.

In figure 6.8 Q_{we} is plotted versus the volume fraction of the dispersed phase. As can be seen from figure 6.8, Q_{We} is a linear function of the volume fraction, as predicted by equation (6.15).

Figure 6.8: *Q_{We} versus volume fraction for different emulsions: [SDBS] = 10^{-2} M, T = 20 °C, stirrer speed 1500 rpm, Q_{We} has been defined by equation (6.15).*

The constant C_5 was calculated to be 0.075 and the constant C_6 was found to be 5.6. These values are slightly different from the value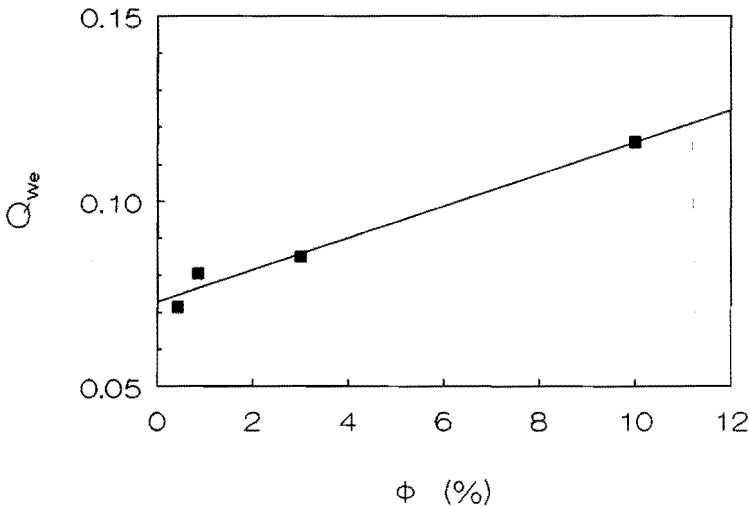s of Lagisetty et al. [9], who found for C_5 a value of 0.125 and for C_6 a value of 4. We used the relationship for $d_{3,2}$, whereas Lagisetty et al. [9] used the relationship for d_{max}. As $d_{max}/d_{3,2}$ is approximately 1.6 in our systems, the value of C_5 will be 1.6 times larger. In that case comparison is satisfactory. We find, however, a stronger dependence of the droplet-size with the volume fraction.

6.5 Influence of surfactants on the break-up of droplets

In figure 6.9 the $d_{3,2}$ is presented as function of the equilibrium interfacial tension (γ_{eq}) for both the surfactants SDBS and Dobanol 91-8. Equation (6.2) can be rewritten as:

$$d_{3,2} = C_2 D_{imp} \left(\frac{\gamma}{\rho \, D_{imp}^3 \, N^2} \right)^{0.6} \tag{6.16}$$

As can be seen from figure 6.9, reasonable straight lines are obtained (disregarding the scatter of the data) in accordance to equation (6.16), but in both cases the slope is not in agreement with the value predicted by equation (6.16). For the emulsions prepared with SDBS a slope of 0.3 is obtained, whereas for Dobanol a value of 0.5 is found. The theoretical prediction is, however, a slope of 0.6.

Another way of showing the differences of figure 6.9, is by plotting $d_{3,2}/\gamma_{eq}^{0.6}$ versus the concentration of surfactant, as is shown in figure 6.10. As can be seen from figure 6.10, distinct deviations are found.

The course of the curves in figure 6.10 shows a maximum, whereas at both high and low surfactant concentrations a constant value of $d_{3,2}/\gamma^{0.6} \approx 3.6\text{-}3.8$ is approached. The reason is that during emulsification the interface is deformed and this causes the concentration of surfactant at the interface to be lower than in the equilibrium situation.

During this break-up process the dynamic interfacial tension (γ_{dyn}) will be higher than the equilibrium interfacial tension (γ_{eq}). In the theory presented in the beginning of this chapter (Weber-theory) the interfacial tension is introduced, but it is obvious from the figures 6.9 and 6.10, that the equilibrium interfacial tension does not account correctly for the case at hand.

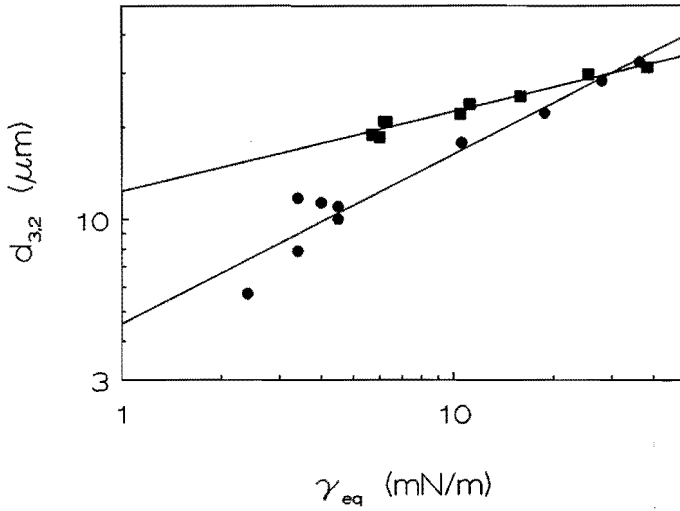**Figure 6.9**: *Dependence of $d_{3,2}$ on the equilibrium interfacial tension for the surfactants SDBS (■) and Dobanol 91-8 (●); emulsions prepared at 20 °C, stirrer speed 1500 rpm, $\phi = 0.01$, dispersed phase decane.*
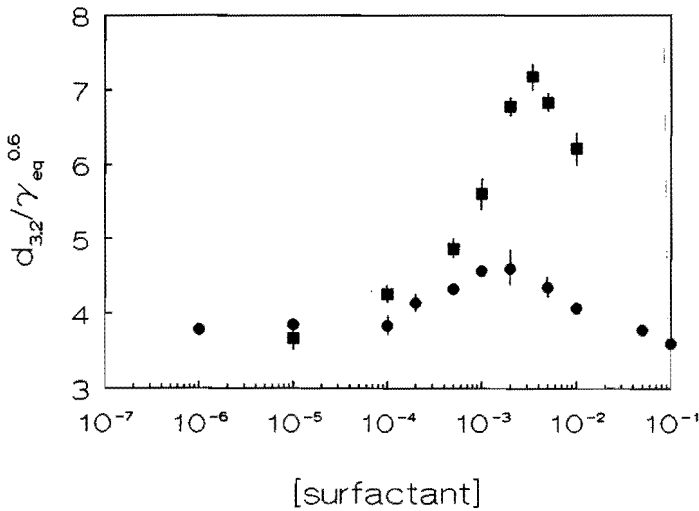

Figure 6.10: *Dependence of $d_{3,2}/\gamma_{eq}^{0.6}$ on surfactant concentration; ■ SDBS, ● Dobanol 91-8; emulsions prepared at similar conditions as in figure 6.9.*

This Weber-theory was originally derived for the case, where no surfactant is present during emulsification, where γ_{dyn} is equal to γ_{eq}. When surfactant is present, apparently at intermediate concentrations a large difference between γ_{dyn} and γ_{eq} is present.

To give an impression of the magnitude of the difference between equilibrium interfacial tension and dynamic interfacial tension, a parameter $\Delta\gamma$ is introduced as defined by:

$$\Delta\gamma = \gamma_{dyn} - \gamma_{eq} \tag{6.17}$$

Since, according to equation (6.13), $d_{3,2}/\gamma^{0.6}$ should be independent of the concentration, a plot of $d_{3,2}/\gamma^{0.6}$ versus surfactant concentration should be a horizontal straight line, if the interfacial tension determining the droplet break-up is equal to the equilibrium interfacial tension. However, this can be claimed only at very low or at very high surfactant concentrations. By assuming that the difference between the values of $d_{3,2}/\gamma^{0.6}$ plotted in figure 6.10 and a horizontal straight line drawn through the values at very low and high surfactant concentrations, is caused only by the difference between γ_{dyn} and γ_{eq}, the values of $\Delta\gamma$ can be calculated.

This calculation was performed in the following way. In figure 6.10 the following relation was plotted:

$$\frac{d_{3,2}}{\gamma_{eq}^{0.6}} = C(conc) \tag{6.18}$$

where $C(conc)$ is the observed value of $d_{3,2}/\gamma_{eq}^{0.6}$ at a certain concentration (conc) of the surfactants. The following relation for the dynamic interfacial tension is used:

$$\frac{d_{3,2}}{\gamma_{dyn}^{0.6}} = C_{We} \tag{6.19}$$

where C_{We} is the Weber number constant, which is found to be 3.8 for the two surfactants and is independent of concentration. Combining equation (6.18) and equation (6.19) we find:

$$\frac{\gamma_{dyn}^{0.6}\, C_{We}}{\gamma_{eq}^{0.6}} = C(conc) \tag{6.20}$$

Combining equations (6.20) and (6.17) we find:

$$\frac{C(conc)}{C_{We}} = \left(\frac{\gamma_{eq} + \Delta\gamma}{\gamma_{eq}}\right)^{0.6} \tag{6.21}$$

Using equation (6.21) the values of $\Delta\gamma$ were calculated and are presented in figure 6.11 for the surfactants SDBS and Dobanol 91-8.
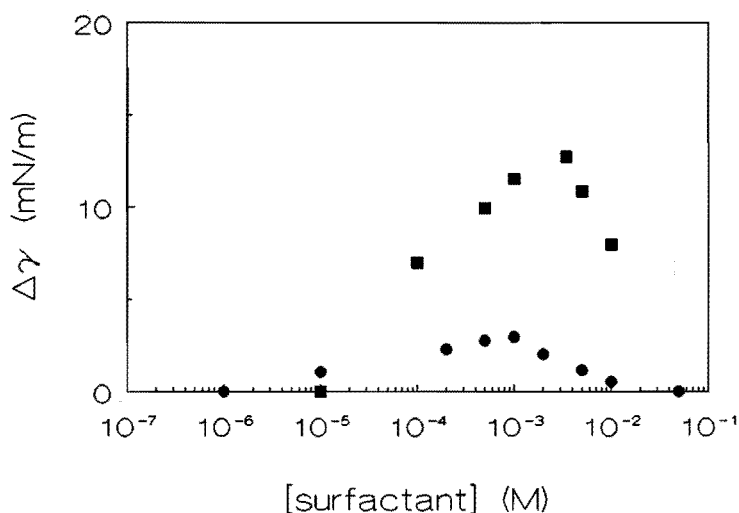
Figure 6.11: $\Delta\gamma$ versus surfactant concentration :● Dobanol 91-8, ■ SDBS.

As can be seen from figure 6.11 the magnitude of $\Delta\gamma$ is higher for SDBS than for Dobanol 91-8. In both cases can be seen, that for high and low concentration of surfactant the value for $\Delta\gamma$ tends to zero. The maximum of $\Delta\gamma$ is in both cases found at concentrations of about 10^{-3} M, which is incidentally close to the cmc.

6.6 Influence of cosurfactants on the break-up of droplets

Under various circumstances cosurfactants are added in the preparation of emulsion-type fluids. For micro-emulsion systems it is known [29],[30], that the addition of a cosurfactant leads to a decrease in interfacial tension, even at low cosurfactant concentrations with respect to the surfactant concentration. As cosurfactant usual lower alcohols (such as pentanol and hexanol) are used. In mini-emulsions [31], [32] higher alcohols (such as dodecanol and cetylalcohol) have been used. Addition of these cosurfactants results also in lower interfacial tensions, but the best effect is found at [cosurfactant]-[surfactant] ratios larger than one. This effect is also described in chapter 4 for the adsorption of SDBS on PS-particles. The largest decrease in adsorption area for a SDBS-molecule was found at [cosurfactant]/[surfactant] larger than one. This effect was most pronounced at temperatures above the melting point of the cosurfactant. It is expected that the adsorption behaviour of surfactants in presence of cosurfactants at an oil-water interface will show the same trends as for the adsorption at the PS-water interface.

In this section the break-up of emulsion droplets in the presence of different cosurfactants (dodecanol and cetylalcohol) at different temperatures will be described.

In figure 6.12 results are shown for the cosurfactant cetylalcohol. The [SDBS] of 10^{-2} M is above the cmc, the temperature is below the melting point of cetylalcohol. As a reference the change in droplet-size in absence of cetylalcohol is shown. As can be seen from figure 6.12, the addition of cetylalcohol results in a smaller droplet-size, even at the lowest [cetylalcohol] used. This smaller droplet-size results from the lower interfacial tension in the presence of cetylalcohol. The equilibrium droplet-size is reached after approx. 120 minutes and this time scale is not influenced by the presence of the cosurfactant. Addition of cetylalcohol at concentrations higher than $2*10^{-4}$ M does not result in smaller droplet-sizes.

In figure 6.13 results are shown for lower surfactant and cosurfactant concentrations. From figure 6.13 can be seen, that at lower [SDBS] addition of cetylalcohol results also in smaller droplet-sizes, although the influence is less pronounced than at higher [SDBS].

Figure 6.12: *Change in droplet-size versus time at various [cetylalcohol] for [SDBS] = 10^{-2} M, stirrer speed 1500 rpm, $\phi = 4.3*10^{-3}$, T = 20 °C, cetylalcohol is dissolved in the aqueous phase, dispersed phase decane; $\triangle$ no cetylalcohol, $\blacksquare$ 1*10^{-3} M, $\bullet$ 2*10^{-3} M, $\bigcirc$ 5*10^{-3} M.*
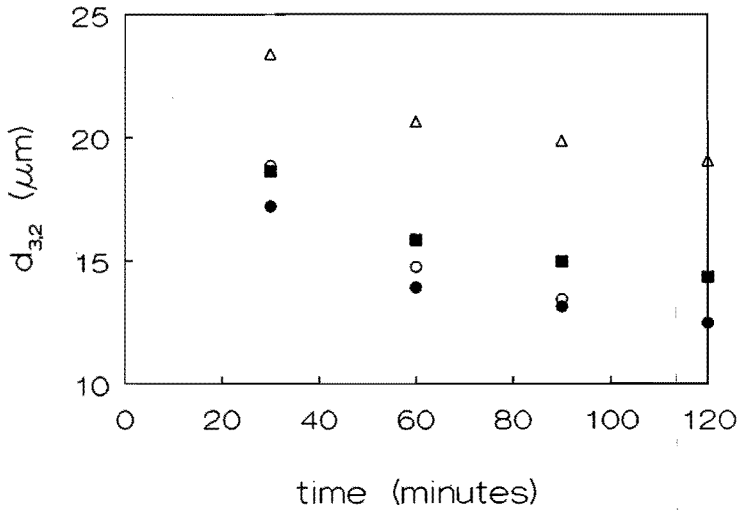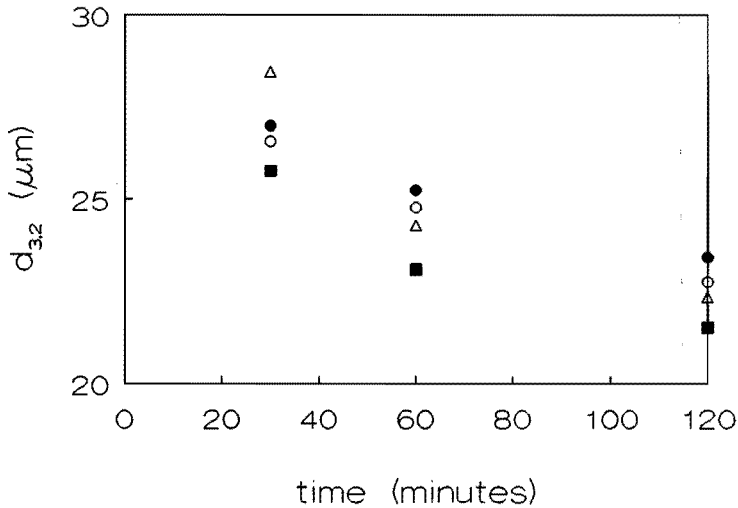

Figure 6.13: *Change in droplet-size versus time at various [cetylalcohol] for [SDBS] = 10^{-3} M, stirrer speed 1500 rpm, $\phi = 4.3*10^{-3}$, T = 20 °C, cetylalcohol is dissolved in the aqueous phase, dispersed phase decane; $\bullet$ no cetylalcohol, $\blacksquare$ 1*10^{-4} M, $\bigcirc$ 2*10^{-4} M, $\triangle$ 5*10^{-4} M.*

The optimum effect of cetylalcohol is found at [cetylalcohol]/[SDBS] ratios of about 1-2. This optimum is found at lower ratios than in mini-emulsion system.

As was stated in the introduction of this section, the temperature can have a large effect on the effectiveness of the cosurfactants. This is shown in figure 6.14 for the cosurfactants dodecanol and cetylalcohol.
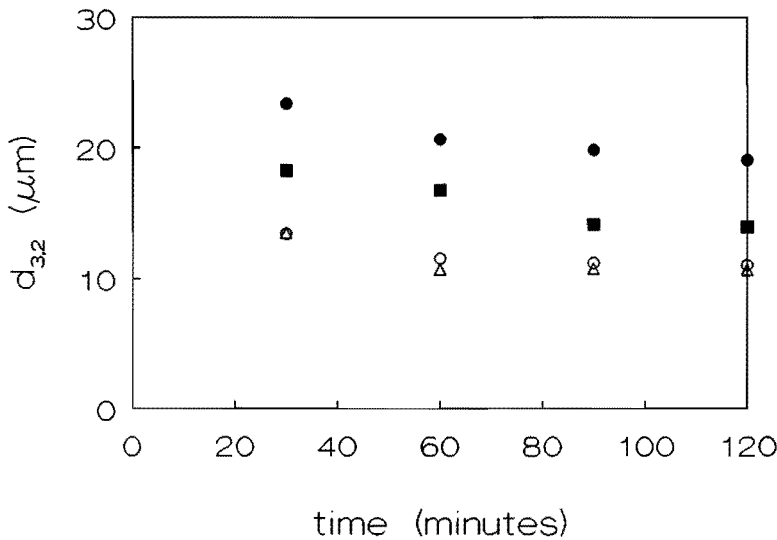
Figure 6.14: Change in droplet-size versus time for [SDBS] = 10^{-2} *M, stirrer speed 1500 rpm,* ϕ = $4.3*10^{3}$, *cosurfactants are dissolved in the aqueous phase, dispersed phase decane;* ● *T = 20 °C, no cosurfactant* ■ *T = 65 °C, no cosurfactant,* ○ *T = 65 °C, [cetylalcohol]* = $1*10^{3}$ *M,* △ *T = 65 °C, [dodecanol]* = $1*10^{3}$ *M.*

The influence of temperature was already described in section 6.4.4. The lower droplet-size results from the interfacial tension being lower at higher temperatures. A higher temperature does not seem to influence the time necessary to reach an equilibrium droplet-size.

The temperature of 65 °C used in these experiments is above the melting point of both dodecanol and cetylalcohol. The addition of a small amount of cosurfactant ([cosurfactant]/[surfactant] = 0.1) of cosurfactant results in a lower droplet-size and the time necessary to reach equilibrium is reduced by 50%.

It may be obvious, that the addition of small amounts of cosurfactant (with respect to the surfactant concentration) results in smaller droplet-sizes. This reduction of droplet-size is more than would be achieved when the surfactant concentration was increased by the same amount. The effectiveness of the cosurfactant is most pronounced at high surfactant concentrations and at temperatures above the melting point of the cosurfactant. When the cosurfactant is dissolved in the aqueous phase at high surfactant concentrations (concentrations above the cmc), the cosurfactant can be solubilized within the micelles.

It is also possible to dissolve the cosurfactant in the oil phase. Results are presented in the figures 6.15 and 6.16.
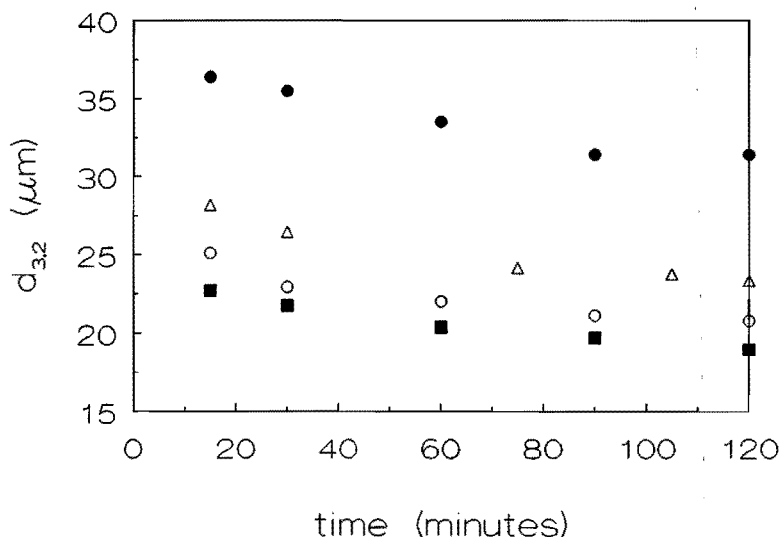
Figure 6.15: *Change in droplet-size versus time at various [dodecanol] in the oil phase for [SDBS] = 10^{4} M, stirrer speed 1500 rpm, $\phi = 4.3*10^{3}$, T = 20 °C, dispersed phase decane, [dodecanol] based on oil phase; ● 0%, △ 1%, ○ 5%, ■ 10%.*

In these figures the dodecanol concentration is expressed as a w/w % based on the oil phase. The fractions used result in a high concentration of cosurfactant within the oil droplets, but because of the small volume fraction used, the total concentration of dodecanol is low compared to the surfactant concentration.

At 10% dodecanol dissolved in the oil phase, this results in a [dodecanol] of 0.42 M.

This is orders of magnitude higher than the [SDBS] of 10^{-4} M. At a volume fraction of $4.3*10^{-3}$, this results in a [dodecanol] being 18 times higher than the [SDBS]. At a [SDBS] of 10^{-2} M and a dodecanol concentration of 10% the [SDBS] is 5 times larger than the [dodecanol].
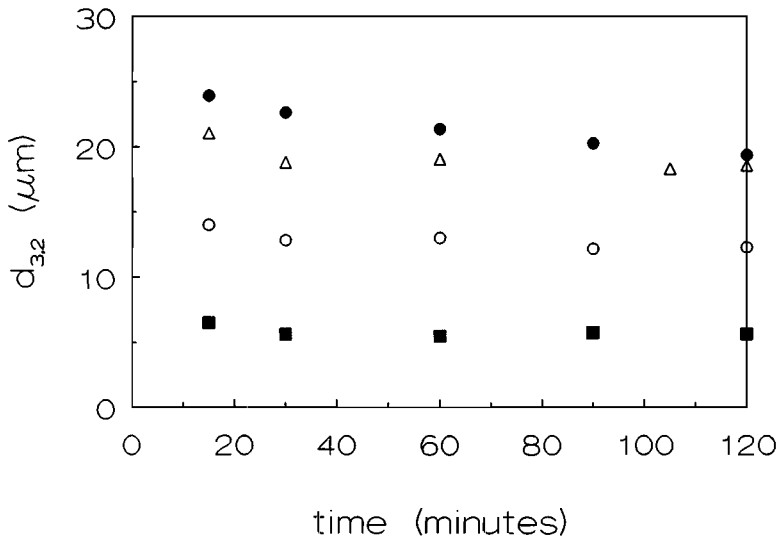
Figure 6.16: Change in droplet-size versus time at various [dodecanol] in the oil phase for [SDBS] = 10^{-2} M, stirrer speed 1500 rpm, ϕ = $4.3*10^{-3}$, T = 20 °C, dispersed phase decane, [dodecanol] based on oil phase; ● 0%, △ 1%, ○ 5%, ■ 10%.

As can be seen from figure 6.15 and figure 6.16, the presence of dodecanol in the oil-phase, results in a lower droplet-size. At higher [dodecanol] the reduction in droplet-size is larger. This is in contrast to the presence of cosurfactant in the water phase, where an optimum concentration was observed.

The influence of cosurfactants is the most pronounced when dissolved in the oil phase. For a constant [SDBS] of 10^{-4} M and varying concentrations dodecanol in the oil-phase equilibrium interfacial tensions were performed and in appendix B results are presented. Using the values of the droplet-sizes and the values of the equilibrium interfacial tension, the values of $d_{3,2}/\gamma_{eq}^{0.6}$ were calculated The results are presented in figure 6.17.
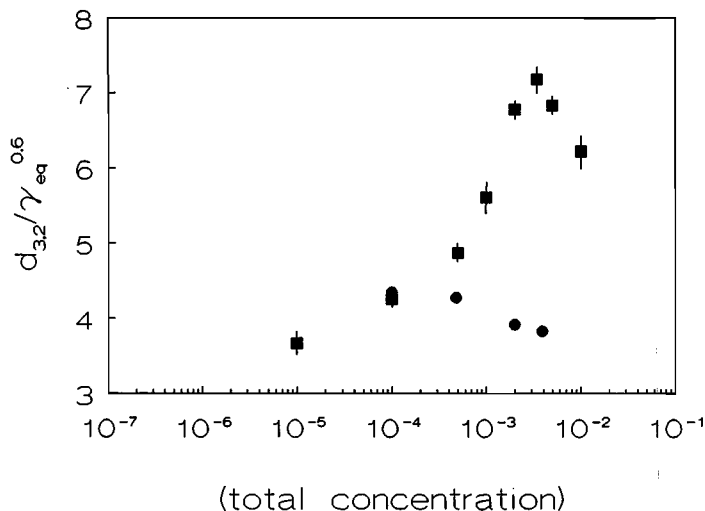
Figure 6.17: *Change in $d_{3,2}/\gamma_{eq}{}^{0.6}$ versus total concentration of surfactant and cosurfactant:* ■ *in absence of dodecanol, total concentration is [SDBS];* ● *[SDBS] kept constant at 10^{-4} M, total concentration varies with increasing concentration of dodecanol in the oil-phase.*

As can be seen from figure 6.17, the magnitude of $d_{3,2}/\gamma_{eq}{}^{0.6}$ decreases with increasing total concentration of surfactant and cosurfactant, whereas when increasing the [SDBS] the value of $d_{3,2}/\gamma_{eq}{}^{0.6}$ as function [SDBS] shows a maximum. In both cases the equilibrium interfacial tension was used for the calculation of $d_{3,2}/\gamma_{eq}{}^{0.6}$.

It may be concluded form the results in figure 6.17, that when dissolving dodecanol in the oil-phase, the equilibrium interfacial tension is very close to the dynamic value, in contrast to the situation is absence of dodecanol, where this fact is only observed at very low and very high surfactant concentrations. In that situation the diffusion process from the bulk to the interface is only at very high surfactant concentrations fast enough to compensate for depletion of surfactant due to deformation. When a cosurfactant is present in the oil-phase in combination with a surfactant in the water-phase, this diffusion process is fast as the cosurfactant has a much smaller diffusion length, which leads to an dynamic interfacial tension very close to the equilibrium interfacial tension.

6.7 Discussion

The results presented in this chapter clearly indicate that:

- the Weber number theory is correct;

- if surfactants are present a dynamic interfacial tension has to be introduced in the Weber number theory.

From the results presented it is clear, that droplet break-up occurs in the inertial subrange under experimental conditions prevailing. The dependence on N is the most direct proof of it, as $d_{3,2} \propto N^{1.2}$ (see figure 6.6), while if break-up would have occurred under viscous conditions $d_{3,2} \propto N^{1.5}$ should have been found [7]. The constants found in the various equations (such as equation (6.2) and equation (6.4)) are very close to those reported in the literature.

The occurrence of a dynamic interfacial tension during the droplet break-up process is evident from figure 6.10. In this figure it is clearly shown, that in a certain surfactant concentration range the interfacial tension is not equal to the equilibrium value. The difference, as depicted in figure 6.11 as $\Delta\gamma$, can be of the order of 12 mN/m for the experimental conditions chosen.

The graph of $\Delta\gamma$ against surfactant concentration is qualitatively very similar to the plot of the surface elasticity modulus as a function of surfactant concentration. That property has been researched extensively and is also found to have a maximum at a particular surfactant concentration. The theory presented by Lucassen and Van den Tempel [33] explained that quite well. In appendix B the essential elements of this theory are presented. The result is, that the elasticity modulus $\mid \epsilon \mid$ for a non-ionic surfactant, obeying a Langmuir adsorption isotherm, is given by:

$$|\epsilon| = \frac{\epsilon_0}{\sqrt{1 + 2\,\xi + 2\,\xi^2}} \qquad (6.22)$$

where

$$\epsilon_0 = RT\Gamma^{\text{max}} \left(\frac{c}{a} \right) \qquad (6.23)$$

and

$$\xi = \frac{a + 2c + (c^2/a)}{\Gamma^{max}} \sqrt{\frac{D}{2\omega}} \qquad (6.24)$$

where D is the diffusion coefficient of the surfactant, $1/\omega$ is the time scale of the interfacial deformation, c is the concentration of the surfactant and Γ is the surface excess of the surfactant.

Under purely elastic conditions $|\epsilon| = \epsilon_0$ where the surface coverage is conserved during deformation and no exchange from or to the bulk solution takes place. The correction to the elastic behaviour originates from the diffusion process, which scales with ξ. This parameter scales the time scale of the interface deformation to the time scale of the diffusion process, where the diffusion length scale is given by $(\partial\Gamma/\partial c)$.

Experimental evidence is available that surfaces behave as given by equation (6.22). Recently it has been proven [34], that dynamic interfacial tensions that had to be introduced in droplet break-up phenomena, can be interpreted by introducing an elasticity modulus. In that study droplet-size during viscous break-up also went through a maximum as a function of surfactant concentration. There the maximum was found far below the cmc, in contrast to what has been observed in figure 6.11, where the maximum is found close to the cmc.

In order to test if the theory of Lucassen and Van den Tempel [33] could also be applied in the case of break-up of emulsion droplets in stirred vessels, a frequency has to be chosen. This frequency is the inverse of the time scale of deformation of the interface.

In turbulent flows there are three time scales to be distinguished: the time needed to obtain an equilibrium droplet-size distribution, the circulating time and the time scale of deformation of the interface of emulsion droplets.

The time needed to obtain an equilibrium droplet-size distribution is for the emulsions presented here in the order of 100 minutes. This is not the time scale which determines the break-up of emulsion droplets.

The circulation time (t_m) is given by $N t_m$ = constant [35], where N is the stirrer speed. The constant is found to be approx. 30 for low viscosity fluids at high Reynolds numbers [36]. The results presented in figure 6.9 and figure 6.10 are obtained at a stirrer speed of 25/s. The mixing time is thus in the order of 1 second. The droplets are

being circulated in the vessel with a frequency of 1 second and every second the interface is being deformed when a droplet is passing the stirrer.

The characteristic time scale of deformation of a droplet subjected to normal oscillations is given by [37]:

$$\frac{1}{\omega_{def}} \approx \frac{1}{6} \sqrt{\frac{\rho d^3}{\gamma}} \qquad (6.25)$$

where ω_{def} is the frequency of deformations caused by drop oscillations, ρ is the density and d is the diameter of the droplets.

Drop deformation is also caused by fluctuating pressure differences across their sides, due to turbulence. The time scale of these fluctuations may be estimated from [38]:

$$\frac{1}{\omega_p} = \frac{d}{2 \pi \, \overline{(u^2(d)}^{0.5}} \qquad (6.26)$$

where ω_p is the frequency of pressure fluctuations and $\overline{u^2(d)}$ is the variance of the velocity and is estimated from Kolmogorov's theory as:

$$\overline{u^2(d)} \sim \epsilon^{\frac{2}{3}} d^{\frac{2}{3}} \qquad (6.27)$$

Using the values for $d_{3,2}$ and γ_{eq} presented in figure 6.9, ω_{def} was calculated to be of the order of $3*10^5$ s^{-1}. The value of ω_p depends on the value of ϵ, which can be much higher in the break-up zone near the impeller than its average value. Taking $\epsilon = 400*\epsilon_{av}$, ω_p was calculated to be 10^5 s^{-1}. In view of the uncertainty of the value of ϵ, it can be stated that it is very likely that $\omega_{def} = \omega_p$, as should be the case as the Weber number theory holds. This means, that the frequency in ξ is fixed by the inertial break-up process and is of the order of 10^5 s^{-1}. This value was used to calculate $|\epsilon|$ versus concentration as presented in figure 6.18. For the diffusion coefficient of Dobanol a value of $5*10^{-10}$ m^2/s was used [33], whereas for the diffusion coefficient of SDBS a value of 10^{-11} m^2/s was chosen.

In figure 6.18 it can be seen, that qualitatively the elasticity modulus has the same shape as the $\Delta\gamma$ versus concentration curve presented in figure 6.11. It is however observed, that the maximum of the curve for both surfactants is found at a too low concentration.
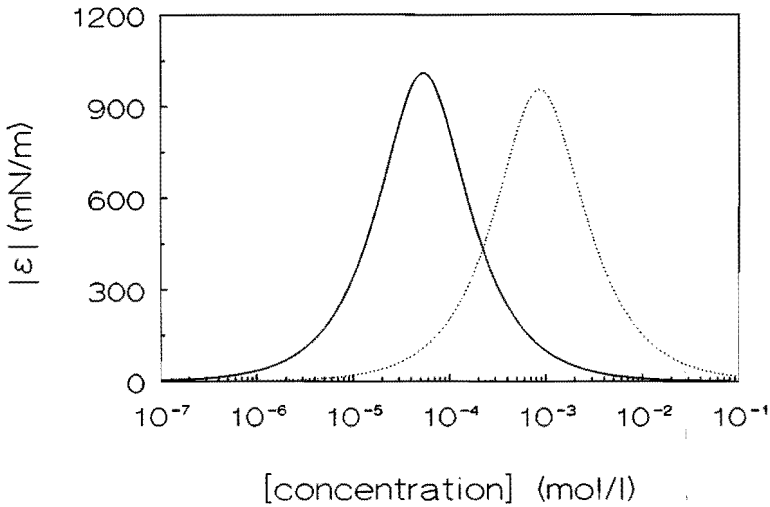
Figure 6.18: $|\epsilon|$ *versus surfactant concentration at* $\omega = 10^5$ s^{-1} *for Dobanol (solid line) and SDBS (dashed line).*

The maximum can be found close to the cmc, if a higher value for the frequency ω is used. In appendix B the change in concentration, where the maximum in $|\epsilon|$ is observed, with increasing frequency is shown (figure B.3). From that figure it can be seen, that ω should be of the order of 10^9 to find the maximum at the cmc. This value of ω is, however, too high to be realistic.

This does not mean, that a correction of γ_{eq} via an equation like

$$\gamma_{dyn} = \gamma_{eq} + \alpha \ |\epsilon| \qquad\qquad (6.28)$$

where α is a constant, can not be applied. Qualitatively the model of Lucassen and Van den Tempel [33] can still be correct, where at higher concentrations a diffusion process eliminates the elastic surface modulus. However, that occurs at a much higher concentration than theory predicts. Using a too high ω is equivalent to using a much higher value for $\partial\Gamma/\partial c$. This means, that the concentration gradient scales over a much larger distance than is assumed in the theory used here. The consequence is, that the theory of Lucassen and Van den Tempel [33] can not be applied straightforward, but that a non-

linear theory has to be used. Such theory is not available however. It can be expected, based on the above results, that such theory predicts $|\epsilon|$ to behave qualitatively the same as equation (6.22) does.

6.8 Conclusions

In this chapter the preparation of emulsions in a stirred vessel is described. The relationships found in the literature for larger vessel and other liquids, could also be used for our small scale vessel. It is found, that the equilibrium droplet-size is determined by break-up processes, which have very long time scales. The equilibrium droplet-size was in most of the experiments reached after more than 100 minutes. This time scale seems not to be strongly influenced by process-variables, such as the concentration of surfactant (and consequently the interfacial tension), stirrer speed, volume fraction dispersed phase or temperature.

The Weber number theory has found to be correct, with the exception that in this theory a dynamic interfacial tension should be used instead of the equilibrium value. The difference between dynamic and equilibrium interfacial tension was found to be 10 mN/m for the experimental conditions prevailing.

An attempt has been made to correlate this difference between dynamic and equilibrium interfacial tension ($\Delta\gamma$), by using the elasticity modulus of expanding interfaces. It was found, that the curves of $\Delta\gamma$ and the elasticity modulus versus concentrations have the same shape, but the concentration where the maximum is found is located at a too low concentration with the theory used. This fact is attributed to the fact, that this theory assumes deformations of the interface at situations close to equilibrium. In our case this is not the case, but theories for deformations far from equilibrium have not been developed so far.

The importance of interfacial tensions during break-up of emulsion droplets was already observed by Koshy et al. [17]. They made the same correction to the equilibrium interfacial tension as in our case, but did not attempt to correlate this deviations to diffusion processes.

Higher volume fractions (up to 0.1) result in larger droplet-sizes, because of turbulence damping and the correlation found agrees with literature relations.

The addition of cosurfactants results in smaller droplet-sizes and a reduction in the time to reach a steady state situation. The smaller droplet-size is attributed to the fact, that the interfacial tension decreases by the addition of cosurfactants. The influence of cosurfactants is the most pronounced, when they are added to the oil-phase. In this case the difference between equilibrium and dynamic interfacial tension is close to zero.

6.9 References

(1)   Becher, P., *Emulsions: Theory and practice*, 2nd ed., Reinhold, New York, **1965**, chapter 7.

(2)   Kolmogorov, A. M., *C. R. Acad. Sci. U. R. S. S.*, **1941**, *30*, 301.

(3)   Kolmogorov, A. M., *C. R. Acad. Sci. U. R. S. S.*, **1941**, *32*, 16.

(4)   Batchelor, G. K., *The theory of homogeneous turbulence*, Cambridge University Press, **1953**.

(5)   Tritton, D. J., *Physical Fluid Dynamics*, Clarendon Press, Oxford, **1988**, p. 312.

(6)   Hinze, J. O., *A. I. Ch. E. J.*, **1955**, *1*, 289.

(7)   Shinnar, R., *J. Fluid Mech.*, **1961**, *10*, 259.

(8)   Sprow, F. B., *Chem. Eng. Sci.*, **1967**, *22*, 435.

(9)   Lagisetty, J. S., Das, P. K., Kumar, R., Gandhi, K. S., *Chem. Eng. Sci.*, **1986**, *41*, 65.

(10) Shinnar, R., Church, J. M., *Ind. Engng. Chem.*, **1960**, *52*, 253.

(11) Chen, H. T., Middleman, S., *A. I. Ch. E. J.*, **1967**, *13*, 989.

(12) Godfrey, J. C., Obi, F. I. N., Reeve, R. N., *Chem. Eng. Progr.*, **1988**, *85(12)*, 61.

(13) Sharma, S. K., Goswami, A. N., Rawat, B. S., *Ind. J. Techn.*, **1991**, *29*, 254.

(14) Berkman, P. D., Calabrese, R. V., *A. I. Ch. E. J.*, **1988**, *34(4)*, 602.

(15) Coulaloglou, C. A., Tavlarides, L. L., *A. I. Ch. E. J.*, **1976**, *22*, 289.

(16) Grosso, J. L., Briceno, M. I., Paterno, J., Layrisse, I., In *Surfactants in Solutions*; Mittal, K. L., Ed.; Academic press, Marcel Dekker, New York, **1986**, p.1653.

(17) Koshy, A., Das, T. R., Kumar, R., *Chem. Eng. Sci.*, **1988**, *43*, 649.

(18) Princen, L. H., Kwolek, W. F., *Rev. Scient. Instrum.*, **1965**, *36*, 646.

(19) Rushton, J. H., Costich, E. W., Everett, H. J.,
     Chem. Engng. Prog., **1950**, *46*, 395.

(20) Bates, R. L., Fondy, P. L., Corpstein, R. R., *Ind. Eng. Chem. Proc. Des. Dev.*,
     1963, *2*, 311-314.

(21) Höcker, H., *Ph. D. Thesis*, University of Dortmund, **1979**.

(22) Einekel, W. D., *Ph. D. Thesis*, Technical University of Munich, **1979**.

(23) Bujalski, W., Nienow, A. W., Chatwin, S., Cooke, M., *Chem. Eng. Sci.*,
     1987, *42(2)*, 317.

(24) Laufhütte, H. D., Mersmann, A. B., in *Proceedings of the 5th European Conf. on
     Mixing*, BHRA Fluid Engineering, Wurzburg, West-Germany, **1985**, 331-340.

(25) Cutter, L. A., *A. I. Ch. E. J.*, **1966**, *12*, 35.

(26) Okamoto, Y., Nishikawa, M., Hashimoto, K., *Int. Chem. Eng.*, **1988**, *21*, 88.

(27) Chatzi, E. G., Boutris, C. J., Kiparissides, C., *Ind. Eng. Chem. Res.*,
     1991, *30*, 536.

(28) Park, J. Y., Blair, L. M., *Chem. Eng. Sci.*, **1975**, *30*, 1057.

(29) Guo, J.S., El-Aasser, M. S., Vanderhoff, J. W., *J. Polym. Sci., Polym. Chem Ed.*,
     1989, *27*, 691.

(30) Verhoeckx, G. J., De Bruyn, P. L., Overbeek, J. Th. G., *J. Colloid Interface Sci.*,
     1987, *119*, 409.

(31) El-Aasser, M. S., Lack, C. D., Vanderhoff, J. W., Fowkes, F. M.,
     Colloids Surfaces, **1988**, *29*, 103.

(32) Brouwer, W. M., El-Aasser, M. S., Vanderhoff, J. W., *Colloids Surfaces*,
     1988, *21*, 69.

(33) Lucassen, J., Van den Tempel, M., *Chem. Eng. Sci.*, **1972**, *27*, 1283.

(34) Janssen, J. J. M., Boon, A., Agterof, W. G. M., *A. I. Ch. E. J.*, accepted.

(35) Hoogendoorn, C. J., Den Hartog, A. P., Chem. Eng. Sci., 1967, *22*, 1689.

(36) Bouwmans, I., The blending of liquids in stirred vessels, Ph. D. thesis, Delft, 1992.

(37) Lamb, H., *Hydrodynamics*, 6th Edition, Cambridge University Press, New York,
     1945, p. 475.

(38) Muralidhar, R., Ramkrishna, D., *Ind. Eng. Chem. Fundam.*, **1986**, *25*, 554.

CHAPTER 7

CONSEQUENCES OF THE PRESENCE OF COSURFACTANTS DURING EMULSION POLYMERIZATION

Summary: In this chapter the consequences of the presence of cosurfactants during the emulsion polymerization process is discussed, based on the results obtained in foregoing chapters. Addition of cosurfactant results in a decrease of the cmc, an increase of adsorption, surface charge density of the micelles and size of micelles and a smaller emulsion droplet-size. It is expected, that of these effects, the increase of adsorption and smaller droplet-size are the most relevant to polymerization processes.

7.1 Introduction

Emulsion polymerization is the radical polymerization of a dispersion of monomer droplets, stabilized by surfactants, in which the radical formation and initiation takes place in the continuous (aqueous) phase. This results in a reaction medium consisting of submicron particles swollen with monomer and dispersed in the continuous phase. In contrast to the monomer droplets with diameters in the range of 1-50 μm, the polymer particles have diameters ranging from 50 to 500 nm. The final product is called a latex and is a dispersion of polymer particles in water.

Emulsion polymerization is a very important industrial process for the production of latices, as it has a number of advantages over other processes:

1. the emulsion polymerization process allows the preparation of high molecular weight polymers at high polymerization rates.

2. due to the relatively low viscosity of the continuous phase, heat can be excellently transferred and a good temperature control is possible.

3. the molecular weight of the polymer particles can be easily controlled by chain transfer agents

4. the latex formed can directly be used in many final products.

Surfactants are used during emulsion polymerization as they provide loci for polymerization and they stabilize the latices formed. The use of surfactants has disadvantages in

certain applications, such as relatively poor film forming properties when the latex is used as paint.

In this chapter a review is given of the literature concerning the role of surfactants in emulsion polymerization and this will be combined with results of this thesis. In particular the possible advantages of the use of cosurfactants will be presented.

7.2 Emulsion polymerization

7.2.1 Theory of emulsion polymerization

The theory of emulsion polymerization has been reviewed extensively and the reader is referred to reviews by Blackley [1], Basset and Hamielec [2], Piirma [3] and Candau and Ottewill [4].

A basic recipe for emulsion polymerization contains monomer, surfactant, water and initiator. The monomer is dispersed as large droplets in the aqueous phase at the beginning of the reaction. Depending on the amount of surfactant, micelles can be present and some monomer can be solubilized in the hydrophobic core of the micelles. The emulsion polymerization is started when the initiator is added to the reaction system.

In a batch emulsion polymerization the process can be divided into three intervals [1]-[4]. In interval I polymer containing particles are formed in a nucleation process described later in this section. Free radicals formed by dissociation of the initiator, will enter the monomer swollen micelles and initiate polymerization, when the surfactant concentration is above the cmc. The micelles will then be converted into polymer particles. The formed particles will be stabilized by the adsorption of surfactant from the not yet initiated micelles. This model for particle generation is called the micellar nucleation model; other models will be presented later. This particle forming mechanism is thought to be the reason for the increase in reaction rate in interval I. Due to adsorption of surfactant on the growing polymer particles, the surfactant concentration eventually drops below the cmc and initiation can only occur in the aqueous phase [5] or in the monomer droplets [6]. As the monomer concentration in the aqueous phase is usually low, due to the low solubility of the monomer in the aqueous phase, initiation in the aqueous phase is not a very effective source of polymer particles. Due to the low surface area of the monomer droplets with respect to the polymer particles, monomer droplets do not play a significant

role in the initiation process. The end of interval I is signalled by the cessation of nucleation.

Interval II follows during which particle growth proceeds. In this interval the particle number and the polymerization rate are constant. The monomer in the polymer particles is polymerized and the monomer concentration in the polymer particles is kept constant by diffusion of monomer from the emulsion droplets through the aqueous phase. The monomer (emulsion) droplets act as reservoirs only. At a certain conversion the emulsion droplets have disappeared; this marks the end of interval II.

In interval III the monomer remaining in the particles and the monomer dissolved in the aqueous phase are polymerized. Due to the decreasing concentration of monomer the polymerization rate decreases. For a batch process the end of interval III coincides with the complete conversion of monomer to polymer.

The above model was first described by Harkins [7], [8]. The model assumes, that the monomer is essentially insoluble in the aqueous phase and that the polymer and monomer are miscible in all proportions.

7.2.2 Particle nucleation theories

All discussions on particle nucleation start with the Smith-Ewart theory [9], in which Smith and Ewart in a quantitative treatment of Harkins' micellar theory [7], [8] managed to obtain an equation for the particle number as a function of initiation and polymerization rates. This equation was developed mainly for systems of monomers of low solubility (e.g. styrene), partly solubilized in micelles of an emulsifier with low cmc and seemed to work well [10]. Other authors have argued against the Smith Ewart theory on the grounds that particles can be formed even when no micelles are present and that for more water-soluble monomers the theory does not fit at all.

A model accounting for the fact, that emulsion polymerization can be performed without added surfactant, is the homogeneous nucleation mechanism. This mechanism is based on the observation, that polymer particles can be formed by an emulsion polymerization in the absence of added surfactant, provided that a suitable initiator is used (see chapter 2). Such an initiator is usually potassium persulphate, which gives by dissociation, negatively charged sulphate ($SO_4 \bullet^-$) radicals. The radicals can initiate polymerization by reacting

with dissolved monomer droplets, leading to a negative charge on the growing polymer particle. The number concentration of polymer particles is usually low and the final particle size is therefore large. These observations imply that the presence of micelles is not necessary for particle nucleation; the possibility is, however, not excluded, that micelles, when formed by combination of molecules generated by reaction of radicals with monomer molecules, are involved in the nucleation process. A radical will react in the aqueous phase with dissolved monomer to give a growing polymer chain dissolved in the aqueous phase. This oligomeric chain will grow, having surfactant like properties. These species may adsorb on already formed latex particles. The latex particles may be postulated to be generated by the soluble surfactant like species adding on monomers to such an extent, that they precipitate from solution and form polymeric nuclei. The nucleated particles then grow by monomeric diffusion from the monomer droplets, followed by polymerization therein. The primary role of micelles in this theory lies in the provision of reservoirs of the surfactant that impart colloidal stability to the nucleated particles. This model was first described by Priest [11] and later quantified by Roe [12], Ugelstad and Hansen [13] and Fitch and Tsai [14].

Usually, particle formation by initiation in the monomer droplets is not considered important. This is because of the low absorption rate of radicals into the monomer droplets, relative to the other particle formation rates. Only in the case where the monomer droplets are very small, they can be an important source of particle formation. This mode of initiation was described by Ugelstad et al. [15], [16], Hansen et al. [17], Azad et al. [18] and Hansen and Ugelstad [19]. Such fine monomer droplets were produced either by spontaneous emulsification by means of a mixed emulsifier system, consisting of an ionic emulsifier and a long chain fatty alcohol or amine, or by high pressure homogenization of monomer and water in the presence of a water-insoluble compound (e.g. hexadecane) to stabilize the droplets against degradation by Ostwald ripening. It has therefore been pointed out [19], that particle nucleation models should include all three initiation mechanisms (micellar, homogeneous/coagulative and droplet), since all these mechanisms may compete and coexist in the same system, even if one of them usually dominates.

7.2.3 The role of surfactants in emulsion polymerization

In emulsion polymerization the role of surfactants are numerous: (i) solubilizing highly water-insoluble monomers, (ii) determining the mechanism of particle nucleation, (iii) determining the number of particles nucleated, thus the rate of polymerization, (iv) maintaining colloidal stability during the particle growth stage and (v) controlling average particle size and size distribution of the final latex.

The adsorption isotherm of a surfactant on a polymer particle is determined by the physical and chemical nature of the polymer surface. A correlation was found between the saturation adsorption of a surfactant and the polymer water interfacial tension [20]. The saturation cross-sectional area of Sodium lauryl sulphate (SDS) on a latex particle surface decreases with increasing polymer-water interfacial tension and decreasing polarity of the particle surface.

The charged head groups of adsorbed ionic surfactants repel each other because of electrostatical repulsion; this results in a lower packing density (an increase in adsorption area). The addition of a non-ionic surfactant to an anionic surfactant gave a smaller adsorption area for the anionic surfactant [21]. In such a mixture, the nonionic surfactants apparently acted as a shield to reduce electrostatic repulsion between the adsorbed anionic surfactants and a decrease in adsorption area was observed. A similar effect was described by Tuin et al. [22] for the adsorption of an anionic surfactant (SDBS) on PS-particles in presence of long chain fatty alcohols. The adsorption area for SDBS decreases when using relatively large amounts of alcohols. This effect was especially noticeable at temperatures above the melting point of the alcohols.

Piirma et al. [23] investigated the emulsion polymerization of styrene using a mixture of an ionic and a non-ionic surfactant. At the optimal ratio of ionic surfactant to non-ionic surfactant of 0.2, the highest polymerization rate, the smallest particle size and narrowest particle size distribution were found. These findings were correlated with an optimal micellar size and a maximum in the ratio of the final number of particles to the initial number of micelles.

The chain length of the surfactant molecule plays an important role in determining the adsorption isotherm on a given polymer surface. The longer the chain length, the lower the concentration at which saturation adsorption is attained, for a homologous series of

surfactants. The number of surfactant molecules adsorbed per unit area of surface at saturation is expected to be independent of the surfactant chain length. However, the increase of the surfactant chain length was found to increase the packing density, presumably because of the lateral interaction between adsorbed surfactant molecules and because of the physical orientation of surfactants on the surface [24], [25].

Surfactants play a major role in determining the number of latex particles formed during the nucleation stage of emulsion polymerization. Each of the nucleation mechanisms outlined before, dictates a certain role for the surfactants, although the actual role may be more complex, because of the different nucleation mechanisms operating simultaneously.

In the micellar nucleation mechanisms the role of surfactants is to provide the micelles, which, when swollen with monomer, become the main loci of particle nucleation and maintain colloidal stability in a later stage of the process. The Smith-Ewart theory was found to hold for monomers with low water solubility (such as styrene) [26], [27], [28]. In the homogeneous/coagulative nucleation mechanisms the role of surfactants is less straightforward.

When nucleation in monomer droplets occurs, the role of surfactants is to stabilize the submicron particles. The mixed emulsifier systems result in small particle sizes, but also lead to high surfactant and cosurfactant concentrations at the droplet-water interface. This interfacial layer seems to retard the radical capture efficiency, as is observed by a relatively long nucleation stage, as described by Choi et al. [29], Chamberlin et al. [30], Delgado et al. [31] and Guo et al. [32].

It is obvious from the foregoing literature survey, that emulsion polymerization has several connections with colloid chemistry. In the case of micellar nucleation the cmc, the size and degree of dissociation of the micelles are important parameters. In the case of droplet initiation the size of the droplets is important, because too large droplets do not result in droplet initiation. In the following section results on the micellization of SDBS in presence of cosurfactants will be discussed. These results, combined with other results of surfactant/cosurfactant combinations described in this thesis, will be used to give some consequences of the presence of a cosurfactant on emulsion polymerization.

7.3 Experimental

7.3.1 Materials

Sodium dodecylbenzenesulfonate (SDBS): ex. Albright and Wilson (Nansa 1260, 25% w/v in water) was used without further purification, because surface tension (γ) measurements showed no minimum in the γ versus concentration curves, indicative for the absence of surface active impurities.

Water was distilled twice using an all glass apparatus.

Dodecanol: ex. Merck, purity > 95%, was used without further purification.

7.3.2 Conductivity measurements

The critical micelle concentration was determined at different temperatures by measuring the electrical conductivity of aqueous solutions as a function of concentration. The conductivity was measured using a Jenway 4020 conductivity meter (Jenway, U. S. A.), equipped with a Schott (Schott, Germany) conductivity cell. The cell constant was determined using standard KCl solutions. The conductivity measurements were carried out in a Pyrex vessel, kept at the ambient temperature using a thermostat bath, keeping the temperature within 0.1 °C. In the Pyrex vessel approx. 200 ml double distilled water was placed and the conductivity probe was installed. After having established thermal equilibrium, a small amount of a high concentration surfactant solution (0.05 M) was added. After equilibrium was reached, the conductivity was recorded and a further amount was added, until the cmc was surpassed.

The determination of the cmc in presence of dodecanol was performed at a temperature of 30 °C, which is above the melting point of dodecanol. It was shown in chapter 4, that the performance of cosurfactants increased significantly above the melting point of the cosurfactants. The procedure of the measurements was slightly different from the case, that no cosurfactant was present. One problem arising with the cosurfactant at hand, is its very low solubility in water. Dodecanol can, however, be solubilized in the micelles to some extent (see e.g Fendler and Fendler [33] and Attwood and Florence [34]). SDBS-solutions were made up to 0.01 M, which is well above the cmc. To this solutions different amounts of dodecanol were added in such a way, that the [SDBS]/[Dodecanol] ratios (on molar basis) were 8.5, 4.6, 3.5 and 2.0. These solutions were shaken at 35 °C

for about two hours. Only the lowest ratio did not clear at this temperature, which means that this ratio is above the maximum amount of dodecanol that can be solubilized in the micelles at that concentration and temperature. After cooling down to room temperature, the same situation was observed. Except the lowest ratio, all solutions were clear.

To keep the [Dodecanol] as constant as possible, instead of using pure water a surfactant solution with concentration below the cmc was used. To this surfactant solution a combination of surfactant and cosurfactant solution was added, in a similar way as described before.

7.4 Results

7.4.1 Results in absence of cosurfactants

In figure 7.1 the change in specific conductivity (κ_c) with increasing surfactant concentration in the waterphase at different temperatures is shown as an example. The specific conductivity versus concentration curves show all the same behaviour. As can be seen from figure 7.1, the value of κ_c increases linearly with concentration until a gradual transition in conductivity with concentration is observed. After this point, the conductivity again varies linearly with concentration. The change in conductivity with concentration can be represented by two straight lines, as is also shown in figure 7.1. The point were the two straight lines intersect, is designed as the cmc. This point was calculated using linear regression, in a similar way as was done by Van Os et al. [35]. For this linear regression the points (both at low and high concentration) far from the cmc are used. The determined values of the cmc are shown in figure 7.2 and are also listed in table 7.1.

Surfactants can be regarded as strong electrolytes in solution at concentrations below the cmc, but micelles attract a substantial number of the counter ions into an attached layer. A mono-valent surfactant with aggregation number n, may have an effective charge of p units only and the degree of dissociation of the micelle is p/n. For such an ionic surfactant, represented by Na^+S^-, the aggregation process may be represented by:

$$nS^- + (n-p)\,Na^+ \rightleftharpoons M^{p-} \tag{7.1}$$

where the factor p/n accounts for the degree of dissociation and can be calculated from the slopes of the plots of κ_c versus [SDBS] above and below the cmc. This approximate

method gives a too low value for p/n. This procedure was used by other investigators [36], [37]. A more precise method was described by Kahlweit et al. [38] and Attwood et al. [39]. The degree of dissociation of the micelles, p/n, can be calculated from the slope, S_m, of plots of κ_c against [SDBS] above the cmc, as proposed by Evans [40]. Assuming that the micelles do not contribute significantly to the conductivity, S_m may be approximated by [41]:

$$S_m = \frac{\lambda_m}{n} + \frac{p\,\lambda_{Na^+}}{n} \qquad (7.2)$$

where λ_m and λ_{Na+} are the molar ionic conductivities of micelles and counterions respectively. Since the cmc is found at low concentrations, the ionic conductivities of equation (7.2) may be approximated by the limiting ionic conductivities $\lambda_{0,m}$ and $\lambda_{0,Na+}$. The value of $\lambda_{0,m}$ can be calculated using Stokes' law giving:

$$S_m = \left(\frac{p}{n}\right)\left(\frac{F^2}{6\pi N_A \eta_0 r_m} + \lambda_{0,Na^+}\right) \qquad (7.3)$$

where F is Faraday's constant, N_A is Avagadro's constant and η_0 is the solvent viscosity. The values of the limiting conductivity of Na^+ and the viscosity of water at the different temperatures are listed in table 7.1. An approximate value for r_m was calculated, assuming micellar sphericity for all temperatures studied, from [42]:

$$l_c = 0.15 + 0.1265 * n_c + l_{ph} \qquad (7.4)$$

where l_c is the length of the extended alkylchain (in nm), n_c is the number of carbon atoms in the alkylchain and l_{ph} is the length of the phenyl ring. The value of l_{ph} was estimated from [43] to be 0.266 nm. The value of r_m is therefore approximately 1.93 nm. As a consequence of these assumptions, the value of the degree of dissociation must be regarded as approximate only. The determined values of p/n using both methods are listed in table 7.1.
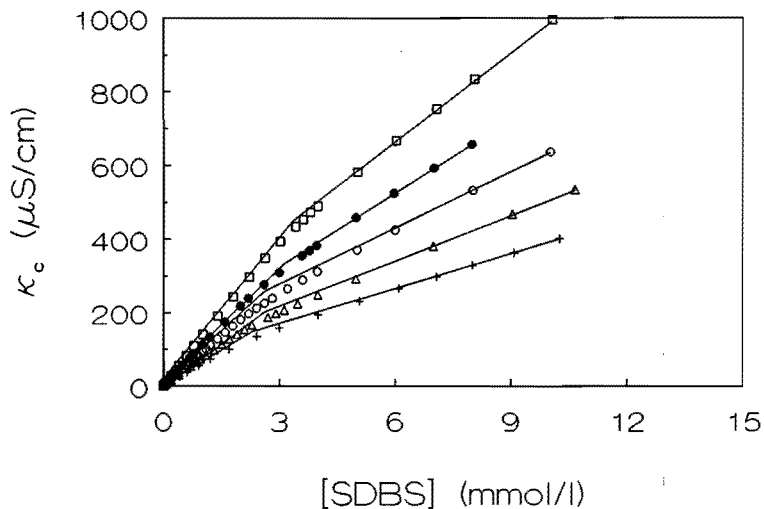
Figure 7.1: *Change in specific conductivity (κ_c) versus SDBS concentration at different temperatures:* + *20 °C,* $\triangle$ *30 °C,* $\bigcirc$ *40 °C,* $\bullet$ *50 °C,* $\square$ *60 °C.*

Table 7.1: *Determined values of the cmc and degree of dissociation.*

Temperature (K)	cmc (mmol/l)	cmc *10^5 (molfraction)	η_0[a] (μPa S)	λ_{Na+}[b] (cm^2 S mol^{-1})	p/n[c]	p/n[d]
293	2.3	4.13	1002	45.9	0.52	0.64
303	2.6	4.7	797.7	56.9	0.58	0.68
313	2.9	5.3	653.2	68.7	0.61	0.71
323	3.1	5.7	547.0	81.2	0.62	0.76
333	3.4	6.2	466.5	94.6	0.62	0.79

[a] Data taken from [44].

[b] From interpolation of Smithsonian Physical Tables [45].

[c] Determined from the slopes of κ_c versus [SDBS] above and below the cmc.

[d] Determined using equation (7.3).

In table 7.1 it can be seen, that the cmc increases as the temperature is increased. An increase in cmc with increasing temperature was also observed by Van Os [35] for Sodium Decylbenzenesulphonate. From table 7.1 can be seen also, that the degree of dissociation, calculated by the two methods, both show an increase with increasing temperature. The value of p/n, determined from the slopes of the κ_c versus [SDBS] above and below the cmc, is lower than the value determined by using equation (7.3), as stated before. The degree of dissociation at 20 °C of 0.64 (determined by equation (7.3)) is comparable to values reported by Lindman et al. [46]. A value of 0.60 was reported for the surfactant Sodium Octylbenzenesulphonate. The higher value of p/n with increasing temperature was also noted by other investigators for Sodium alkylsulphates [47], for Sodium perfluorooctanate [48] and a homologous series of Octyltrimethylammonium bromide to Tetradecyltrimethylammonium bromide [49].

In figure 7.2 the change of the cmc and ln [cmc] is plotted versus temperature.

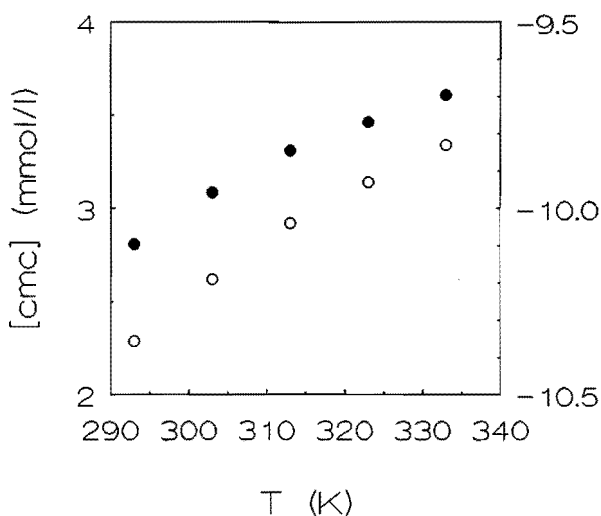*Figure 7.2*: *Determined values of the cmc and logarithm of cmc versus temperature:*
○ *[cmc] expressed in mmol/l;* ● *ln [cmc], [cmc] expressed in molfractions.*

7.4.2 Results in presence of cosurfactants

In figure 7.3 the change in equivalent conductivity versus surfactant concentration in absence and presence of cosurfactant is shown as an example.
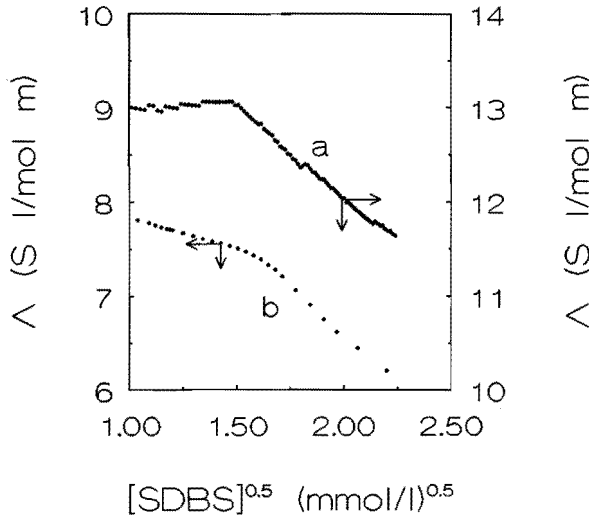

Figure 7.3: Change in equivalent conductivity (Λ) versus surfactant concentration at temperature 30 °C; a: for [Dodecanol] = $5.2*10^{-5}$ mol/l, b: in absence of dodecanol.

In figure 7.3 the equivalent concentration Λ (κ_c/[SDBS]) is plotted versus the square root of the [SDBS]. This method was preferred above the method used for the determination of the cmc in absence of cosurfactant. In presence of cosurfactants the slopes of the line after and below the cmc (when plotted as in figure 7.1) do not differ as much as in the case in absence of cosurfactants. In presence of cosurfactants the method used before is subject to a larger error than is the method used here. The method used here in presence of cosurfactants can, however, lead to different cmc values to be determined. This fact was noted before by other authors [35], [48].

In figure 7.3 the cmc is found at the concentration where Λ changes most. The results are presented in figure 7.4.
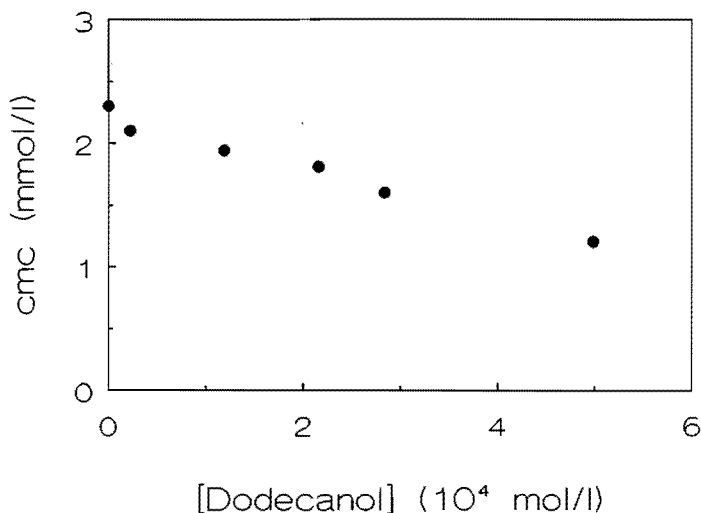
Figure 7.4: Change in cmc with varying dodecanol concentrations, temperature is 30 °C.

As can be seen from figure 7.4, the cmc is shifted to lower concentrations. It should be noted, that the Dodecanol concentrations used are low, with regard to the surfactant concentration. With a low concentration of Dodecanol, it is possible to lower the cmc by 50 %. The lowering of the cmc is limited by the low solubility of Dodecanol in the water phase.

From the data, the degree of dissociation can be calculated. For this calculation the slopes of the lines above and below the cmc were used, as was also done by other authors [36], [37]. This method was preferred above the method used before, because the micellar size in presence of Dodecanol is not known. The change in micellar size with addition of cosurfactant can be significant, as was shown by Candau and Zana [50]. The results are presented in figure 7.5. As can be seen from figure 7.5, the degree of dissociation increases with increasing Dodecanol concentration. This phenomenon was also observed by Attwood [39], who studied the effect of lower alcohols (butanol to hexanol) on the micellization of CTAB, DTAB and TTAB. It was found, that the degree of dissociation increased as the concentration of alcohol was increased. This effect was more pronounced as the alkyl chain of the alcohol increased. A similar increase was found by Zana et al.

[51] for the micellization of TTAB in 0.1 M KCl when using butanol, pentanol and hexanol. For anionic surfactants similar trends have been observed. The degree of dissociation increases for micelles of SDS on the addition of alcohols (ranging from butanol to heptanol), as was reported by Manabe et al. [37], [52] and Jain et al. [53]. This increase in degree of dissociation is thought to be the result of a reduction in the surface charge density of the micelles due to the presence of solubilized alcohols. This causes in return a release of counter ions from the micelles to compensate for this decrease [52]. The influence of higher alcohols on the degree of dissociation are, to the author's knowledge, not known.
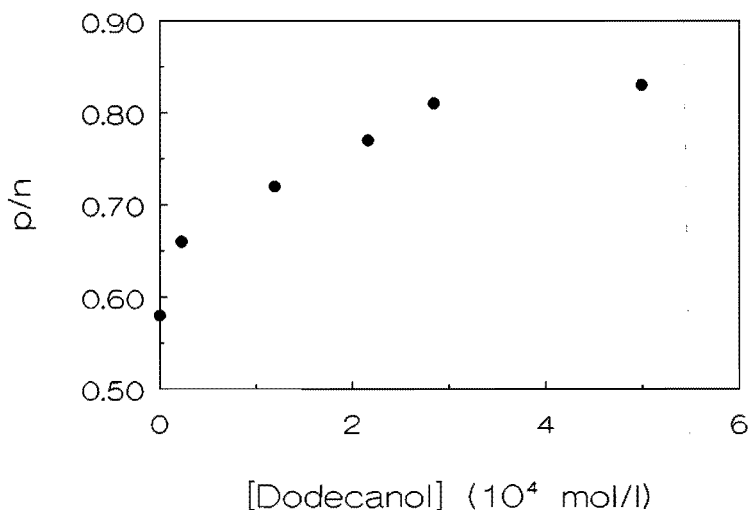
Figure 7.5: *Change in degree of dissociation (p/n) versus concentration Dodecanol at the cmc.*

The addition of Dodecanol to SDBS solutions causes the cmc to decrease, as was already noted by Shinoda [54]. He postulated that alcohols solubilize in the surfactant micelles, with their head group located in the palisade layer of the surfactant micelles and the tail located between the surfactant tails. The alcohol head group, being non-ionic,

serves to lessen the electrostatic interactions with the neighbouring charged surfactant head groups, while the hydrocarbon tail of the alcohol contributes to the hydrophobic interactions. These two effects result in the observed decrease of the cmc with an increase of alcohol concentration. The influence of higher alcohols on the micellization of SDBS and other surfactants has not yet been studied very extensively. Most research has been performed using lower alcohols, with up to 8 Carbon atoms.

The addition of lower alcohols to surfactants also results in a lowering of the cmc. This was found by Attwood et al. [39], Marangoni et al. [55] and Reekmans et al. [56]. They all found a significant decrease in the cmc as the alcohol concentration was increased. Their results are comparable with the results presented here, but differ in the amount of alcohol used. As the lower alcohols are more soluble in water, the concentration of alcohols can be increased to a higher level and consequently the reduction of the cmc is increased further.

Another effect of the addition of cosurfactants on micellar solutions, which has not been shown by the results presented here, is that the size of the micelles may change on addition of cosurfactants. When using short and medium chain length alcohols, a decrease in micellar size is observed, as was found e.g. by Candau and Zana [50] and Yiv et al. [57]. On the other hand, using medium to long chain alcohols increases the aggregation number producing larger alcohol-surfactant mixed micelles (see e.g. Reekmans et al. [56]).

7.5 Possible consequences of cosurfactants during emulsion polymerization

From the results of this thesis, it has become clear that the addition of cosurfactants results in:

- a decrease of the cmc;
- an increase of the degree of dissociation (p/n) of the micelles;
- an increase of the size of micelles;
- an increase of adsorption of surfactant at interfaces;
- a decrease in emulsion droplet-size.

These results will be discussed in relation to emulsion polymerization in the following sections.

7.5.1 Decrease of the cmc

The nucleation period (the time in which particles are formed, interval I) ends when the surfactant concentration drops below the cmc. When using the same amount of emulsifier above the cmc, the addition of cosurfactants leads to a decrease in the cmc. In this case, the nucleation period will continue for a longer time. The number of particles will become larger. If, however, the same micellar concentrations (defined as c-cmc, with c > cmc) are used, the number of particles does not change when adding cosurfactant. In this case it is possible to decrease the concentration of surfactant by adding a small amount of cosurfactant, in order to reach the cmc. The total amount of surfactant and cosurfactant is smaller than the amount of surfactant originally needed to reach the cmc. In view of the decreased amount of surfactant used, it is expected, that properties of the latices prepared will improve (e.g. a lower water sensitivity).

7.5.2 Increase of the degree of dissociation of the micelles

Addition of higher alcohols results simultaneously in a higher degree of dissociation of the micelles and a larger micellar size. It is therefore difficult to predict, if the surface charge density decreases or increases. This has to measured experimentally.

The radicals, generated by dissociation of the initiator, are not directly captured by the micelles. The initiator fragments grow in the aqueous phase, before entering the micelles, where polymerization is started. The oligomeric species and the micelles both have a negative charge, which means that there is an electrostatic barrier to overcome.

In seeded emulsion polymerization nucleation takes place in the seed polymer particles, because no micelles are present. It was suggested that in these systems, the entering species is a large oligomer [58], [59], whose entry rate coefficient is governed by colloidal considerations. As was shown by Maxwell et al. [60], this is not the case. When, by adsorption of surfactants on the seed polymer particles, the surface charge density was changed, no influence was found on the radical capture efficiency [61]. It was also found, that when changing the ionic strength (resulting in a smaller repulsive barrier) no influence was found in the radical capture efficiency [61]. These results indicate, that the surface charge density plays only a minor role (if any) in the entry of oligomeric radicals during seeded emulsion polymerization. The length of this oligomeric

species is of the order of 2 monomeric units for a typical styrene polymerization [60]. It is therefore expected, that the change in degree of dissociation plays a minor role only.

7.5.3 Increase of the size of micelles

At constant surfactant concentration, a larger micellar size will result in a decrease of the number of micelles. Particle numbers varied with micellar size in mixed emulsifier systems, as was shown by Piirma and Wang [23]. For a homologous series of Sodium alkyl sulphates (C_8-C_{16}) it was shown, that in absence of cosurfactant for given micellar concentration, the aggregation number increased with increasing alkyl chain length from 27 to 100 [62]. Consequently the number of micelles decreases as their size increases at constant micellar concentration. For the emulsion polymerization of styrene, using the same surfactants and the same micellar concentrations as in [62], the conversion versus time curves were found to be equal for the different surfactants studied. Clearly the number of micelles initially present does not determine the number of latex particles formed. This was observed by Al-Shahib [63], who found that the total surface area of the micelles was a constant quantity and this may be the factor determining the rate at which initiator radicals are captured by the micelles and hence the number of latex particles formed.

The radical capture efficiency of the micelles depends on their size [64]. The larger the micellar size, the higher is the radical capture efficiency per micelle. At constant number of micelles per unit volume, in case of larger micelles the duration of interval I will be shorter and the size distribution of the final latex particles will be narrower. This effect is expected to be operational by adding small amounts of cosurfactants.

7.5.4 Increase of adsorption of surfactant

In chapter 4 it was shown, that the adsorption of ionic surfactant (SDBS) in presence of cosurfactants was increased significantly, especially at high [cosurfactant]/[surfactant] ratios and above the melting point of the cosurfactants.

In both the homogeneous and coagulative nucleation mechanism the adsorption of surfactant on the particles plays an important role, because of changing the surface charge

density and hence decreasing the coagulation rate. As the adsorption of surfactants on polymer particles is increased in presence of cosurfactant [22], this would result in a higher particle stability at even lower conversion levels.

This effect may be especially noticeable when using polar (non-ionic) monomers, on which surfactant adsorption may be limited. The presence of higher alcohols may decrease the polarity and hence the adsorption of surfactant may be increased leading to a higher stability.

7.5.5 Decrease in emulsion droplet-size

Particle formation by initiation in monomer droplets is usually not considered to be very important, because of the low adsorption rate of radicals compared to the other particle formation rates. Only if very small droplets can be produced, this nucleation mechanism can be competitive to the other mechanisms.

Droplet initiation is most effective when the free surfactant concentration is below the cmc (no micelles present). When a certain concentration of surfactant is present in the aqueous phase, the droplet diameter can be calculated at which the free surfactant concentration drops below the cmc, because of adsorption of surfactant on the droplet interface [65]. It was shown, that the droplet diameters have to be of the order of 0.5 μm to become the main locus of initiation.

The emulsion droplets described in chapter 6, have diameters of the order of 5-25 μm and can not be considered to be an important locus of initiation. A stirred vessel is, however, not the most efficient apparatus to produce emulsions [66], because a stirrer dissipates much energy at levels where it can not break-up small emulsion droplets. Using a high-pressure homogenizer is a much more effective way to produce small droplets, because the energy input is much higher [66]. In order to obtain smaller droplets either a higher stirrer speed or a high-pressure homogenizer has to be used.

The emulsions can, however, be used in suspension polymerization, where the droplet sizes are of the order of 100 μm and larger. In these systems an oil-soluble initiator is used. After initiation each monomer droplet is considered to be a small bulk polymerization system. The final latex particles have diameters resembling those of the emulsion droplets.

If a certain droplet-size is necessary, the surfactant concentration can be decreased if a small amount (compared to the amount of surfactant) is added. In this way the droplet-size can be varied, without the need to vary the surfactant concentration.

7.6 Conclusions

The addition of cosurfactants results in an increase of the micellar charge, an increase in micellar size and a decrease of the cmc. In addition, from results of this thesis it is clear, that the adsorption of surfactant is increased and emulsion droplet-size decreases. These results were discussed in relation to emulsion polymerization.

Of these effects, the increased adsorption of surfactant in the presence of surfactant in the presence of cosurfactants and the decreased droplet-size were found to be of most importance in relation to emulsion polymerization.

When using polar monomers, the adsorption of surfactants (and consequently stability of polymers formed) may be difficult. Addition of a highly water-insoluble cosurfactant may decrease the polarity and consequently the adsorption of surfactant may be increased and as a result an increased stability of the polymers.

The decrease of emulsion droplet-size by addition of cosurfactant, gives the opportunity to control droplet-size without changing the surfactant concentration. This result may especially be useful during suspension polymerization.

7.7 References

(1) Blackley, D. S., *Emulsion Polymerisation*, Applied Science Publishers Ltd., London, **1975**.

(2) Basset, D. R., Hamielec, A. E., *Emulsion Polymers and Emulsion Polymerization*, ACS Symp. Ser. *165*, Washington, **1981**.

(3) Piirma, I., Ed., *Emulsion Polymerization*, Academic Press, New York, **1982**.

(4) Candau, F., Ottewill, R. H., Eds., *Scientific Methods for the Study of Polymer Colloids and Their Applications*, Kluwer Academic Publishers, London, **1990**.

(5) Harkins, W. D., *J. Chem. Phys.*, **1945**, *13*, 381.

(6) Harkins, W. D., *J. Chem. Phys.*, **1946**, *14*, 47.

(7) Harkins, W. D., *J. Am. Chem. Soc.*, **1947**, *69*, 1428.

(8) Harkins, W. D., *J. Polym. Sci.*, **1950**, *5*, 217.

(9)   Smith, W. V., Ewart, R. H., *J. Phys. Chem.*, **1948**, *16*, 592.

(10) Gerrens, H., *Ber. Bundesges. Phys. Chem.*, **1963**, *67*, 741.

(11) Priest, W. J., *J. Phys. Chem.*, **1952**, *56*, 1077.

(12) Roe, C. P., *Ind. Eng. Chem.*, **1968**, *60*, 20.

(13) Ugelstad, J., Hansen, F. K., *Rubber Chem. Technol.*, **1976**, *49*, 536.

(14) Fitch, R. M., Tsai, C. H., In *Polymer Colloids*; Fitch, R. M., Ed.,
      Plenum Press, New York, **1971**, p. 71.

(15) Ugelstad, J., El-Aasser, M., Vanderhoff, J. W., *J. Polym. Sci., Polym. Lett. Ed.*,
      1973, *11*, 505.

(16) Ugelstad, J., Hansen, F. K., Lange, S., *Makromol. Chem.*, **1974**, *175*, 507.

(17) Hansen, F. K., Ofstad, E. B., Ugelstad, J., In *Theory and Practice of Emulsion
      Technology*, Smith, A. L., Ed., Academic Press, New York, **1976**, p. 13.

(18) Azad, A. R. M., Ugelstad, J., Fitch, R. M., Hansen, F. K.,
      Am. Chem. Soc. Symp. Ser., **1976**, *24*, 1.

(19) Hansen, F. K., Ugelstad, J., *J. Polym. Sci., Polym. Chem. Ed.*, **1979**, *17*, 3047.

(20) Vijayendran, B. R., *J. Appl. Polym. Sci.*, **1979**, *23*, 733.

(21) Orr, R. J., Breitman, L., *Can. J. Chem.*, **1960**, *38*, 668.

(22) Tuin, G., Stein, H. N., *Langmuir*, **1994**, *10(4)*, 1054; see also chapter 4.

(23) Piirma, I., Wang, P. C., In *Emulsion Polymerization*, Piirma, I., Gardon, J. L.,
      Eds., Am. Chem. Soc. Symp. Ser., *24*, Washington D. C., **1976**, p. 34-61.

(24) Maron, S. H., Elder, M. E., Moore, C., *J. Colloid Sci.*, **1954**, *9*, 382.

(25) Connor, P., Ottewill, R. H., *J. Colloid Interface Sci.*, **1971**, *37*, 642.

(26) Vanderhoff, J. W., In *Vinyl Polymerization II*, Ham, G. E., Ed., Marcel Dekker,
      New York, **1969**, p. 210.

(27) Hansen, F. K., Ugelstad, J., In *Emulsion Polymerization*, Piirma, I., Ed.,
      Academic Press, **1982**, p. 51.

(28) Bartholome, E., Gerrens, H., Herbeck, R., Weitz, N. M.,
      Elektrochem., **1956**, *60*, 334.

(29) Choi, Y. T., El-Aasser, M. S., Sudol, E. D., Vanderhoff, J. W., *J. Polym. Sci.,
      Polym. Chem.*, **1985**, *23*, 2973.

(30) Chamberlin, B. J., Napper, D. H., Gilbert, R. G., *J. Chem. Soc.,
      Faraday Tans. I.*, **1982**, *78*, 591.

(31) Delgado, J., El-Aasser, M. S., Silebi, C. A., Vanderhoff, J. W., *J. Polym. Chem., Polym. Chem.*, **1989**, *27*, 193.

(32) Guo, J. S., El-Aasser, M. S., Vanderhoff, J. W., *J. Polym. Sci., Polym. Chem.*, **1989**, *27*, 691.

(33) Fendler, J. H., Fendler, E. J., *Catalysis in Micellar and Macromolecular Systems*, Academic Press, New York, **1975**, p. 42-85.

(34) Attwood, D., Florence, A. T., *Surfactant Systems, Their Chemistry, Pharmacy and Biology*, Chapmann and Hall, London, **1983**, p. 245-257.

(35) Van Os, N. M., Daane, G. J., Bolsman, T. A. B. M., *J. Colloid Interface Sci.*, **1987**, *115(2)*, 402.

(36) Zana, R., *J. Colloid Interface Sci.*, **1980**, *78*, 330.

(37) Manabe, M., Kawamura, H., Yamashita, A., Tokunaga, S., *J. Colloid Interface Sci.*, **1987**, *77*, 189.

(38) Kahlweit, M., Teubner, M., *Adv. Colloid Interface Sci.*, **1980**, *13*, 1.

(39) Attwood, D., Mosquera, V., Rodriguez, J., Suarez, M. J., *Colloid Polym. Sci.*, **1994**, *272*, 584.

(40) Evans, H. C., *J. Chem. Soc.*, **1956**, 579.

(41) Van Nieuwkoop, J., Snoei, G., *J. Colloid Interface Sci.*, **1985**, *103*, 417.

(42) Tanford, C., *J. Phys. Chem.*, **1972**, *76*, 3020.

(43) Binana-Limbelé, W., Van Os, N. M., Rupert, L. A. M., Zana, R., *J. Colloid Interface Sci.*, **1991**, *141(1)*, 157.

(44) *CRC Handbook of Chemistry and Physics*, Lide, D. R., Ed., CRC Press, *72 Ed.*, **1992**, p. 6-9.

(45) CRC Handbook of Chemistry and Physics, Hodgman, C. D., Ed., *44 Ed.*, **1962**, p. 2696.

(46) Lindman, B., Puyal, M. C., Kamenka, N., Brun, B., Gunnarson, G., *J. Phys. Chem.*, **1982**, *86*, 1702.

(47) Mukerjee, P., *J. Phys. Chem.*, **1962**, *66*, 1375.

(48) Mukerjee, P., Korematsu, K., Okawauchi, M., Sugihara, G., *J. Phys. Chem.*, **1985**, *89*, 5308.

(49) Barry, B. W., Russell, G. F. J., *J. Colloid Interface Sci.*, **1972**, *40*, 587.

(50) Candau, S., Zana, R., *J. Colloid Interface Sci.*, **1981**, *84*, 206.

(51) Zana, R., Yiv, S., Strazielle, C., Lianos, P., *J. Colloid Interface Sci.*,
     1981, *80*, 208.

(52) Manabe, M., Koda, M., Shirahama, K., *J. Colloid Interface Sci.*, **1980**, *77*, 189.

(53) Jain, A. K., Sing, R. P. B., *J. Colloid Interface Sci.*, **1981**, *81*, 536.

(54) Shinoda, K., *J. Phys. Chem.*, **1954**, *58*, 1136.

(55) Marangoni, D. G., Kwak, J. C. T., *Langmuir*, **1991**, *7*, 2083.

(56) Reekmans, S., Luo, H., Van der Auweraer, M., De Schryver, F.,
     Langmuir, **1990**, *6*, 628.

(57) Yiv, S., Zana, R., Ulbricht, W., Hoffmann, H.,
     J. Colloid Interface Sci., **1981**, *80*, 224.

(58) Penboss, I. A., Gilbert, R. G., Napper, D. H., *J. Chem. Soc., Faraday Trans. 1*,
     1983, *79*, 1257.

(59) Penboss, I. A., Napper, D. H., Gilbert, R. G., *J. Chem. Soc., Faraday Trans. 1*,
     1986, *82*, 2247.

(60) Maxwell, I. A., Morrison, B. R., Napper, D. H., Gilbert, R. G., *Macromolecules*,
     1991, *24*, 1629.

(61) Adams, M. E., Trau, M., Gilbert, R. G., Napper, D. H., *Aust. J. Chem.*,
     1988, *41*, 1799.

(62) Aniansson, E. A. G., Wall, S. N., Almgren, M., Hoffmann, H., Kielmann, I.,
     Ulbricht, W., Zana, R., Lang, J., Tondre, C., *J. Phys. Chem.*, **1976**, *80*, 905.

(63) Al-Shahib, W. A., *Ph. D. Thesis*, Manchester, **1977**.

(64) Dunn, A. S., In *Emulsion Polymerization*, Piirma, I., Ed., Academic Press,
     New York, **1982**, p. 236.

(65) Hansen, F. K., Ugelstad, J., In *Emulsion Polymerization*, Piirma, I., Ed.,
     Academic Press, **1982**, p. 88.

(66) Walstra, P., *Chem. Eng. Sci.*, **1993**, *48(2)*, 333.

COMPARISON OF DROPLET-SIZE MEASUREMENTS USING COULTER COUNTER, LIGHT MICROSCOPY AND LIGHT-SCATTERING

Particle size measurements of emulsion droplets can be performed using different techniques: light scattering, light microscopy or by Coulter Counter. Light scattering techniques, like turbidity measurements, have the disadvantage that only an average particle diameter is obtained. Using light microscopy or Coulter Counter a particle size distribution can be measured.

Particle size measurements of emulsion droplets were performed using the Coulter Counter. This apparatus can measure a large number of particles in a short time and has a high resolution. Light microscopy has the disadvantage that a large number of samples has to be analyzed, which is very time consuming.

In order to validate the accuracy of particle size distributions obtained by Coulter Counter, these were compared to particle size distributions obtained by light microscopy.

For this experiment an emulsion was prepared using 0.001 M SDBS, a volume fraction of decane of 20 % and a stirrer speed of 1500 rpm. After equilibrium was reached the particle size distribution was determined using the Coulter Counter. The Coulter Counter measures approx. 20000 particles within a minute.

The determination of the particle sizes by light microscopy was performed by making photographs of the various samples. For this purpose the light microscope was equipped with a photocamera. Different samples of the emulsion were photographed (total number of droplets approx. 2500). After having developed the film a computer system was used to calculated the droplet-sizes. Using this computer system, it reduces the time for analysis considerably, but it still takes more than a day to analyze ca. 2000 particles.

The computer program (TIM, Difa measuring systems, The Netherlands) uses a video-camera which reads in the photographs. From each droplet the circumference and area is

measured. From the ratio of these values the diameter is calculated, according to the following equation:

$$Diameter = \frac{4 * area}{circumference} \qquad \text{(A.1)}$$

A problem with such analysis is, that the computer program uses the inside of the droplet to calculate the diameter. When making photographs it is not possible to focus in such a manner, that no shadow of the droplet is present on the photograph. Depending on the quality of focusing of the droplets, different shadows are present on the photographs. This means that the calculated droplet-sizes, using this computer program, always lead to smaller droplet-sizes than in reality. In figure A.1 a schematic picture is shown to give an impression of this problem.
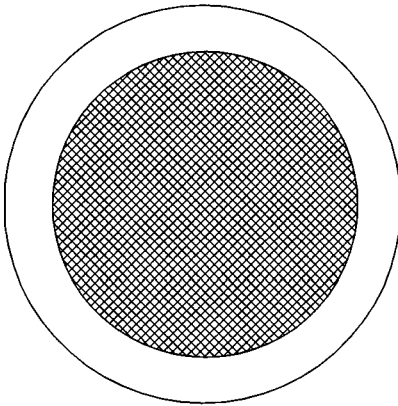

Figure A.1: Schematic view of the droplet contour as a result of focusing. The outer black border line is the actual droplet, the computer program uses the hatched area for the calculation of the particle size.

In figure A.2 the two determined particle size distributions from the same emulsion are shown.

As can be seen from figure A.2 the two distributions are very similar. As a result of the procedure, followed for the processing of the light microscopy photographs, the whole distribution is shifted to lower particle sizes. This difference was also seen for different emulsions.
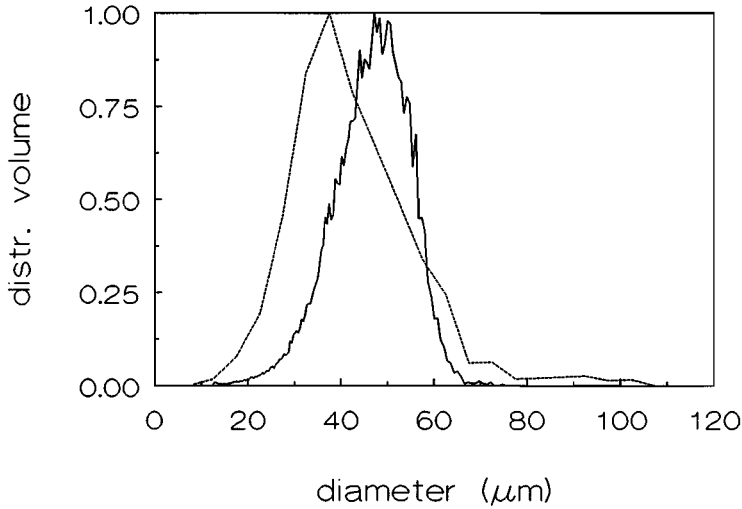
Figure A.2: *Determined particle size distributions (volume averaged) using Coulter Counter and light microscopy. Drawn line: Coulter Counter; broken line: light microscopy.*

The calculated values of the number and volume average diameters for this emulsion is shown in table A.1.

Table A.1: *Calculated values of number average ($d_{1,0}$) and Sauter mean diameter ($d_{3,2}$) from distributions measured with light microscopy and Coulter Counter.*

Apparatus	$d_{1,0}$ (μm)	$d_{3,2}$ (μm)	number of particles
Light microscope	38.7	42.6	2659
Coulter Counter	42.9	45.2	80103

From the values in table A.1 can be seen, that the determined average values are close together. The difference between the two techniques is approx. 10%, which is not very large for two such different techniques and the errors involved in the calculation of particle sizes from photographs.

The fact, that the difference in average particle size is not dependent on the type of averaging confirms the fact, that the measured particle sizes with the Coulter Counter are accurate particle sizes.

The Coulter Counter was also compared with the Coulter LS 130, which uses light-scattering (Fraunhoffer diffraction). Here glass particles were used with different particle sizes, in the range of particle sizes of the emulsion droplets. In figure A.3 the results of these measurements are shown.
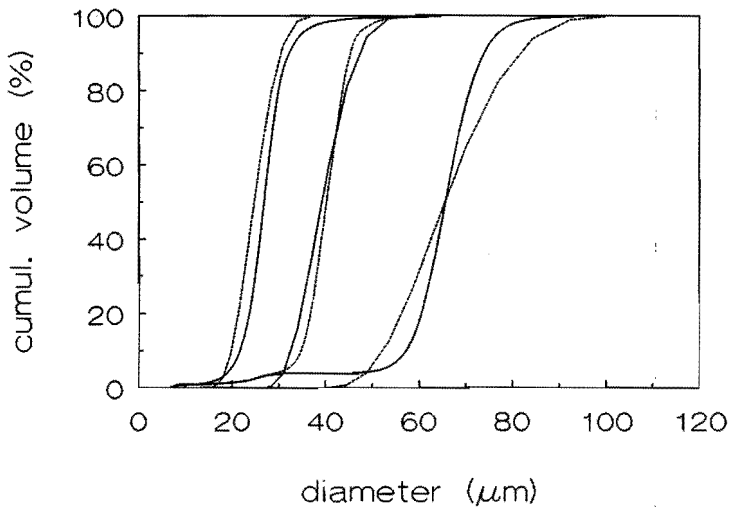

Figure A.3: Cumulative particle size distribution of glass particles measured with Coulter Counter (drawn curve) and Coulter LS 130 (broken curve).

From figure A.3 can be seen that the particle size distributions are very similar. The differences between Coulter Counter and Coulter LS 130 are smaller than found with Coulter Counter and light microscopy. The particle size distribution measured with the Coulter Counter are smaller than measured by Coulter LS 130. This is due to the higher resolution of the Coulter Counter. In table A.2 the measured values for the average particle sizes are listed.

Table A.2: Measured values of number average $(d_{1,0})$ and Sauter mean diameter $(d_{3,2})$ of glass particles from distributions measured with Coulter Counter and Coulter LS 130. Diameters are given in micrometers.

Apparatus	$d_{1,0}$	$d_{3,2}$	$d_{1,0}$	$d_{3,2}$	$d_{1,0}$	$d_{3,2}$
Coulter Counter	21.5	24.1	38.7	41.0	67.8	68.9
Coulter LS 130	25.2	26.6	41.0	42.6	66.8	70.6

From table A.2 can be seen, that the particle sizes with Coulter Counter and Coulter LS 130 are very close, with a difference less than 5%.

The particle size distribution measurements were performed using the Coulter Counter, because of the higher resolution and the short time of analysis.

INTERFACIAL TENSION MEASUREMENTS

B.1 Static interfacial tension measurements

Static interfacial tension measurements were performed using a Krüss K10T automatic tensiometer (Krüss GmbH, Hamburg, Germany) using a platinum Wilhelmy plate. The results of the water-decane interface measurements of the surfactants SDBS and Dobanol 91-8 are shown in figure B.1:
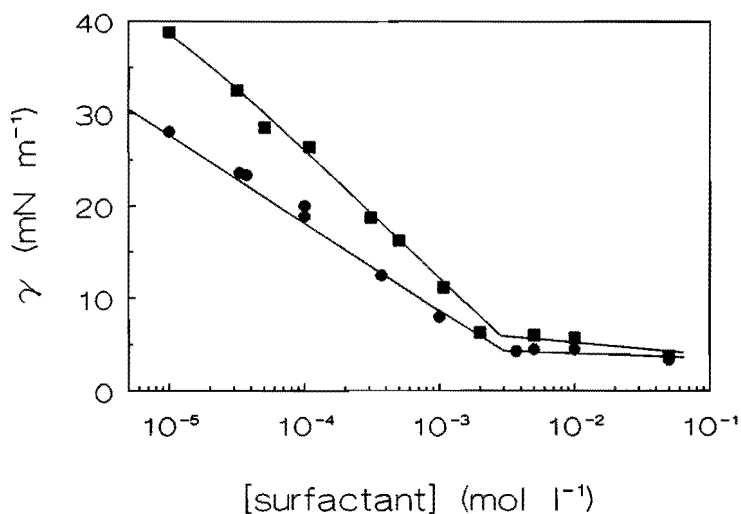

Figure B.1: Equilibrium interfacial tension (γ) for the decane-water interface versus concentration of surfactant : ● Dobanol 91-8, ■ SDBS; the drawn lines before the cmc are the best fit of the Szyszkovski equation, the lines after the cmc are calculated by linear regression.

The Szyszkovski equation [1] relates the interfacial tension to the concentration of surfactant in the waterphase:

$$\gamma - \gamma_0 = -RT\Gamma^{max}\ \ln\left(\frac{c+a}{a}\right) \tag{B.1}$$

where γ is the interfacial tension at concentration c of surfactant in the waterphase, γ_0 is the interfacial tension at concentration 0 of surfactant in the waterphase, R is the gas constant, T is the temperature, a is the Langmuir-Szyszkovski constant and Γ^{max} is the maximum surface excess of the surfactant.

Szyszkowski made the assumption, based on empirical data, that the equation is only valid below the CMC for uncharged particles. It appeared however, that the Szyszkowski equation has a broader validity. The equation was used by Rosen and Aronson [2] for alcohol and anionic surfactant, by Müller [3] for cationic surfactants and Kegel et al. [4] for the system brine, anionic surfactant, alcohol and cyclohexane. They all obtained good results in using the equation to describe their data. The fitting of the equation to the data points was performed using a least-squares method, in the same way as was done by Müller [3].

Equation (B.1) is valid for a non-ionic surfactant or an ionic surfactant in presence of excess salt. For a ionic surfactant (SDBS) the Szyszkovski equation reads:

$$\gamma - \gamma_0 = -2RT\Gamma^{max}\ \ln\left(\frac{c+a}{a}\right) \tag{B.2}$$

In table B.1 the obtained fit parameters for the surfactants SDBS and Dobanol 91-8 are listed.

Table B.1: Szyszkovski fit parameters for the surfactants used.

surfactant	a (mol/l)	Γ^{max} (mol/m^2)
SDBS	$3.0*10^{-6}$	$1.25*10^{-6}$
Dobanol 91-8	$1.2*10^{-7}$	$1.7*10^{-6}$

In figure B.2 the change in equilibrium interfacial tension at constant [SDBS] with varying dodecanol concentration in the oil-phase (decane) is shown. As can be seen from

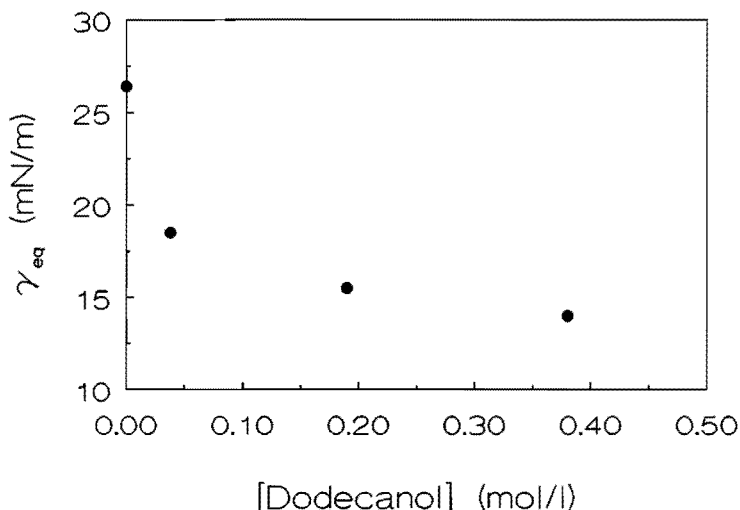figure B.2, the equilibrium interfacial tension decreases as the dodecanol concentration is increased.

Figure B.2: *Change in equilibrium interfacial tension for the water-decane interphase versus concentration of dodecanol at constant [SDBS] = 10^{-4} M. The dodecanol is dissolved in the oil-phase.*

B.2 Interfacial relaxation studies

One of the first to investigate this interfacial visco-elastic behaviour for expanding areas at a constant relative rate were Van Voorst Vader et al. [5]. Later experiments were performed in a Langmuir through, in which a small-amplitude sinusoidal barrier motion provides a well deformed deformation of the interface. The theory for this mechanism was presented by Lucassen and Van den Tempel [6]. In this section this theory will be used to describe the dilatational properties of the interface.

The response of a surface (or interface) to local compression or expansion is described by a surface dilatational modulus ϵ:

$$\epsilon = \frac{d\gamma}{d\ln A} \qquad (B.3)$$

where γ is the interfacial tension and A the area of the surface element considered. This modulus determines the resistance to the creation of surface tension gradients, as well as the speed with which such gradients disappear once the system is left to itself.

The elasticity modulus $|\,\epsilon\,|$ is given by:

$$|\epsilon| = \frac{\epsilon_0}{\sqrt{1 + 2\,\xi + 2\,\xi^2}} \qquad (B.4)$$

where

$$\epsilon_0 = -\frac{d\gamma}{d\ln\Gamma} = \Gamma\frac{d\gamma}{d\Gamma} \qquad (B.5)$$

and

$$\xi = \frac{dc}{d\Gamma}\sqrt{\frac{D}{2\,\omega}} \qquad (B.6)$$

In these equations D is the diffusion coefficient of the surfactant, $1/\omega$ is the time scale of the interfacial deformation, c is the concentration of the surfactant and Γ is the surface excess of the surfactant.

The dependence of γ on c is given by the Szyszkovski equation:

$$\gamma - \gamma_0 = +RT\Gamma^{max}\,\ln\left(1 - \frac{\Gamma}{\Gamma^{max}}\right) = -RT\,\Gamma^{max}\,\ln\left(\frac{c+a}{a}\right) \qquad (B.7)$$

with

$$\frac{\Gamma}{\Gamma^{max}} = \frac{c}{c+a} \qquad (B.8)$$

Using these equations we obtain for ϵ_0:

$$\epsilon_0 = RT\Gamma^{\text{max}} \left(\frac{c}{a} \right) \tag{B.9}$$

and for ξ:

$$\xi = \frac{a + 2c + (c^2/a)}{\Gamma^{\text{max}}} \sqrt{\frac{D}{2\omega}} \tag{B.10}$$

Equations (B.9) and (B.10) are valid for a non-ionic surfactant (Dobanol 91-8) or an ionic surfactant in excess electrolyte. For the surfactant SDBS in absence of added salt we find, using the Szyszkovski equation:

$$\gamma - \gamma_0 = +2RT\Gamma^{\text{max}} \ln \left(1 - \frac{\Gamma}{\Gamma^{\text{max}}} \right) = -2RT\Gamma^{\text{max}} \ln \left(\frac{c+a}{a} \right) \tag{B.11}$$

for ϵ_0:

$$\epsilon_0 = 2RT\Gamma^{\text{max}} \left(\frac{c}{a} \right) \tag{B.12}$$

and for ξ:

$$\xi = \frac{a + 2c + (c^2/a)}{\Gamma^{\text{max}}} \sqrt{\frac{D}{2\omega}} \tag{B.13}$$

Using these equations it is now possible to calculate the $|\epsilon|$ versus log [Dobanol 91-8] curve for different values of ω. The values for a and Γ^{max} are given in table B.1 and the diffusion coefficient D of Dobanol 91-8 is estimated from values by Lucassen and Van den tempel [6] to be $5*10^{-10}$ m^2/s.

In figure B.3 the concentration where the maximum of $|\epsilon|$ is found, together with the value of $|\epsilon|$ at that concentration, is plotted versus ω. From figure B.3 it can be seen, that the position of the maximum of the curve and the maximum value of $|\epsilon|$ shifts to higher values as ω increases. In chapter 6 the maximum was experimentally found to be at a concentration of 10^{-3} M for both SDBS and Dobanol 91-8.
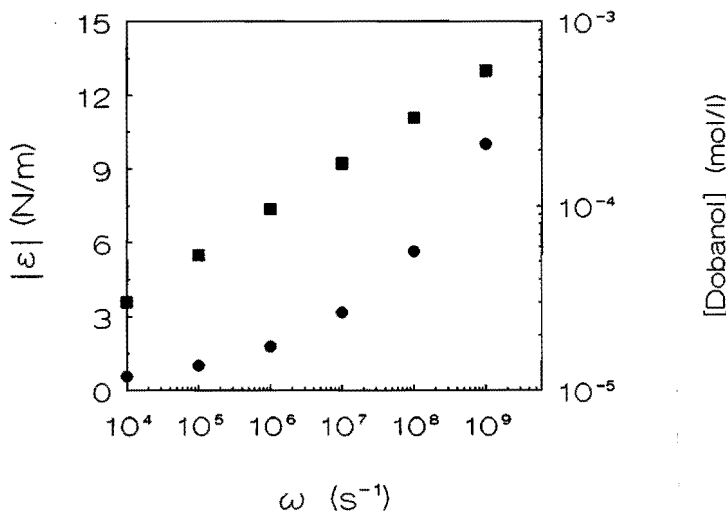
Figure B.3: Value of $|\epsilon|$ at the [Dobanol] where the maximum is found in the $|\epsilon|$ versus [Dobanol] curve as function of ω; ● $|\epsilon|$, ■ [Dobanol].

As can be seen from figure B.3 the frequency has to be higher than 10^9 s^{-1} to find the maximum in the $|\epsilon|$ versus concentration for the surfactant Dobanol. These are un-realistic high values, which agrees with our remark, that a non-equilibrium theory has to be introduced.

B.3 References

(1)   Von Szyszkowski, B., *Z. Phys. Chem*, 1908, *64*, 385.

(2)   Rosen, M. J., Aronson, S., *Colloids Surf.*, 1981, *3*, 201.

(3)   Müller, A., *Colloids Surf.*, 1991, *57*, 219.

(4)   Kegel, W. K., Van Aken, G. A., Bouts, M. N., Lekkerkerker, H. N. W., Overbeek, J. Th. G., de Bruyn, P. L., *Langmuir*, 1993, *9*, 252.

(5)   Van Voorst Vader, F., Erkens, T. F., Van den Tempel, M., *Trans. Faraday Soc.*, **1964**, *60*, 1170.

(6)   Lucassen, J., Van den Tempel, M., *Chem. Eng. Sci.*, **1972**, *27*, 1283.

LIST OF SYMBOLS

This list contains those symbols that are frequently used in this thesis. The symbols that appear only once ore twice are defined in the text itself.

Symbol		SI-units
a	Langmuir-Szyszkovski constant	mol/m^3
A	Surface area per unit mass of polymer	m^2
A$_a$	Adsorption area of surfactant in presence of cosurfactant	m^2
A$_m$	Adsorption area of surfactant in absence of cosurfactant	m^2
A$_n$	Area per charged surface group	m^2
c	Concentration of ions in bulk	mol/m^3
cmc	Critical micelle concentration	mol/m^3
C	Constant	--
C$_a$	Concentration of adsorbed surfactant	mol/m^3
C$_f$	Concentration of unadsorbed surfactant	mol/m^3
C$_t$	Total concentration of surfactant	mol/m^3
d$_{3,2}$	Sauter mean diameter	m
d$_{max}$	Maximum droplet diameter	m
D	Diffusion coefficient	m^2/s
D$_{imp}$	Diameter of impeller	m
D$_n$	Number average diameter ($\sum n_i D_i / \sum n_i$)	m
D$_a$	Surface average diameter ($\sum n_i D_i^2 / \sum n_i D_i$)	m
D$_v$	Volume average diameter ($\sum n_i D_i^3 / \sum n_i D_i^2$)	m
e$_0$	Elementary charge	C
E$_m$	Electrophoretic mobility	m^2/Vs
ΔG^0	Standard Gibbs free energy of adsorption	J/mol
G^E	Excess G-function	J/mol
I	Critical micelle concentration (cmc) of surfactant in pure water	mol/m^3
k	Boltzman's constant	J/K

k_L	Constant in Langmuir-equation	m^3/mol
L_k	Kolmogorov length scale	m
m_p	Mass of polymer per liter of suspension	kg/m^3
n	Number of particles	--
n_∞	Concentration of ions in bulk	mol/m^3
N	Stirrer speed	s^{-1}
N_A	Avogadro's constant	mol^{-1}
N_p	Impeller power number	--
P	Impeller power input	J/s
P_n	Degree of polydispersity (D_v/D_n)	--
R	Gasconstant	J/mol K
Re_D	Impeller Reynolds number (ND_{imp}^2/ν)	--
S_a	Surfactant adsorbed on latex particles	mol/m^2
S_i	Amount of surfactant or cosurfactant initially adsorbed on latex particles	mol/m^2
t	Dropping time	s
t_a	Age of surface	s
t_m	Mixing (circulating) time	s
T	Temperature	K
V	Volume vessel	m^3
V_p	Volume of polymer particles per unit mass	m^3/kg
We_{imp}	Impeller Weber number $(\rho N^2 D_{imp}^3/\gamma)$	--
x	Molfraction	--
z	Valency of ions	--

Greek symbols

$\Delta\gamma$	Difference between dynamic and equilibrium interfacial tension ($\gamma_{dyn} - \gamma_{eq}$)	N/m
γ	Surface or interfacial tension	N/m
γ_0	Surface or interfacial tension of pure liquids	N/m
γ_{dyn}	Dynamic interfacial tension	N/m
γ_{eq}	Equilibrium interfacial tension	N/m
Γ	Surface excess of surfactant or cosurfactant	mol/m^2
Γ^{max}	Maximum surface excess of surfactant or cosurfactant	mol/m^2
ϵ	Energy dissipation per unit mass of fluid	m^2/s^3
ϵ_0	Permittivity of vacuum	F/m
ϵ_{av}	Average energy dissipation per unit mass of fluid	m^2/s^3
ϵ_r	Relative permittivity	--
$|\epsilon|$	Elasticity modulus	N/m
ζ	Zeta-potential	V
θ	Degree of surface coverage (Γ/Γ^{max})	--
κ_c	Conductivity	S/m
κ	Double layer thickness	m
μ	Viscosity	Pa s
μ_{anion}	Chemical potential of surfactant anion	J/mol
μ_{cation}	Chemical potential of surfactant cation	J/mol
μ_{cat+an}	Chemical potential of surfactant molecule	J/mol
ν	Kinematic viscosity (μ/ρ)	kg/ms
ρ	Density	kg/m^3
ρ_p	Density of latex particles	kg/m^3
σ_0	Surface charge density	C/m^2
σ_ζ	Charge density behind electrokinetic shear-plane	C/m^2
σ_Δ	Charge density in Δ-layer	C/m^2
ϕ	Volume fraction	--
ψ_0	Surface potential	V

ψ_δ	Average potential to which adsorbed headgroups of surfactant are subjected	V
ψ_{aver}	Average potential to which counter-ions in electrical double layer are subjected	V
ω	Frequency	s^{-1}

SUMMARY

In this thesis the influence of cosurfactants on the physical properties of surfactants is described. In particular attention is paid to processes, such as adsorption and emulsification, in relation to the stability of coarse emulsions (with diameters larger than 1 μm).

The adsorption of the surfactant Sodium Dodecylbenzenesulphonate (SDBS) on Polystyrene (PS) particles was investigated. Large monodisperse PS-particles were prepared by a one step surfactant-free emulsion polymerization using a lower stirrer speed than applied by previous investigators. The largest PS-particles prepared had a diameter of 3.2 μm. SEM-photographs showed no surface roughness on the PS-particles. In this way PS-particles with uniform surface composition were prepared.

These latices were characterized using conductometric titration and electrophoresis. The charged groups, arising from initiator fragments, were all strong acid groups and no carboxyl groups could be detected. The amount of surface charge groups varies with particles size.

Electrophoresis measurements have shown, that the electrophoretic mobility passes through a maximum as the electrolyte concentration is increased. Converting the electrophoretic mobility to ζ-potentials gives the same picture. The same phenomenon is observed with increasing H^+-concentration. Only at very high electrolyte or H^+-concentrations the ζ-potential reaches values close to zero.

The ζ-potentials were converted to charge densities behind the electrokinetic shear plane (σ_ζ), using the Gouy-Chapman theory and assuming no influence of surface conductivity. In general PS-particles behave as expected without discrepancies between experiment and theory: $|\sigma_0|$ is larger than $|\sigma_\zeta|$, where σ_0 is the surface charge density of the latices. For one particular latex, however, a $|\sigma_\zeta|$ larger than $|\sigma_0|$ was found. This fact was attributed to chemisorption of NO_3^- ions. Chemisorption of NO_3^--ions is not a common fact, but may be attributed to the pronounced hydrophobic character of the PS-particles.

The adsorption of SDBS on the monodisperse PS-particles was investigated. Differences in the surface charge density of the latices have an effect on the adsorption behaviour of this surfactant at very high surface charge densities only.

The areas per adsorbed SDBS-molecule were determined by Maron's soap titration method and were 50-60 $\mathring{A}^2$ at 22 °C and 60-80 $\mathring{A}^2$ at 60 °C for the latices depending on the surface charge density. The higher areas per adsorbed molecule at higher temperatures are explained by the larger thermal motion of the adsorbed molecules.

The addition of long chain fatty alcohols (cosurfactants) such as dodecanol or cetylalcohol influences the adsorption behaviour of the surfactants. When adding the alcohols at low cosurfactant/surfactant ratios there is only little influence, whereas at higher ratios the average area per adsorbed molecule of SDBS decreases sharply.

This is explained by the fact that when adding alcohols there is a positive attraction between the tails of surfactant and alcohol, without simultaneously introducing additional repulsion through negatively charged groups. This positive effect is more pronounced at larger ratios of cosurfactant/surfactant than at lower ratios. At higher temperatures smaller average areas per adsorbed SDBS molecule are found.

The adsorption of SDBS on PS-particles is described by the Langmuir equation only superficially: on closer look there are small but systematic differences with the experiments. This is expressed here as an excess G function (G^E) of the surfactant electrolyte on adsorption, which changes with increasing degree of occupation of adsorption sites (θ). At low θ values, G^E changes in positive direction with increasing θ; at large θ values, this trend levels off and may even be in the opposite direction (depending on the value assumed for total saturation of the surface with surfactants). This is explained by changes in adsorption energy of the surfactant chain on the polystyrene surface: at very low θ values the chain is adsorbed in a flat configuration; at larger θ values this is no longer possible, but this is partially compensated by interaction between the hydrocarbon chains of surfactant ions adsorbed on neighbouring sites. This explanation is confirmed by the effect of cosurfactant molecules on the adsorption.

The preparation of emulsions in a stirred vessel was investigated and it was found, that the equilibrium droplet-size is determined by break-up processes, which have very long time scales. The equilibrium droplet-size was in most of the experiments reached after more than 100 minutes. This time scale seems not to be strongly influenced by process-variables, such as the concentration of surfactant (and consequently the interfacial tension), stirrer speed, volume fraction dispersed phase or temperature, but does depend

on the presence or absence of cosurfactant.

The Weber number theory has found to be correct, with the exception that in this theory a dynamic interfacial tension should be used instead of the equilibrium value. An attempt has been made to correlate this difference between dynamic and equilibrium interfacial tension ($\Delta\gamma$), by using the elasticity modulus of expanding interfaces. It was found, that the curves of $\Delta\gamma$ and the elasticity modulus versus concentrations have the same shape, but the concentration where the maximum is found is located at a too low concentration with the theory used. This fact is attributed to the fact, that this theory assumes deformations of the interface at situations close to equilibrium. In the system studied, this is not the case, but theories for deformations far from equilibrium have not been developed so far.

The addition of cosurfactants results in smaller droplet-sizes and a reduction in the time to reach a steady state situation. The smaller droplet-size is attributed to the fact, that the interfacial tension decreases by the addition of cosurfactants. The influence of cosurfactants is more pronounced, when they are added to the oil-phase. In this case the difference between equilibrium and dynamic interfacial tension is close to zero.

In the last chapter the consequences of the presence of cosurfactants during the emulsion polymerization process is discussed, based on the results obtained in foregoing chapters. Addition of cosurfactant results in a decrease of the cmc, an increase of adsorption, surface charge density of the micelles and size of micelles and a smaller emulsion droplet-size. It is expected, that of these effects, the increase of adsorption and smaller droplet-size are the most relevant to polymerization processes.

SAMENVATTING

In dit proefschrift wordt de invloed van cosurfactants op de fysische eigenschappen van surfactants beschreven. In het bijzonder wordt aandacht besteed aan processen, zoals adsorptie en emulgering, in relatie tot de stabiliteit van emulsies (met een deeltjesgrootte groter dan 1 μm).

De adsorptie van de surfactant Natrium Dodecylbenzeensulfonaat (SDBS) op Polystyreen (PS) deeltjes werd onderzocht. Grote monodisperse PS-deeltjes (met een deeltjesgrootte vergelijkbaar met de emulsiedruppels) werden gemaakt door middel van een één-staps surfactant-vrije emulsiepolymerisatie, door gebruik te maken van een lagere roersnelheid dan werd toegepast door eerdere onderzoekers. De grootste PS-deeltjes hadden een diameter van 3.2 μm. Op SEM-foto's kon geen oppervlakteruwheid van de PS-deeltjes gezien worden. Op deze manier kunnen PS-deeltjes met een uniforme oppervlakte-compositie gemaakt worden.

Deze deeltjes werden gekarakteriseerd d.m.v conductometrische titraties en electroforese. De geladen groepen, afkomstig van initiator fragmenten, bleken sterk zure groepen te zijn en er werden geen carboxylgroepen gevonden. Het aantal geladen groepen per opper-vlakte eenheid (de oppervlakteladingsdichtheid, σ_0) varieerde met de deeltjesgrootte.

Electroforese metingen hebben aangetoond, dat de electroforetische snelheid door een maximum gaat, als de zout- of H$^+$-concentratie wordt verhoogd. Hetzelfde resultaat werd gevonden voor de ζ-potentiaal, die berekend werd uit de electroforetische snelheid. Alleen bij zeer hoge zout- of H$^+$-concentraties worden ζ-potentialen gevonden met waarden dicht bij nul.

De ladingsdichtheid achter het electrokinetisch afschuifvlak (σ_ζ) werd berekend uit de gemeten ζ-potentialen, door gebruik te maken van de Gouy-Chapman theorie en aan te nemen, dat er geen oppervlaktegeleiding plaatsvindt. In het algemeen gedragen de PS-deeltjes zoals verwacht zonder afwijkingen tussen theorie en experiment: $|\sigma_0|$ is groter dan $|\sigma_\zeta|$. Voor één latex werd echter een $|\sigma_\zeta|$ gevonden, die hoger was dan $|\sigma_0|$. Dit feit werd toegeschreven aan de chemisorptie van NO$_3^-$-ionen. Alhoewel chemisorptie van NO$_3^-$-ionen een niet algemeen verschijnsel is, kan dit worden verklaard door het sterk hydrofobe karakter van de PS-deeltjes.

De adsorptie van SDBS op de monodisperse PS-deeltjes werd onderzocht en alleen bij zeer hoge oppervlakteladingsdichtheden bleek dat de adsorptie te beïnvloeden.

Het oppervlak per geadsorbeerd SDBS-molecuul werd bepaald d.m.v. Maron's zeep titratie methode en bleek 50-60 Å^2 bij 22 °C en 60-80 Å^2 bij 60 °C te zijn voor de verschillende PS-deeltjes, afhankelijk van de oppervlakteladingsdichtheid. Het hoger oppervlak per geadsorbeerd molecuul bij hogere temperatuur werd verklaard door een hogere thermische beweging van de geadsorbeerde moleculen.

Toevoeging van hogere alcoholen (cosurfactants), zoals dodecanol of cetylalcohol, beïnvloedt het adsorptiegedrag van surfactants. Bij toevoeging van de alcoholen bij een lage cosurfactant/surfactant-verhouding is er weinig invloed, maar bij hogere ver-houdingen daalt het gemiddeld oppervlak per geadsorbeerd SDBS-molecuul scherp. Dit werd verklaard door het feit, dat bij toevoeging van een alcohol er een positieve interactie is tussen de staarten van de surfactant en het alcohol, zonder dat er tegelijkertijd een repulsie door negatief geladen groepen van de surfactant wordt geïntroduceerd. Dit positieve effect wordt belangrijker bij hogere cosurfactant/surfactant-verhoudingen dan bij lagere. Bij hogere temperaturen werd een lager oppervlak per geadsorbeerd SDBS-molecuul gevonden.

De adsorptie van SDBS op PS-deeltjes kan slechts in eerste benadering door de Langmuir vergelijking beschreven worden; bij nadere beschouwing worden er kleine, maar syste-matische verschillen tussen de theorie en de experimenten gevonden. Deze verschillen werden beschreven door een exces G-functie (G^E) van de surfactant electroliet tijdens adsorptie, die wijzigt met een hogere bezettingsgraad van de adsorptieplaatsen (θ). Bij lage θ-waarden verandert G^E naar de positieve kant bij groter wordende θ; bij hoge θ-waarden vlakt deze trend af en kan zelfs omslaan in de andere richting (afhankelijk van de waarde die wordt aangenomen voor de maximale oppervlaktebezetting van surfactants). Dit werd verklaard door veranderingen in adsorptie-energie van de surfactant staart op het PS-oppervlak: bij zeer lage θ-waarden is de staart geadsorbeerd in een vlakke configura-tie, terwijl bij hogere θ-waarden dit niet langer mogelijk is. Dit wordt ten dele gecompen-seerd door de interactie tussen de koolwaterstof staarten van surfactants die geadsorbeerd zijn op naburige adsorptieplaatsen. Deze verklaring wordt bevestigd door het effect van cosurfactants op de adsorptie van surfactants.

De bereiding van emulsies in een geroerd vat werd onderzocht en het bleek, dat de evenwichtsdruppelgrootteverdeling werd bepaald door opbreekprocessen met een zeer lange tijdsschaal.

De evenwichtsdruppelgrootteverdeling werd in de meeste experimenten na meer dan 100 minuten bereikt. Deze tijdsschaal lijkt niet erg te worden beïnvloed door de procesvariabelen, zoals de surfactantconcentratie (en dus de grensvlakspanning), roersnelheid, volumefractie van de gedispergeerde fase of de temperatuur, maar hangt wel af van de aan- of afwezigheid van een cosurfactant.

De Weber theorie bleek de experimentele resultaten goed te beschrijven, als in deze theorie de dynamische- i.p.v. de evenwichtsgrensvlakspanning wordt gebruikt. Om het verschil tussen de dynamische- en evenwichtsgrensvlakspanning ($\Delta\gamma$) te kunnen verklaren, werd geprobeerd dit te beschrijven door gebruik te maken van de elasticiteitsmodulus van expanderende grensvlakken. De curves van $\Delta\gamma$ en de elasticiteitsmodulus versus concentratie hebben dezelfde vorm, maar de concentratie waar het maximum van $\Delta\gamma$ experimenteel wordt gevonden, ligt bij een hogere concentratie dan de theorie voorspelt. Dit wordt veroorzaakt door het feit, dat in de theorie deformaties van het grensvlak dicht bij evenwicht worden beschouwd. In ons systeem is dit niet het geval, maar tot nu toe zijn dergelijke niet-evenwichts theorieën niet ontwikkeld.

Toevoeging van cosurfactants leidt tot kleinere druppelgroottes van de emulsies en een verkleining van de tijdsduur om een evenwichtssituatie te bereiken. De kleinere druppelgroottes zijn het gevolg van een lagere grensvlakspanning na toevoeging van de cosurfactants. Het grootste effect van de cosurfactants wordt waargenomen, als zij worden opgelost in de olie-fase. In dat geval is het verschil tussen dynamische- en evenwichtsgrensvlakspanning zeer klein.

In het laatste hoofdstuk wordt de invloed van de aanwezigheid van cosurfactants tijdens emulsiepolymerisatie beschreven, gebaseerd op de resultaten, die in dit proefschrift staan beschreven. Toevoeging van een cosurfactant leidt tot een verlaging van de cmc, een toename van de adsorptie, een hogere ladingsdichtheid van de micellen, een toename van de grootte van de micellen en een kleinere emulsie-druppelgrootte. Het is aan te nemen, dat van deze effecten de toename van de adsorptie en de kleinere emulsie-druppelgroottes het meest belangrijk zijn voor het emulsiepolymerisatie proces.

DANKWOORD

De mensen van de technische dienst verdienen dank voor de wijze, waarop zij mijn gedachten omzetten in technisch realiseerbare apparatuur.

Mijn ouders, Trix en mijn vrienden hebben altijd interesse getoond voor mijn onderzoek. Ik wil mijn ouders bedanken voor de steun, die zij mij hebben gegeven. Zonder hun steun was ik niet gaan studeren en had dit proefschrift er nu niet gelegen.

Tenslotte wil ik Caroline bedanken. Caroline, bedankt voor alle keren dat je mij met raad en daad terzijde hebt gestaan en voor jouw steun, ook in die tijden dat het wat moeizamer ging.

Gert

CURRICULUM VITAE

De schrijver van dit proefschrift werd geboren op 10 april 1967 in Winschoten. Het atheneum werd op de Winschoter Scholengemeenschap te Winschoten gevolgd, waar in 1985 het diploma werd gehaald. In hetzelfde jaar werd begonnen met de studie Scheikunde aan de Rijksuniversiteit Groningen. Het afstudeeronderzoek "Template-polymerisatie van N-Vinylimidazool langs isotactisch polymethacrylzuur" werd verricht bij de vakgroep Polymeerchemie van Prof. dr. G. Challa, onder leiding van Ir. Y. Y. Tan en Dr. H. T. van de Grampel. Het doctoraal-diploma werd in 1990 behaald en in hetzelfde jaar begon hij als A. I. O. bij de vakgroep Colloïdchemie en Thermodynamica aan de Technische Universiteit Eindhoven aan het in dit proefschrift beschreven onderzoek, onder leiding van Prof. dr. H. N. Stein en Prof. dr. W. G. M. Agterof.

Resultaten van het promotie-onderzoek werden gepresenteerd op het "First world congres on emulsions" in oktober 1993 in Parijs, Frankrijk en op het "8th International conference on surface and colloid science" in februari 1994 in Adelaide, Australië.

Vanaf 1 mei 1995 zal hij werkzaam zijn als post-doc aan het "Institut Charles Sadron" in Straatsburg.

Stellingen

behorende bij het proefschrift van

G. Tuin

1. Onder turbulente stromingscondities is de dynamische grensvlakspanning een belangrijke parameter die mede de uiteindelijke deeltjesgrootteverdeling van emulsiedruppels bepaalt.

   Dit proefschrift, Hoofdstuk 6.

2. In tegenstelling tot mini-emulsies, leidt bij emulsies het oplossen van cosurfactants in de olie-fase niet tot onstabiliteit.

   Dit proefschrift, Hoofdstuk 6.

3. De adsorptie van surfactants op Polystyreen deeltjes wordt, ten onrechte, door Kusters beschreven door gebruik te maken van de Langmuir adsorptie isotherm.

   Kusters, J. M. H., *Inisurfs: Surface-Active Initiators, Their Synthesis and Application in Emulsion Polymerization*; Proefschrift, Eindhoven 1994, p. 102.

4. De methode om de adsorptie van surfactants op polymeerdeeltjes te bepalen, die Maurice als verbeterd omschrijft, blijkt dat bij nadere bestudering niet te zijn, omdat tussen de data-punten en de gefitte vergelijking de grootste afwijking optreedt in het punt waar de informatie over de adsorptie wordt bepaald.

   A. M. Maurice, *J. Appl. Pol. Sci.*, **1985**, *30*, 473.

5. Het gebruik van constantes met een ordegrootte van 1, maakt de formules onnodig ingewikkeld en komt de duidelijkheid van het verhaal niet ten goede.

   A. Chesters, *Trans. I. Chem. E.*, **1991**, *69(A)*, 259.

6. Lee en Soong komen ten onrechte tot de conclusie, dat de gevonden afwijking tussen hun meetresultaten en de theoretische waarden, moet worden toegeschreven aan andere factoren dan een verandering van de fysische eigenschappen van het bestudeerde systeem.

   J. M. Lee, Y. Soong, *Ind. Eng. Chem. Process Des. Dev.*, **1985**, *24(1)*, 119.

7. De door Jindal en Bahadur gepubliceerde data, over de adsorptie van SDBS aan het water-lucht grensvlak, zijn onjuist.

    V. K. Jindal, P. Bahadur, *Ind. J. Technol.*, **1982**, *20*, 64.

8. El-Aasser et al. gebruiken ten onrechte de term "spontaneous emulsification", omdat tijdens hun experimenten wel degelijk energie wordt toegevoerd.

    M. S. El-Aasser, G. D. Lack, J. W. Vanderhoff, F. M. Fowkes, *Colloids Surfaces*, **1988**, *29*, 103.

9. Het steeds meer uitbesteden van onderzoek door bedrijven aan universiteiten, biedt universiteiten de mogelijkheid om onderzoek te doen en wetenschappers op te leiden, maar heeft als keerzijde dat de opgeleide mensen de opgedane kennis bij bedrijven steeds moeilijker in de praktijk kunnen brengen.

10. Het absorptie-vermogen van de moderne luiers heeft tot gevolg, dat zindelijkheids-training een steeds belangrijker plaats zal innemen tijdens de opvoeding.